https://ntrs.nasa.gov/search.jsp?R=19690005897 2020-03-12T08:23:15+00:00Z

General Disclaimer

One or more of the Following Statements may affect this Document

- This document has been reproduced from the best copy furnished by the organizational source. It is being released in the interest of making available as much information as possible.

- This document may contain data, which exceeds the sheet parameters. It was furnished in this condition by the organizational source and is the best copy available.

- This document may contain tone-on-tone or color graphs, charts and/or pictures, which have been reproduced in black and white.

- This document is paginated as submitted by the original source.

- Portions of this document are not fully legible due to the historical nature of some of the material. However, it is the best reproduction available from the original submission.

Produced by the NASA Center for Aerospace Information (CASI)

AD 677269

TG—977
JULY 1968
Copy No. 8

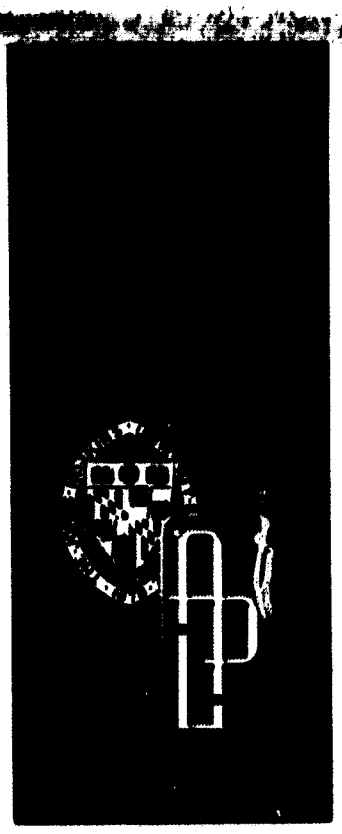

Technical Memorandum

GEOS-B ANTENNA SYSTEM

by C. C. KILGUS

FACILITY FORM 602
N69-15229 (ACCESSION NUMBER)
124 (PAGES)
CR 98916 (NASA CR OR TMX OR AD NUMBER)
(THRU) 1
(CODE) 31
(CATEGORY)
AD 677269

DDC
RETAINED
NOV 7 1968
C

THE JOHNS HOPKINS UNIVERSITY • APPLIED PHYSICS LABORATORY

This document has been approved for public release and sale; its distribution is unlimited.

TG—977
JULY 1968

Technical Memorandum

GEOS-B ANTENNA SYSTEM

by C. C. KILGUS

THE JOHNS HOPKINS UNIVERSITY ■ APPLIED PHYSICS LABORATORY
8621 Georgia Avenue, Silver Spring, Maryland 20910

Operating under Contract NOw 62-0604-c, Bureau of Naval Weapons, Department of the Navy

This document has been approved for public release and sale; its distribution is unlimited.

THE JOHNS HOPKINS UNIVERSITY
APPLIED PHYSICS LABORATORY
SILVER SPRING, MARYLAND

PRECEDING PAGE BLANK NOT FILMED.

ABSTRACT

This report documents the design, performance, fabrication and flight acceptance tests of the GEOS-B antenna system. Measured data is included for the VHF-UHF wideband hemispherical spiral, nine-port multiplexer, S-band conical spiral and C-band cavity helices. Simple theoretical models are included to yield an intuitive insight to the theory of the system; a bibliography aids those seeking detailed information.

THE JOHNS HOPKINS UNIVERSITY
APPLIED PHYSICS LABORATORY
SILVER SPRING, MARYLAND

PRECEDING PAGE BLANK NOT FILMED.

TABLE OF CONTENTS

TABLE OF CONTENTS (Cont'd)

THE JOHNS HOPKINS UNIVERSITY
APPLIED PHYSICS LABORATORY
SILVER SPRING, MARYLAND

LIST OF ILLUSTRATIONS

LIST OF ILLUSTRATIONS (Cont'd)

THE JOHNS HOPKINS UNIVERSITY
APPLIED PHYSICS LABORATORY
SILVER SPRING, MARYLAND

I. INTRODUCTION

GEOS-B, designed by APL and operated by NASA, is to be injected into a near-earth orbit with a 600 nautical mile perigee, 800 nm apogee and 74 degree (retrograde) inclination.(1) The satellite is gravity gradient stabilized so that the bottom surface of the satellite is always oriented toward the center of the earth.

Five separate antennas make up the antenna subsystem: A VHF-UHF wideband hemispherical log spiral with a nine port multiplexer; an S-band conical log spiral; two C-band cavity helices; and a C-band Van Atta array. The location of the antennas on the satellite is recorded on Drawing #7211-0005.* The satellite subsystems feeding each antenna and the frequencies used are detailed below. Each of the antennas will then be discussed separately.

Hemispheric Log Spiral

136.32 mcs - Telemetry and minitrack beacon transmitter

148.98 mcs - Command Receiver

162
324
972 } mcs - Doppler Beacons. The doppler subsystem is to be used in conjunction with the U. S. Navy TRANET doppler network for gravimetric measurements to define the structure of the earth's gravitational field, to refine the location and magnitude of large gravity anomalies, and to improve positional accuracies of the fixed and portable TRANET tracking stations

224.5
421
449 } mcs - Range (SECOR) transponder subsystem. The range transponder is to be used in conjunction with the SECOR system ground stations for ranging to the spacecraft transponder. Trilateration techniques permit determining the unknown position of one of four SECOR stations accurately.

S-Band Antanna

1705
2270 } mcs - Range and Rate Rate transponder subsystem. The RARR transponder subsystem is to be used to perform accurate measurements of

---

This work supported by NASA under Task I of the Navy Contract NOw 62-0604-c.

*Drawings listed are APL documents obtainable from S4M - not a part of this report.

the slant range and rate of change of slant range to the spacecraft.

C-Band Antennas

5690 } mcs - C-Band transponder. The C-band transponder is to
5765 }

be used for range radar calibration and for experimentation to determine the accuracy of the system for geometric and gravimetric geodesy investigations.

Van Atta Array - The radar reflector will passively increase the C-band effective radar cross section of the spacecraft. The effects of long-term variations in the C-band transponder system can be studied if both skin and beacon track are accomplished within the same pass.

II. THE HEMISPHERICAL LOGARITHMIC SPIRAL

Introduction

Many of the properties of the planar log spiral are preserved when it is projected onto a hemisphere. The planar spiral is discussed first to yield an intuitive insight to the operation of this type of antenna.

The Frequency Independent Planar Log Spiral - The design of this class of antenna is based on the principle as stated by Rumsey: If the shape of an antenna can be specified entirely by angles, its performance is independent of frequency.(2)

The infinite planar log spiral described by $r = k\, e^{a\phi}$ satisfies this criteria exactly (Fig.1a). The balanced two arm log spiral (Fig.1b) is more easily excited and has become more popular than the one arm spiral.

Physical model - The "current band theory"(3) provides a very approximate but intuitively satisfying model of the spiral antenna.

The arms of the balanced log spiral can be thought of as the conductors of a balanced two wire transmission line that are distorted into a radiating structure (Fig. 2).

THE JOHNS HOPKINS UNIVERSITY
APPLIED PHYSICS LABORATORY
SILVER SPRING MARYLAND

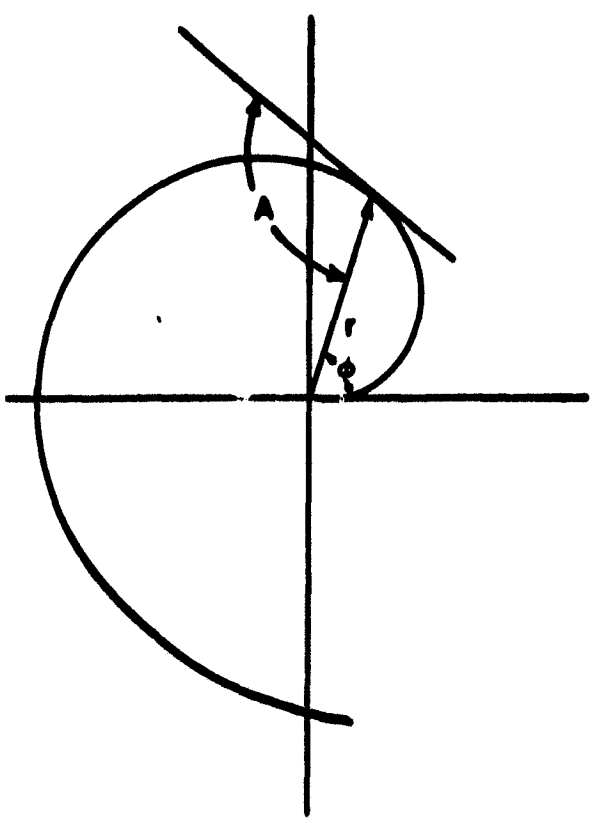

a

Fig. 1a INFINITE PLANAR LOG SPIRAL

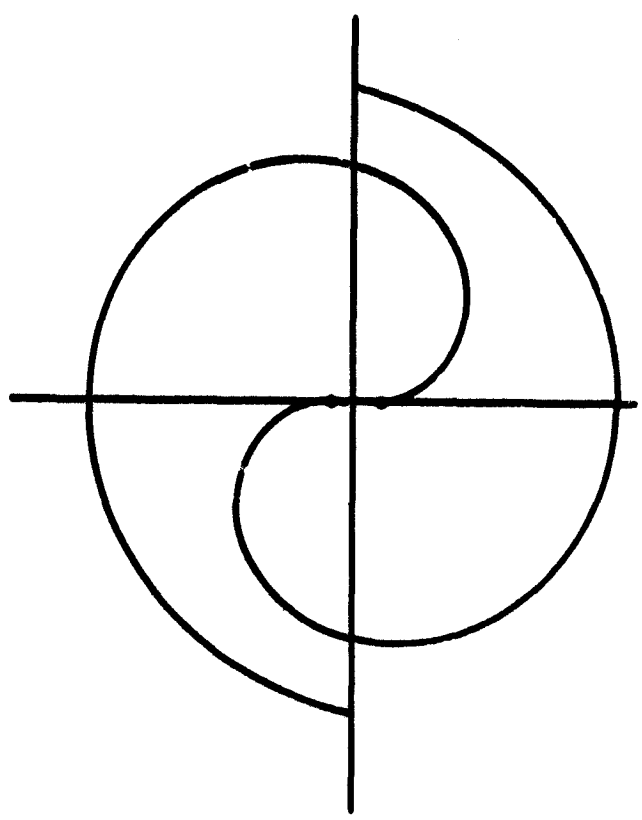

b

Fig. 1b BALANCED TWO-ARM LOG SPIRAL

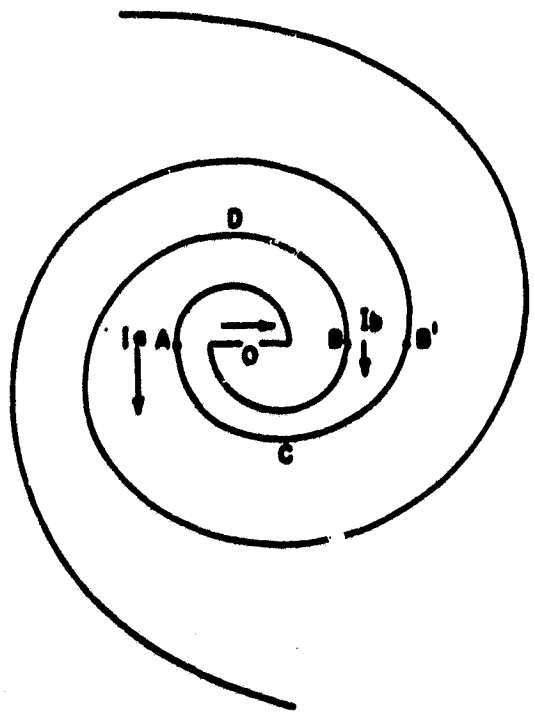

Fig. 2 ARMS OF BALANCED LOG SPIRAL DISTORTED INTO RADIATING STRUCTURE

THE JOHNS HOPKINS UNIVERSITY
APPLIED PHYSICS LABORATORY
SILVER SPRING, MARYLAND

Consider two points at equal distances along the wire, A and B ($\overset{\frown}{oA} = \overset{\frown}{oB}$), where the currents have equal amplitudes and opposite phase. In traveling the additional distance AB' the current is shifted in phase $\frac{2\pi \overset{\frown}{AB'}}{\lambda}$. Near the origin, the shift in phase from A to B' will be small; the currents at B and B' in opposition and radiation from the two points will cancel. At a point further along the spiral where the distance from A to B' is one half wavelength (phase shift 180°) the currents at B and B' will be in the same direction and efficient radiation will take place. The distance $\overline{AB'}$ is approximately πr so radiation occurs at the point on the spiral where the diameter = λ/π. The remainder of the spiral acts as a load to absorb the power that is not radiated.

The currents at C and D are orthogonal in space and phase to those at A and B causing the radiation to be circularly polarized.

The Finite Planar Log Spiral

The introduction of a length, the length of the finite spiral arm, imposes a lower frequency limit on the operation of the antenna. If the last turn is not large enough to allow power dissipation by the efficient radiation noted above to occur, current will be reflected from the end of the spiral. This current will traverse the spiral in the reverse direction causing radiation in the opposite circular polarity. This provides a convenient definition; the lower frequency limit of the antenna is the frequency where the radiation is linearly polarized.

The upper frequency limit of the antenna is determined by the mechanical tolerance or fineness of the small end of the spiral. As will be discussed, convenient methods of exciting the spiral contribute to lowering the upper limit.

Exciting The Balanced Log Spiral

Realization of the wide band potentialities of the log spiral requires a feed network with equally wide bandwidth. The infinite balun[4] is such a feed (Fig.3). A coax cable is bonded to one arm of the spiral. At the

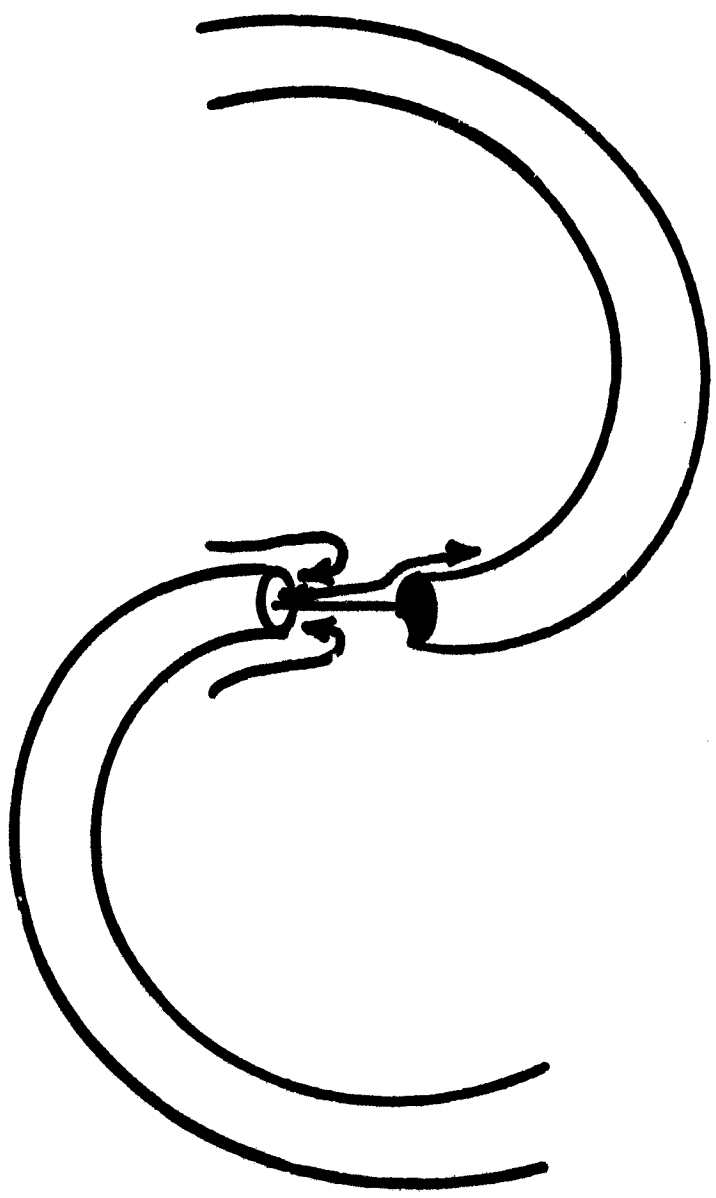

Fig. 3 INFINITE BALUN SHOWING FEED NETWORK WITH EQUALLY WIDE BANDWIDTH

feed point the center conductor is connected to the opposite arm causing the equal and opposite currents inside the coax to become antenna currents. The antenna currents on the outside of the coax are dissipated by radiation, preventing radiation of the feed line past the end of the spiral. The size of the coax used in the feed limits the fineness of the small end of the spiral and therefore the upper frequency limit of the antenna.

III. THE GEOS HEMISPHERICAL LOG SPIRAL SLOT ANTENNA

A balanced spiral antenna is painted on a two-foot diameter, one-sixteenth inch thick fiberglas hemisphere to form the GEOS-B antenna. The slot image of the thin wire spiral is used. The slot is described by the two spirals $r = ke^{a\phi}$ and $r' = ke^{a(\phi-\alpha)}$ where α is the lag angle between equal radius vectors,[5] (Fig. 4). The area remaining is painted with silver loaded paint. To simplify construction of the antenna, the distances r and r' are measured along the surface of the hemisphere rather than measured on a plane and projected onto the hemisphere. Drawing 7211-1302 details the radii at various stations for the GEOS-B hemisphere.

Formulas for the radiation patterns of the hemisphere on a limited ground plane have been calculated but complexity limits their usefulness.[6]

Locally Periodic Structures[7]

A model for the operation of the hemispherical spiral can be obtained by comparison with the cylindrical helix. Figure 5 compares one turn of the hemispherical spiral with one turn of the cylindrical helix with the same pitch. The ratio (s) of pitch to turn length is the ratio of the propagation constant (k) along the arms to the propagation constant (β) along the cylindrical surface. Since this ratio is nearly the same for one turn on the helix or on the hemisphere, there should be good correlation between the operation of this portion of the hemispherical spiral and the corresponding bifilar helical cylinder.

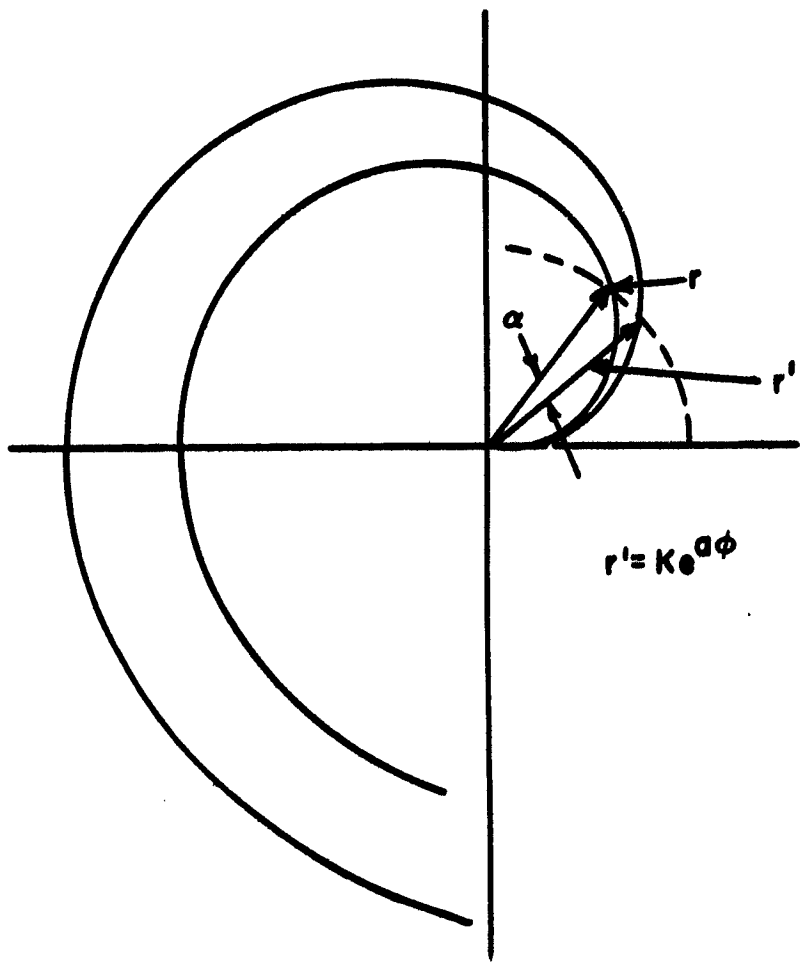

Fig. 4 SLOT DESCRIBED BY TWO SPIRALS, SHOWING LAG ANGLE BETWEEN EQUAL RADIUS VECTORS

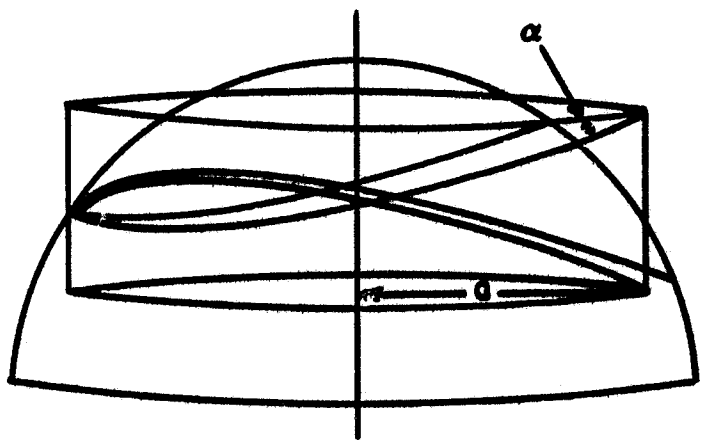

Fig. 5 COMPARISON OF ONE TURN OF HEMISPHERICAL SPIRAL WITH ONE TURN OF CYLINDRICAL HELIX WITH THE THE SAME PITCH

The Brillouin or k/β diagram displays the variation of the propagation constant on periodic antenna structures.(8)(9)

A diagram for the bifilar helix is given in Figure 6. The vertical axis is the pitch distance in free space wavelengths, the horizontal axis is the pitch distance in guide wavelengths on the surface of the antenna. For a given helix (α and a constant) the only variable involved is the frequency of operation.

As frequency is increased there is first a region of closely bound surface waves, then strong coupling to a space wave traveling in the opposite direction. The propagation constant becomes complex as the structure radiates a backfire wave toward the point of excitation(10). At a still higher frequency energy is radiated at an angle to the axis of the structure and then in an end fire beam in the opposite direction.(11)

For the hemispherical antenna the radius r increases with distance from the feedpoint. At a given frequency the propagation constant might be expected to behave in the same manner as the cylindrical helix behaves with increasing frequency. That is, the portion of the helix too small to radiate acts as low loss wave guide carrying energy to the larger region that radiates back toward the feedpoint. This mode of operation causes the hemispherical spiral to radiate in a uni-directional pattern as opposed to the bi-directional pattern of the planar spiral.

Bandwidth of the GEOS Hemisphere

The diameter of the largest turn is 24 inches, placing the calculated lower frequency limit at 158 mcs. Examination of the measured axial ratio (Fig. 13) indicates nearly linear polarization in this frequency range. The fineness of the small end of the spiral limits the upper frequency at about 1200 mcs.

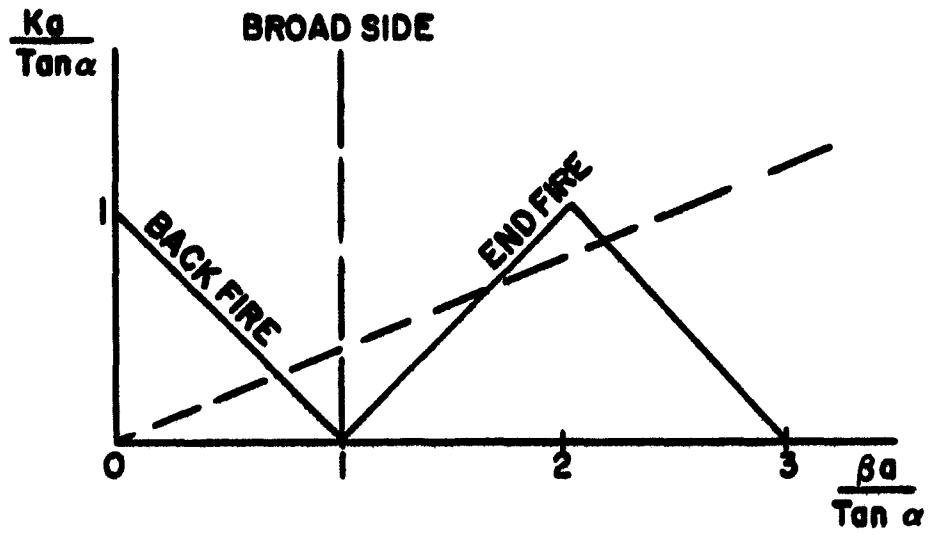

Fig. 6 DIAGRAM OF BIFILAR HELIX

Feed

The hemisphere feed is an infinite balun utilizing Uniform Tubes, Inc., UT-141-C ram extruded coaxitube with copper center conductor. This coax is .141 inches in diameter, limiting the fineness of the feed region as indicated on Drawing #7211-1302, and Figure No. 7. The epoxy across the feedpoint prevents teflon creep during thermal cycling. The coaxitube is bound to the arms with twisted copper wire and silver loaded epoxy. The wires for the solar attitude detector are held in place under the coax by the epoxy.

Measured Parameters

Measured Radiation Patterns - Radiation patterns of the GEOS-B hemispheric antenna mounted on the sheet metal RF mockup of the satellite body were recorded on the S2T-4 antenna range. Figure 8 details the range, Figure 9 the coordinate system used. The measured patterns are grouped as Figure 10. The pattern number for a particular frequency can be found in Table I. Since the patterns are nearly symmetric about the Z axis, only $\phi = 0$ and 90° are given for each frequency.

TABLE I - Pattern Numbers

	$\phi = 0$		$\phi = 90$	
	Polarization		Polarization	
f mcs	Cir.	Lin.	Cir.	Lin.
136	1	2	3	4
148.98	5	6	7	8
162	9	10	11	12
224.5	13	14	15	16
324	17	18	19	20
421	21	22	23	24
449	25	26	27	28
972	29	30	31	32

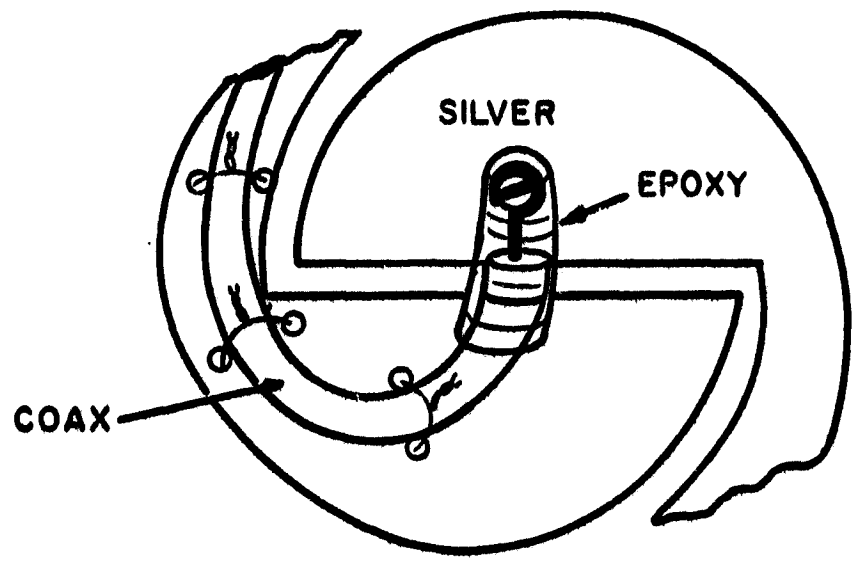

Fig. 7 HEMISPHERICAL SPIRAL FEED REGION

THE JOHNS HOPKINS UNIVERSITY
APPLIED PHYSICS LABORATORY
SILVER SPRING MARYLAND

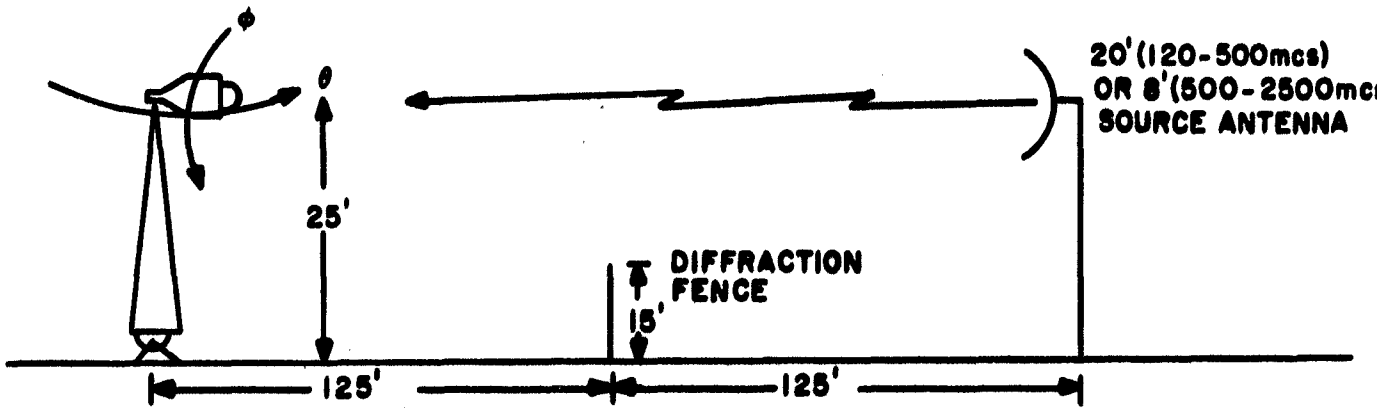

Fig. 8 APL ANTENNA RANGE

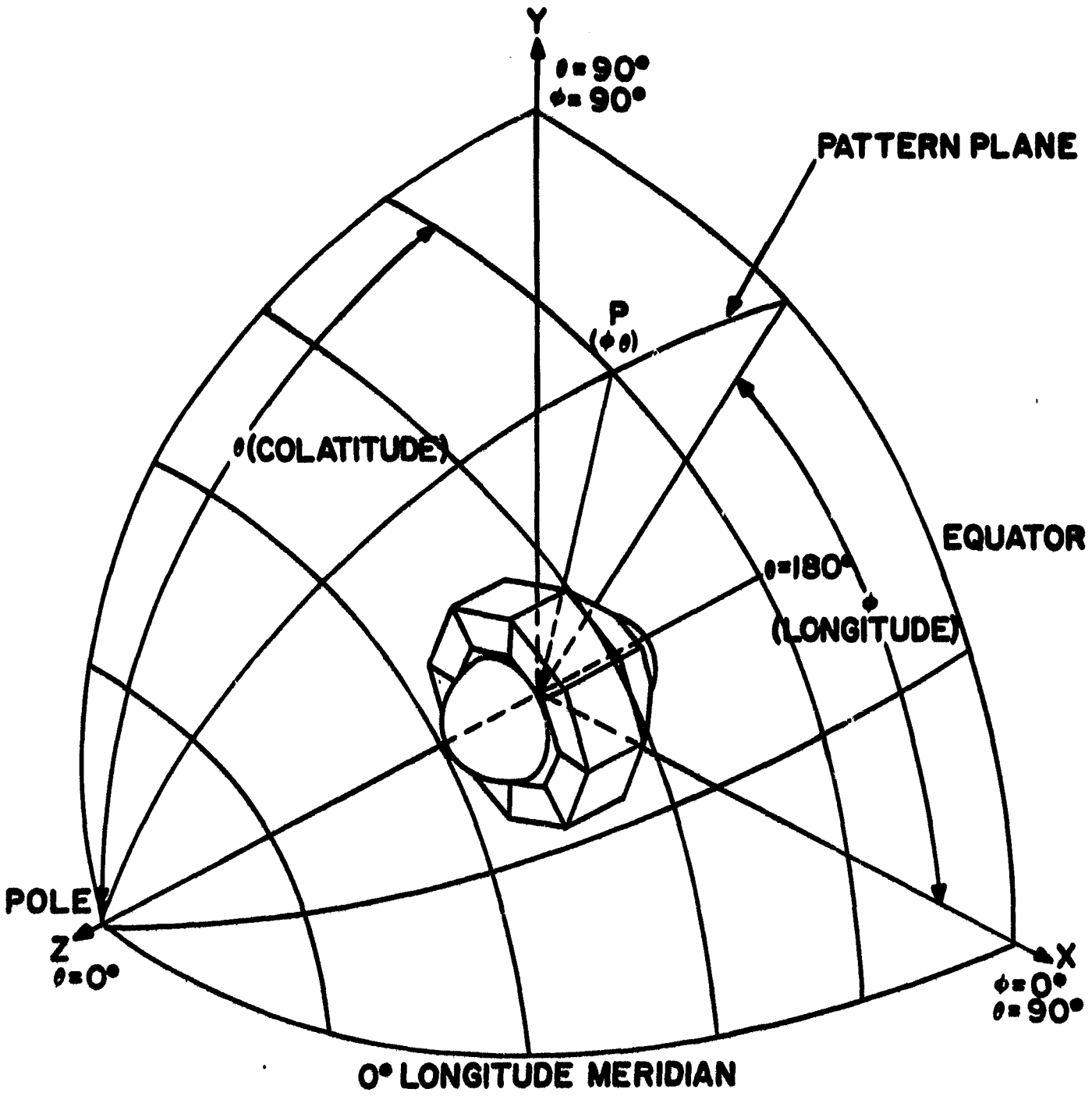

Fig. 9 COORDINATE SYSTEM USED FOR MEASURED RADIATION PATTERNS

Fig. 10 MEASURED RADIATION PATTERNS

THE JOHNS HOPKINS UNIVERSITY
APPLIED PHYSICS LABORATORY
SILVER SPRING MARYLAND

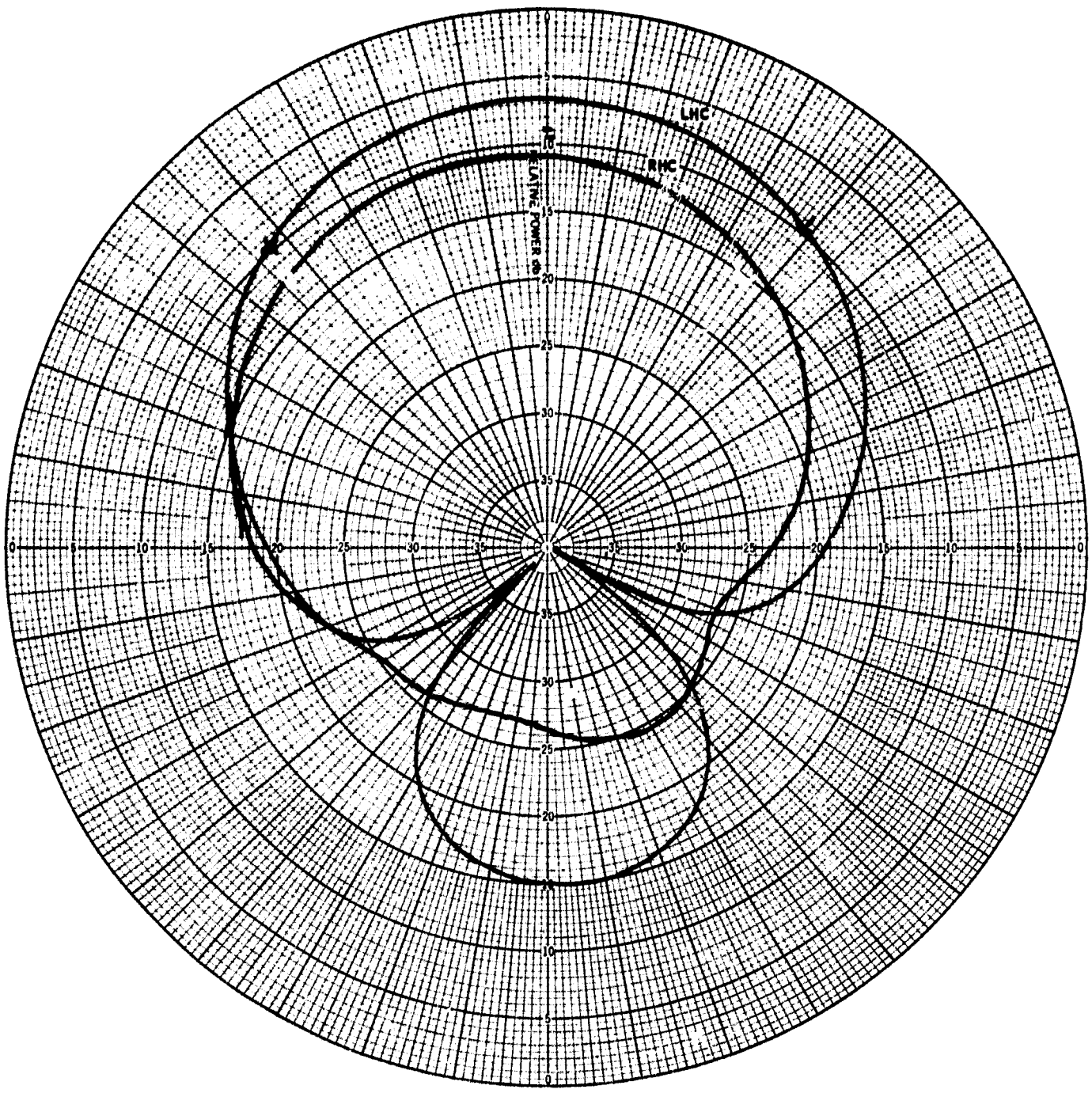

Fig. 10-1

THE JOHNS HOPKINS UNIVERSITY
APPLIED PHYSICS LABORATORY
SILVER SPRING, MARYLAND

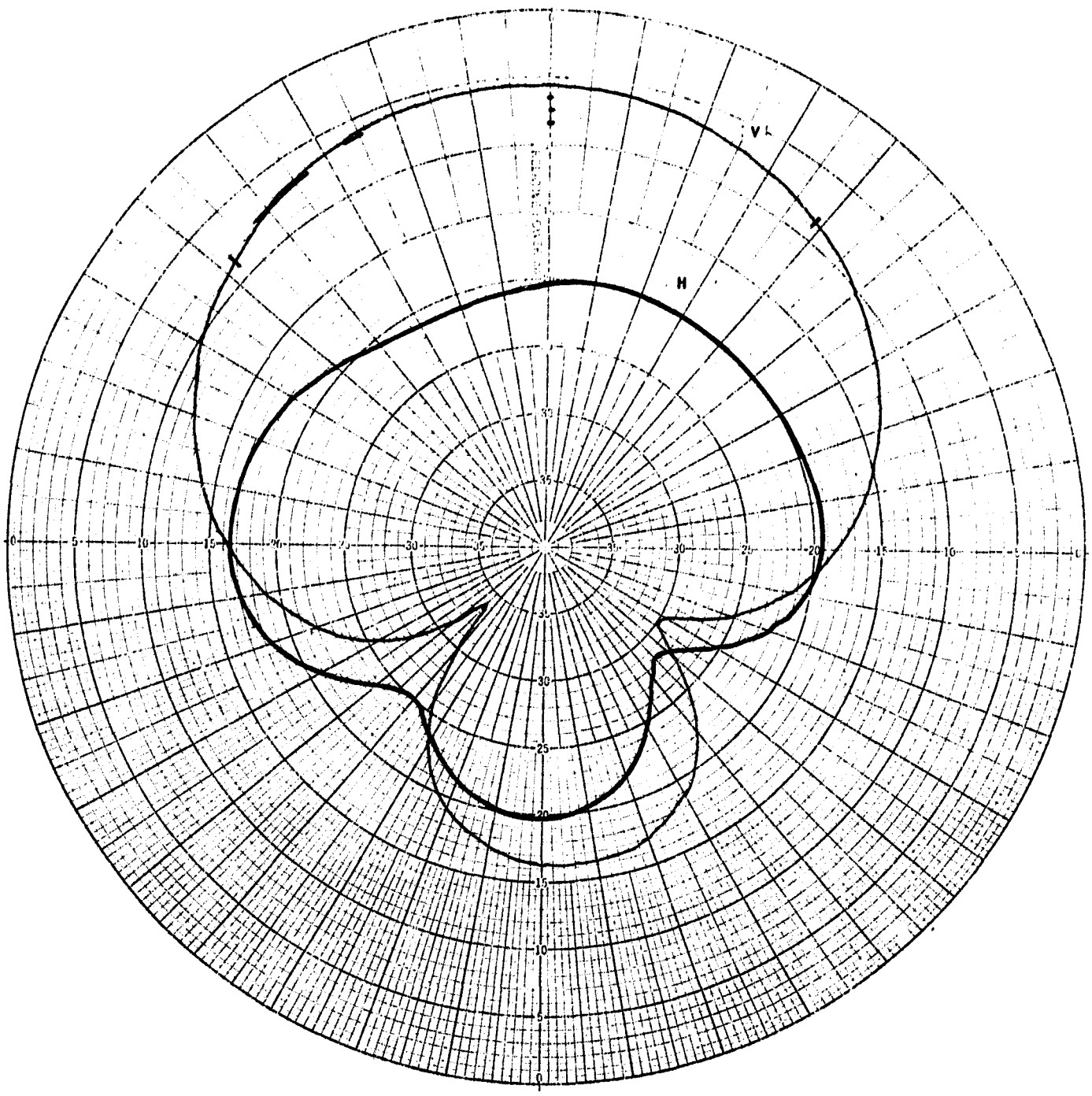

Fig. 10-2

THE JOHNS HOPKINS UNIVERSITY
APPLIED PHYSICS LABORATORY
SILVER SPRING, MARYLAND

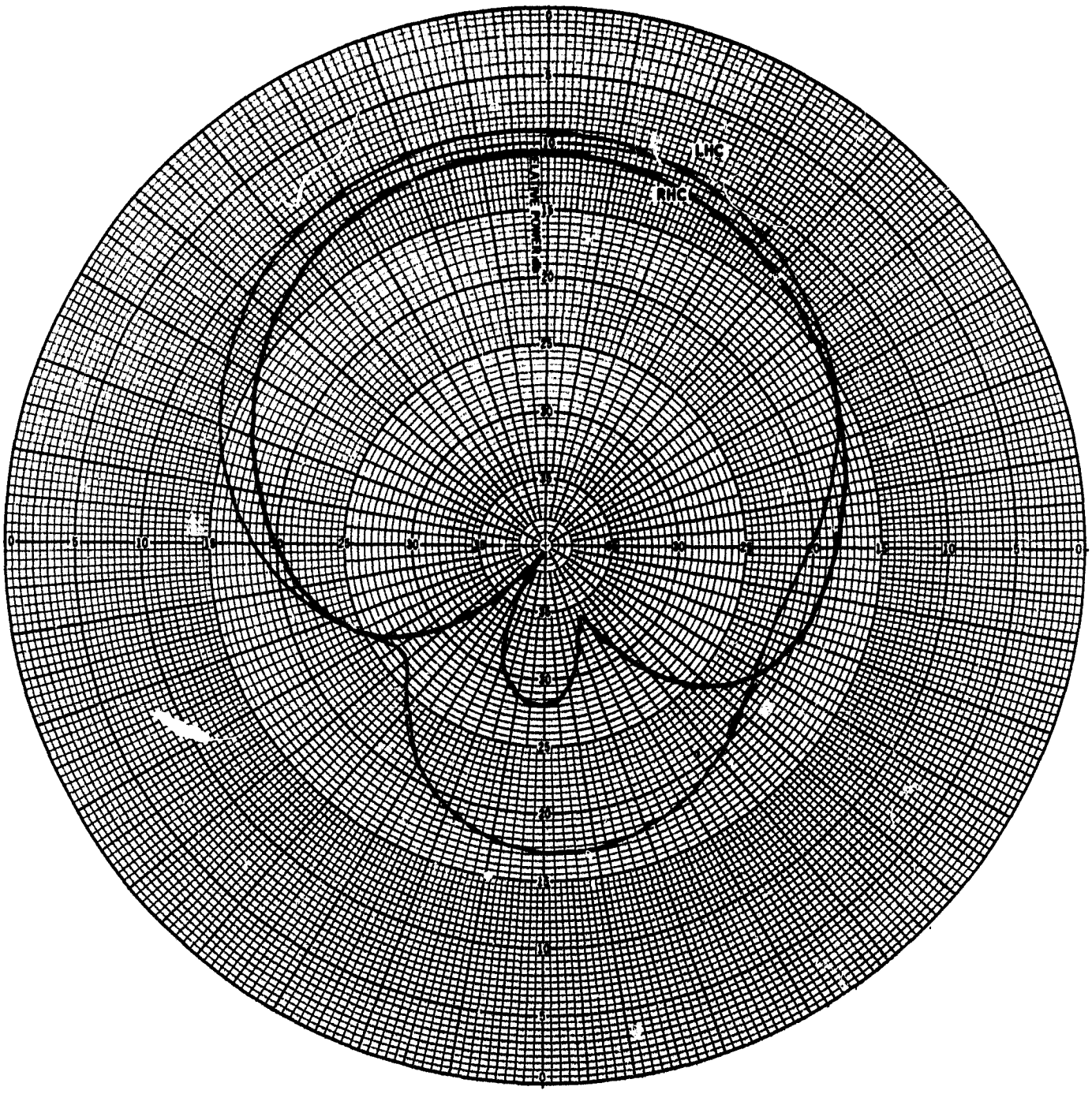

Fig. 10-3

THE JOHNS HOPKINS UNIVERSITY
APPLIED PHYSICS LABORATORY
SILVER SPRING MARYLAND

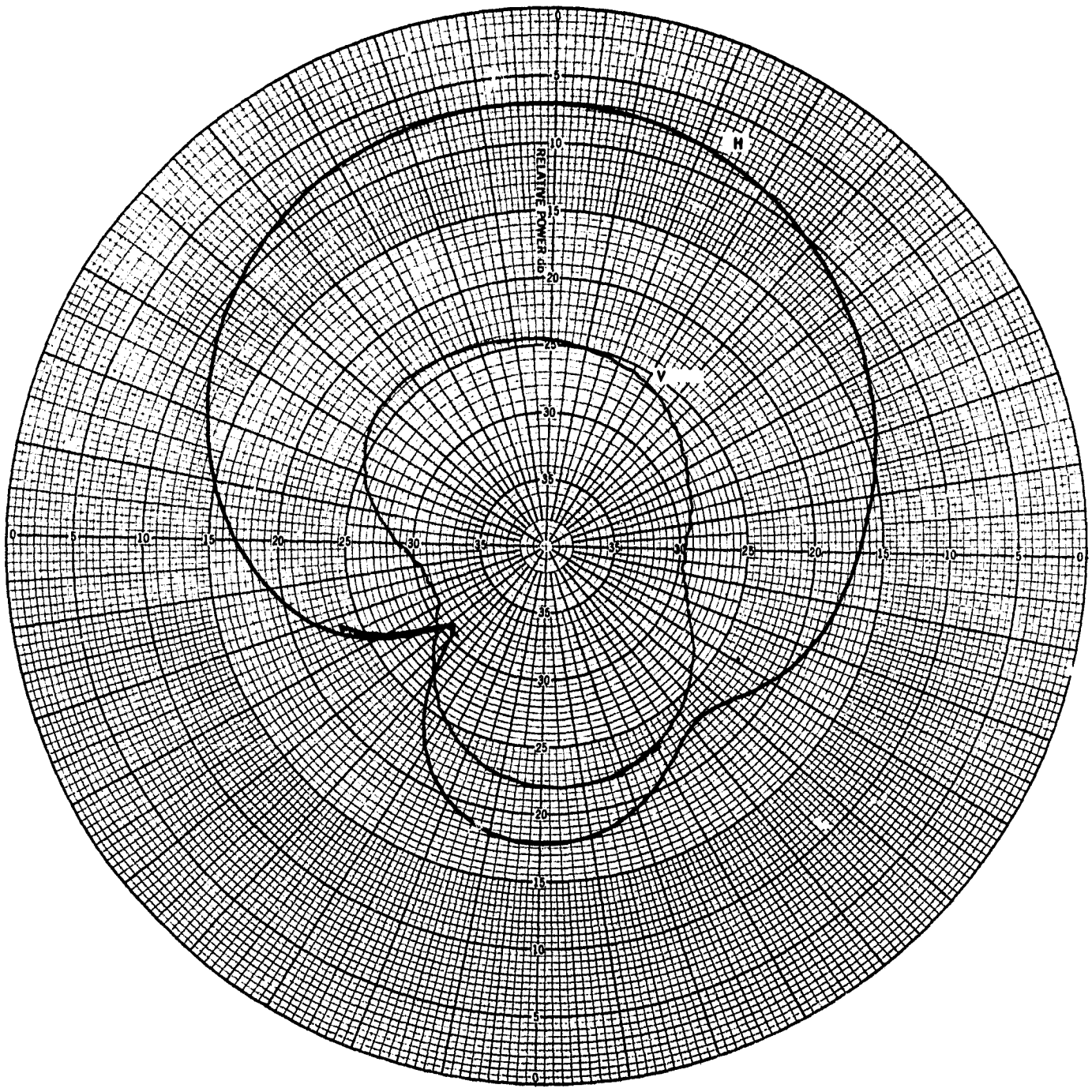

Fig. 10-4

THE JOHNS HOPKINS UNIVERSITY
APPLIED PHYSICS LABORATORY
SILVER SPRING, MARYLAND

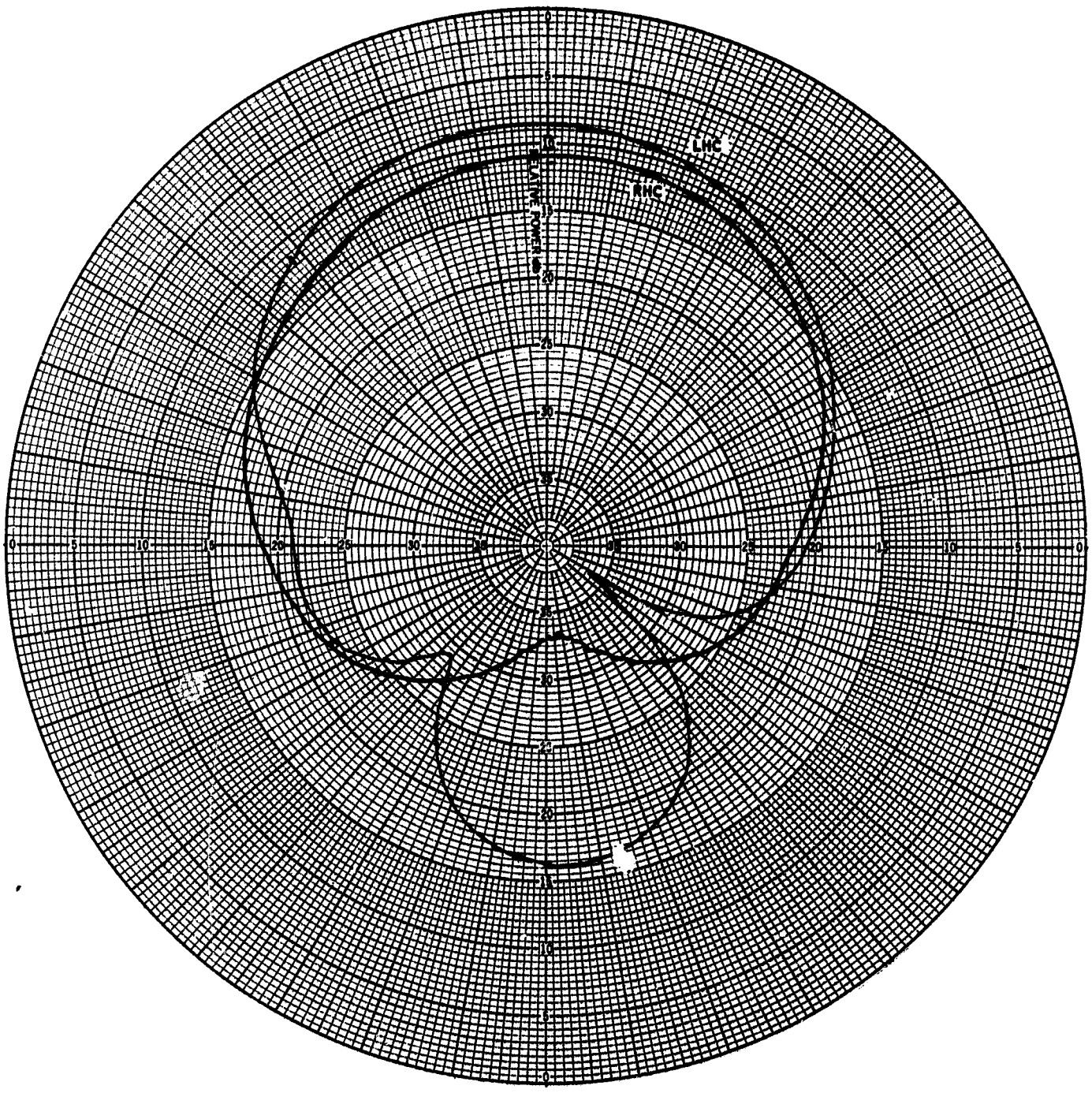

Fig. 10-5

THE JOHNS HOPKINS UNIVERSITY
APPLIED PHYSICS LABORATORY
SILVER SPRING, MARYLAND

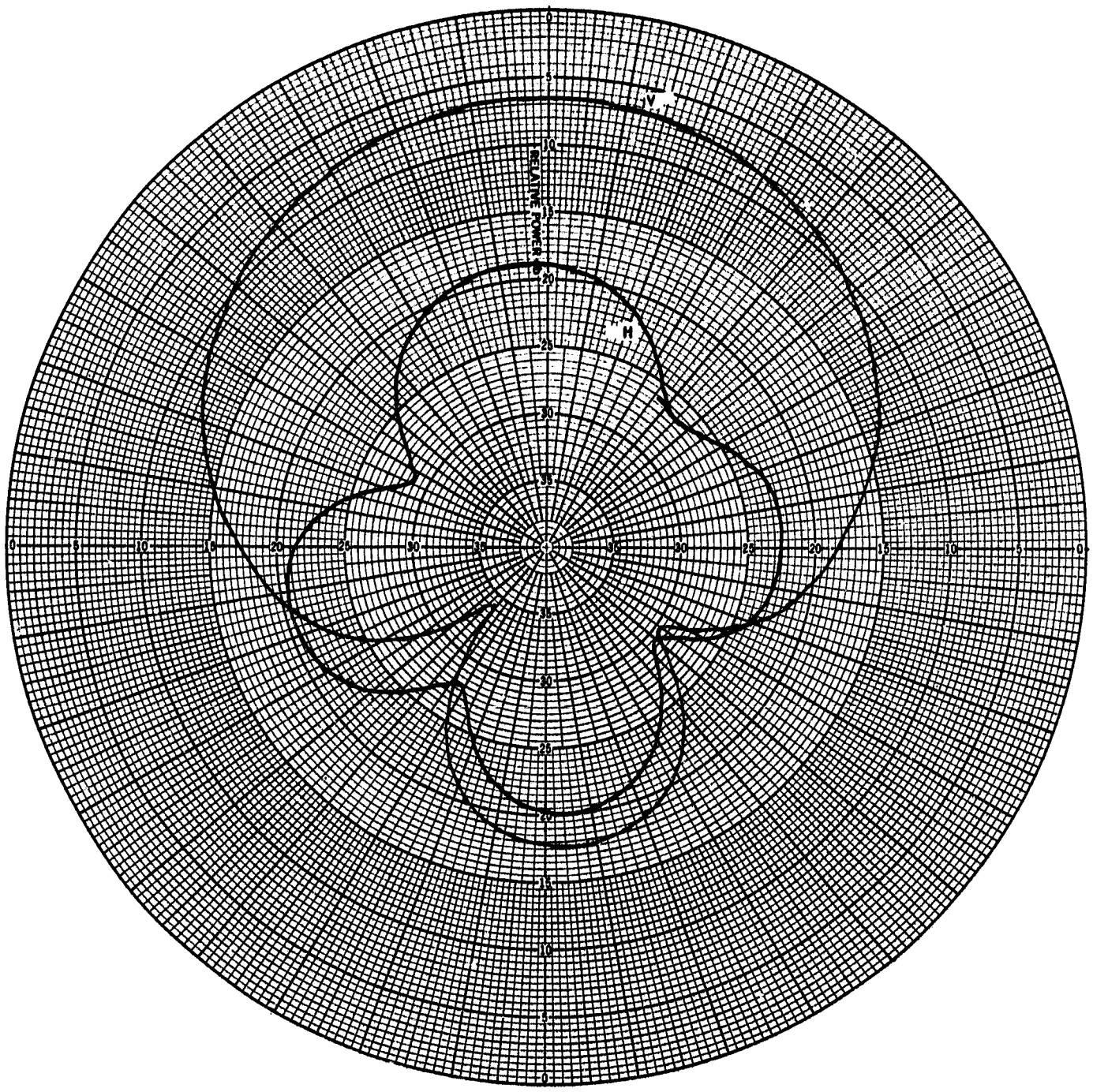

Fig. 10-6

THE JOHNS HOPKINS UNIVERSITY
APPLIED PHYSICS LABORATORY
SILVER SPRING MARYLAND

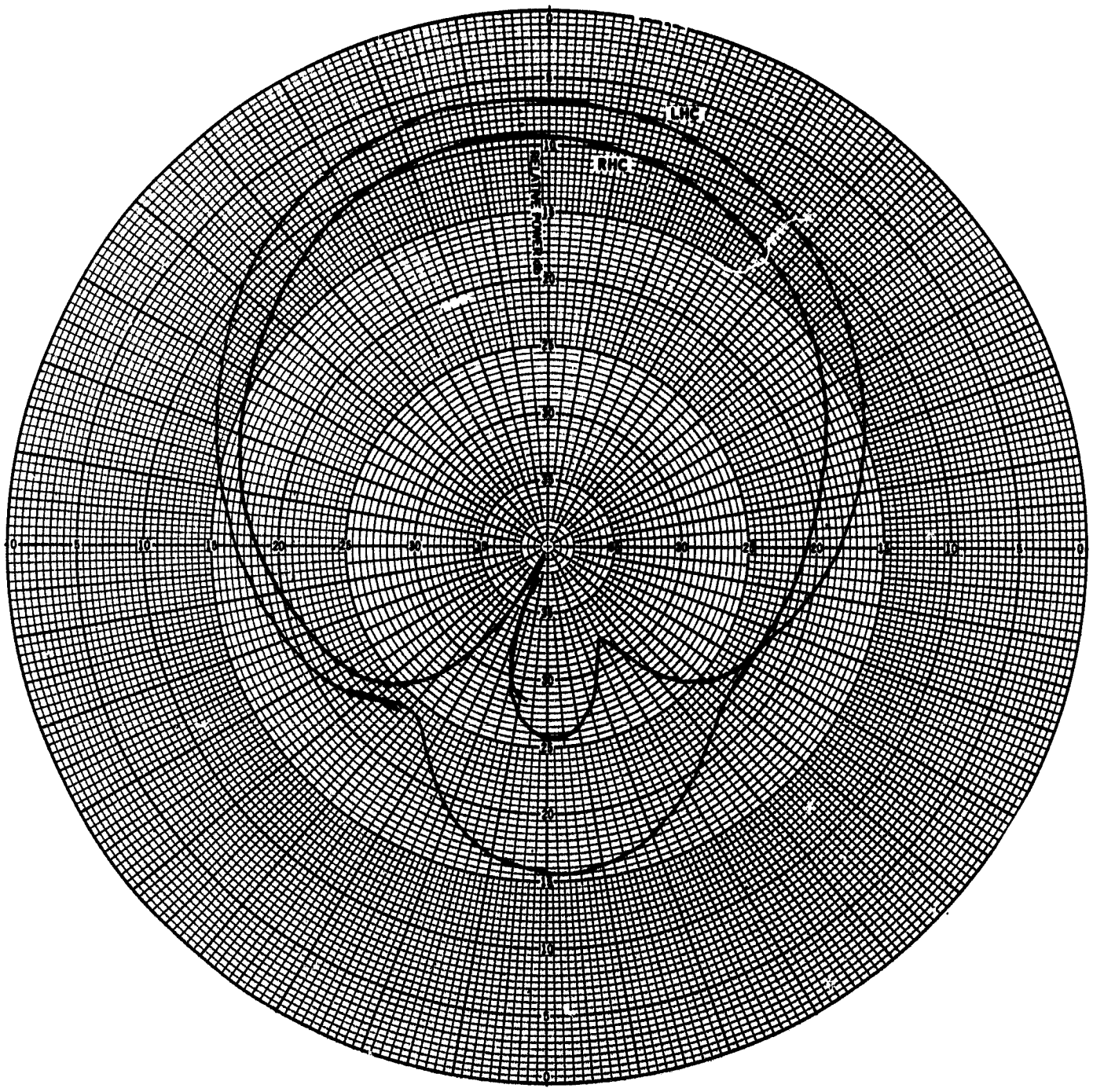

Fig. 10-7

THE JOHNS HOPKINS UNIVERSITY
APPLIED PHYSICS LABORATORY
SILVER SPRING, MARYLAND

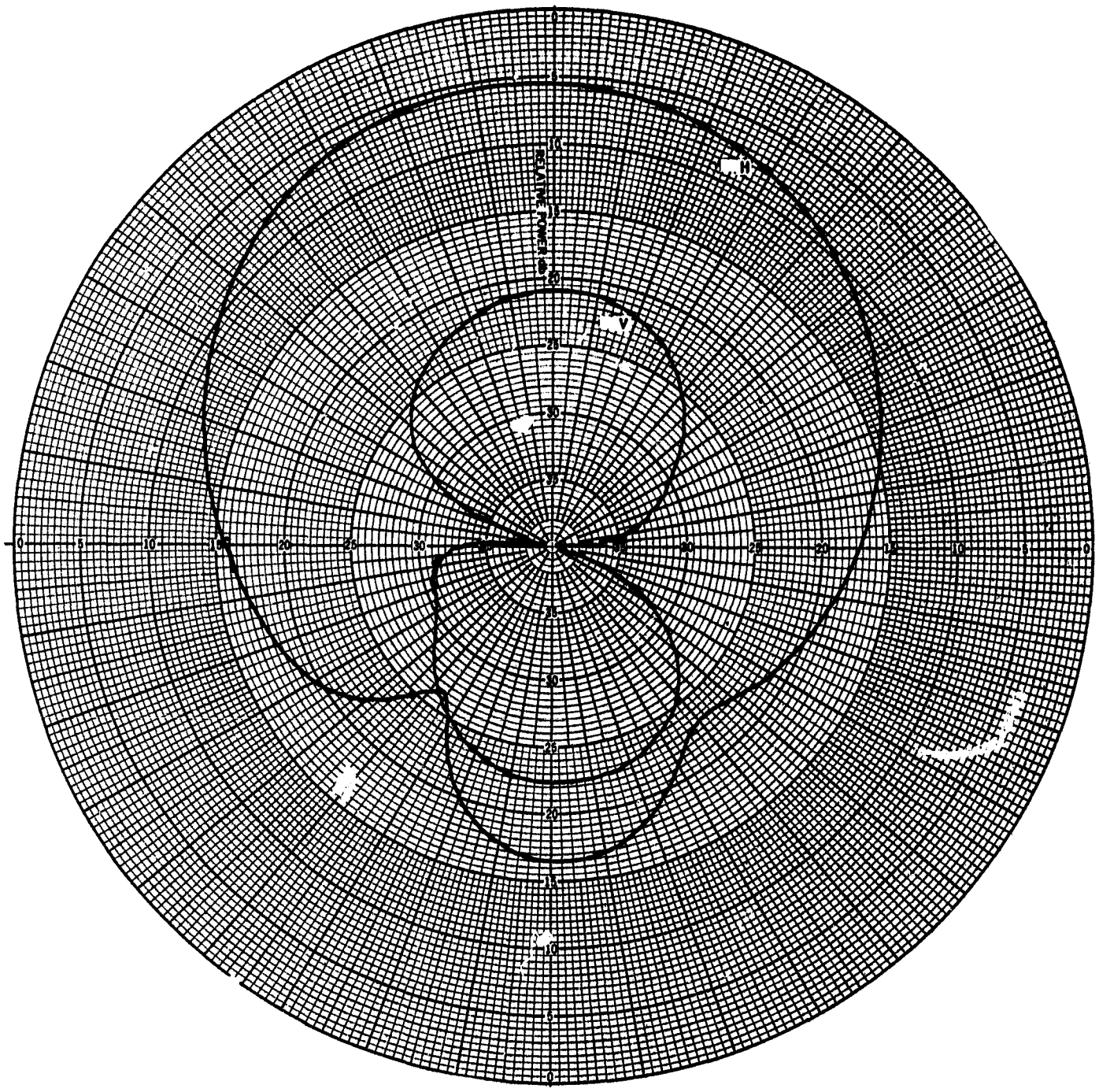

Fig. 10-8

THE JOHNS HOPKINS UNIVERSITY
APPLIED PHYSICS LABORATORY
SILVER SPRING MARYLAND

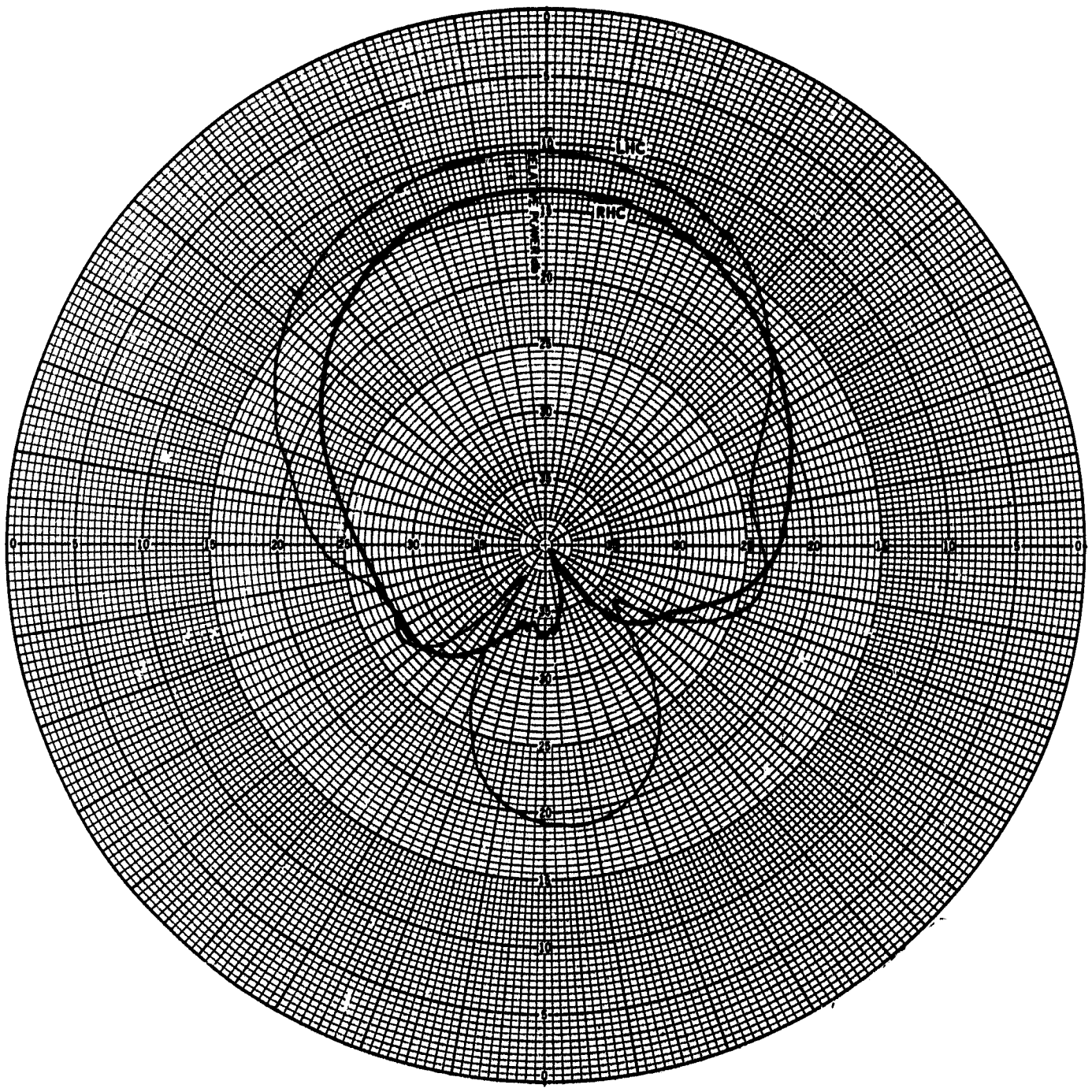

Fig. 10-9

THE JOHNS HOPKINS UNIVERSITY
APPLIED PHYSICS LABORATORY
SILVER SPRING MARYLAND

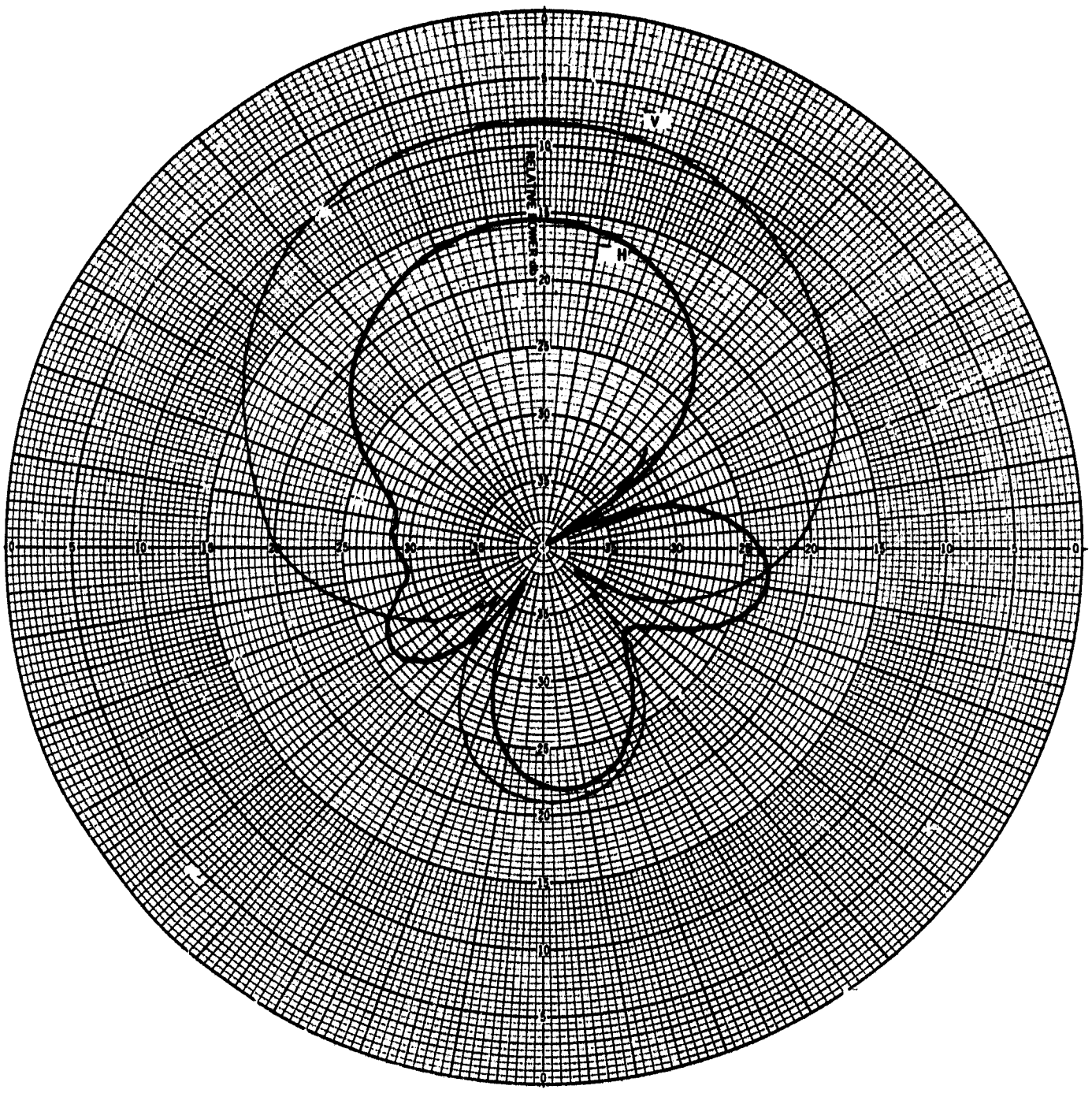

Fig. 10-10

THE JOHNS HOPKINS UNIVERSITY
APPLIED PHYSICS LABORATORY
SILVER SPRING, MARYLAND

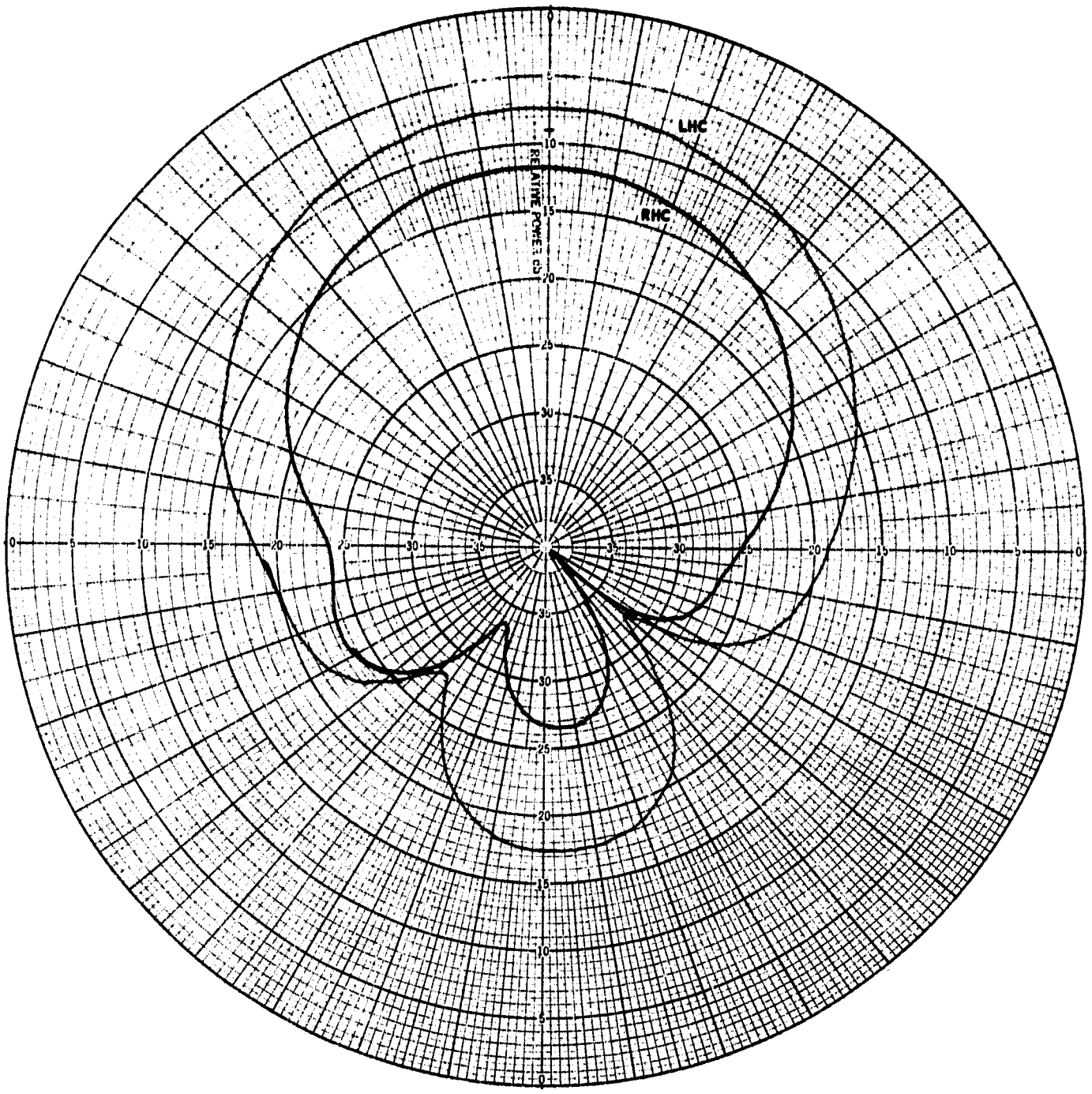

Fig. 10-11

THE JOHNS HOPKINS UNIVERSITY
APPLIED PHYSICS LABORATORY
SILVER SPRING MARYLAND

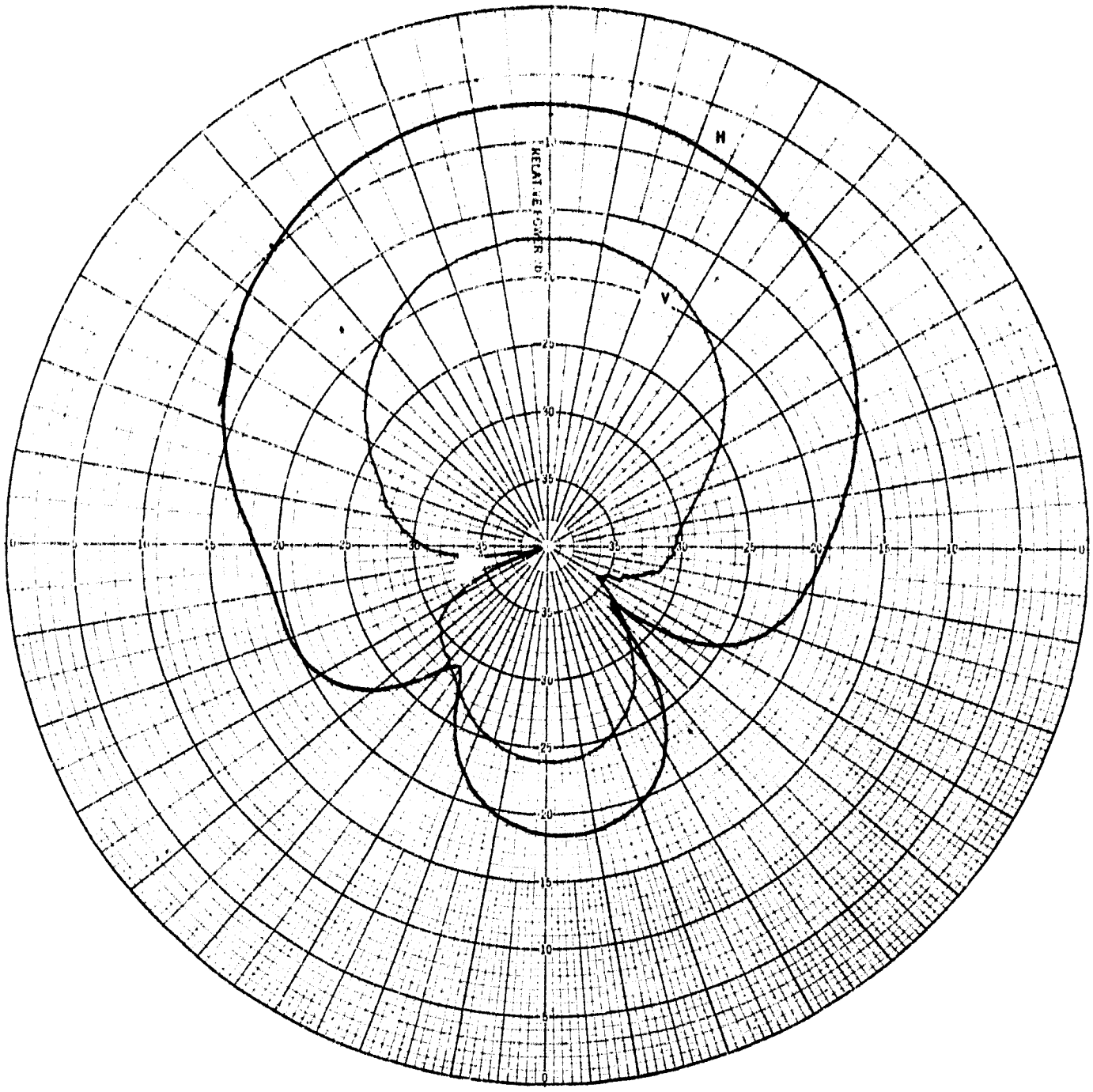

Fig. 10-12

THE JOHNS HOPKINS UNIVERSITY
APPLIED PHYSICS LABORATORY
SILVER SPRING MARYLAND

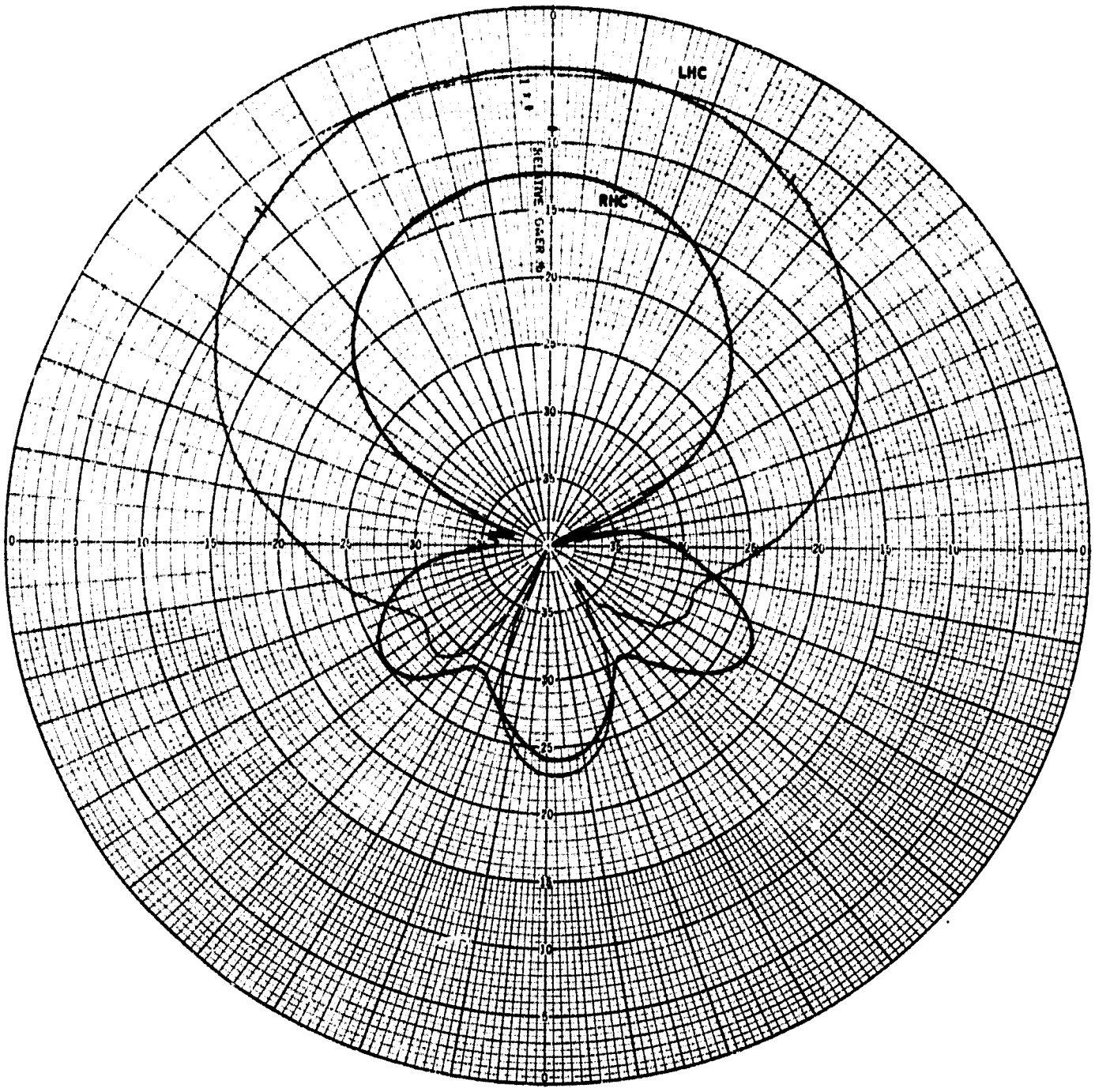

Fig. 10-13

THE JOHNS HOPKINS UNIVERSITY
APPLIED PHYSICS LABORATORY
SILVER SPRING, MARYLAND

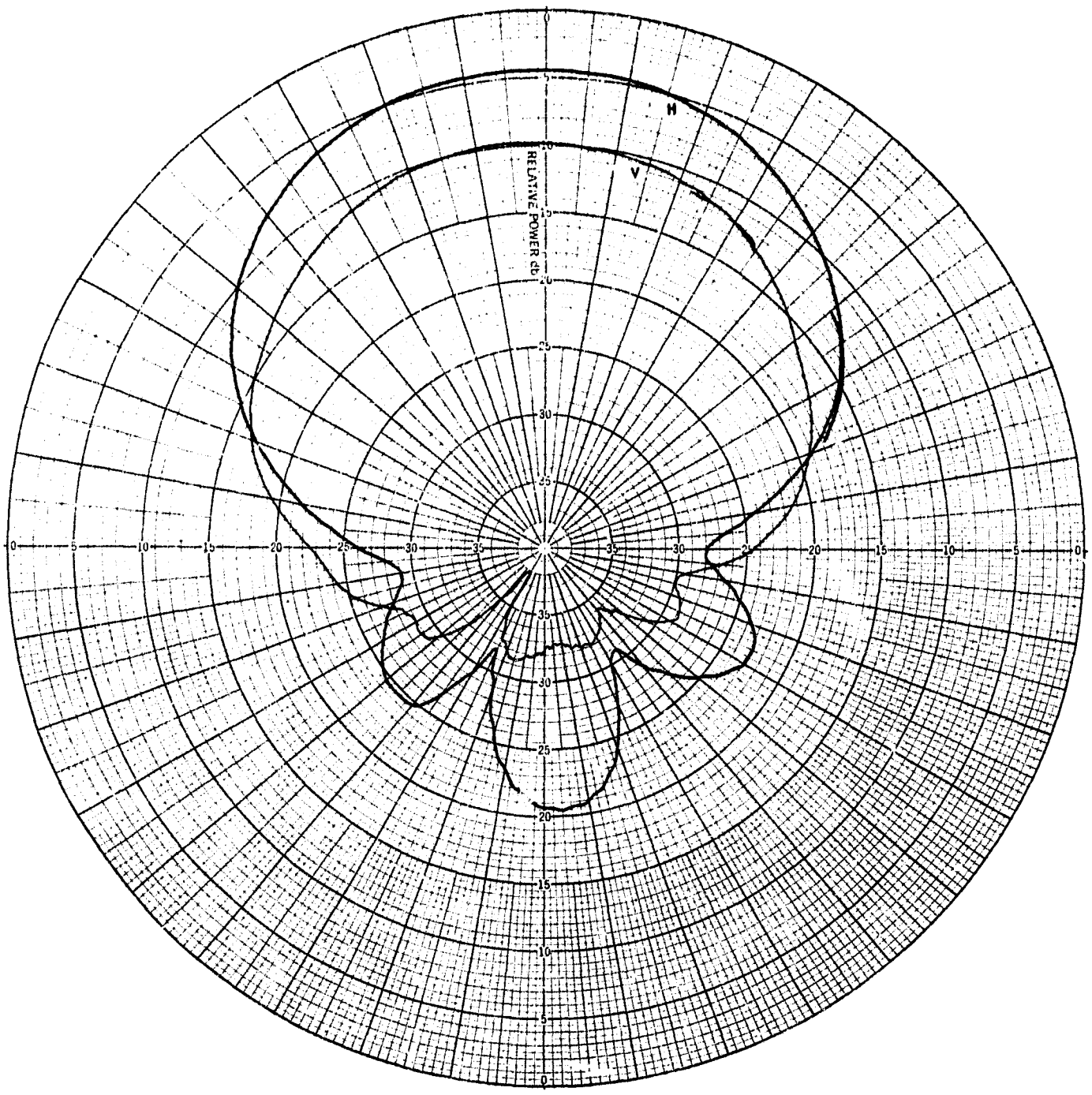

Fig. 10-14

THE JOHNS HOPKINS UNIVERSITY
APPLIED PHYSICS LABORATORY
SILVER SPRING, MARYLAND

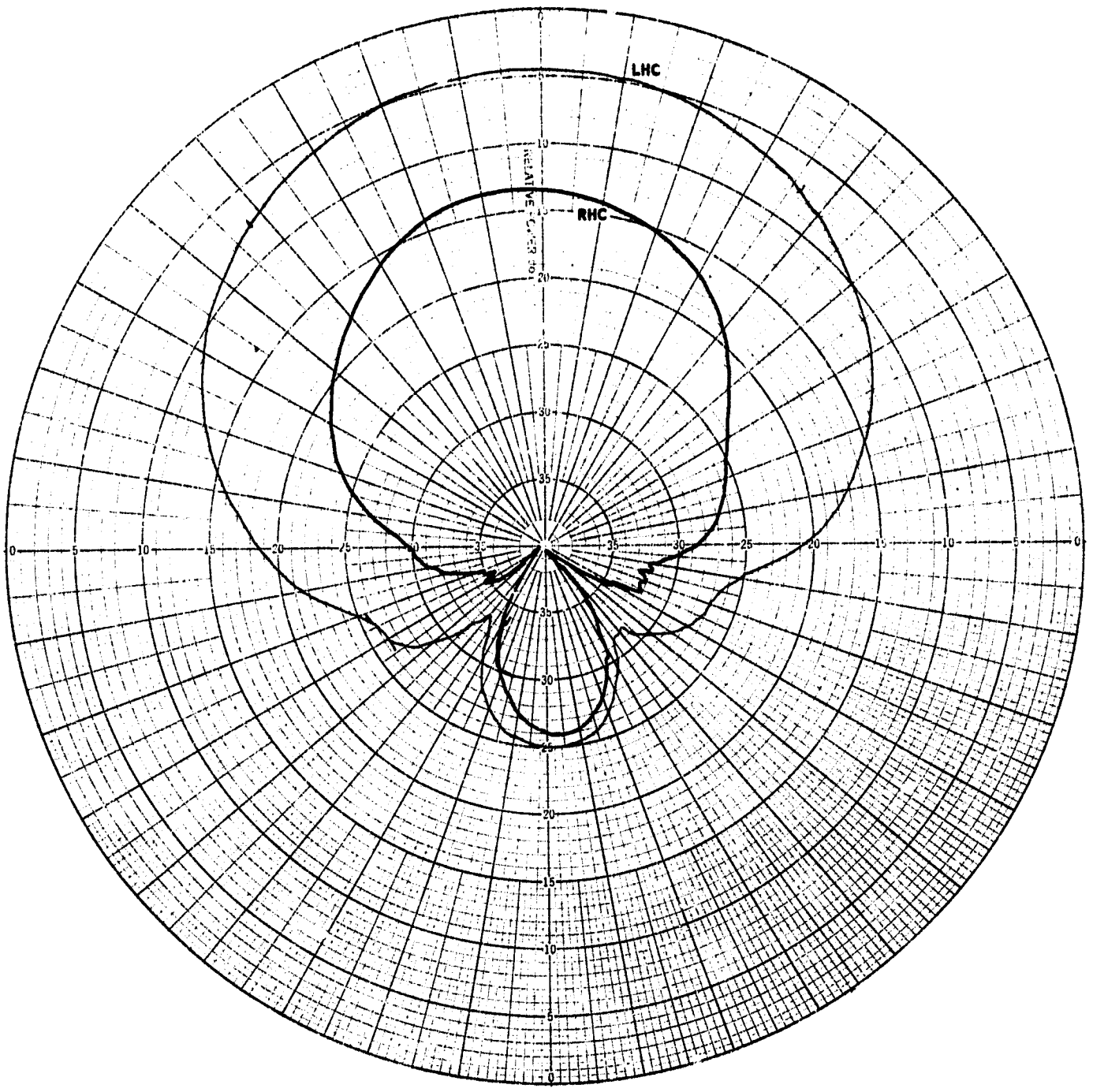

Fig. 10-15

THE JOHNS HOPKINS UNIVERSITY
APPLIED PHYSICS LABORATORY
SILVER SPRING MARYLAND

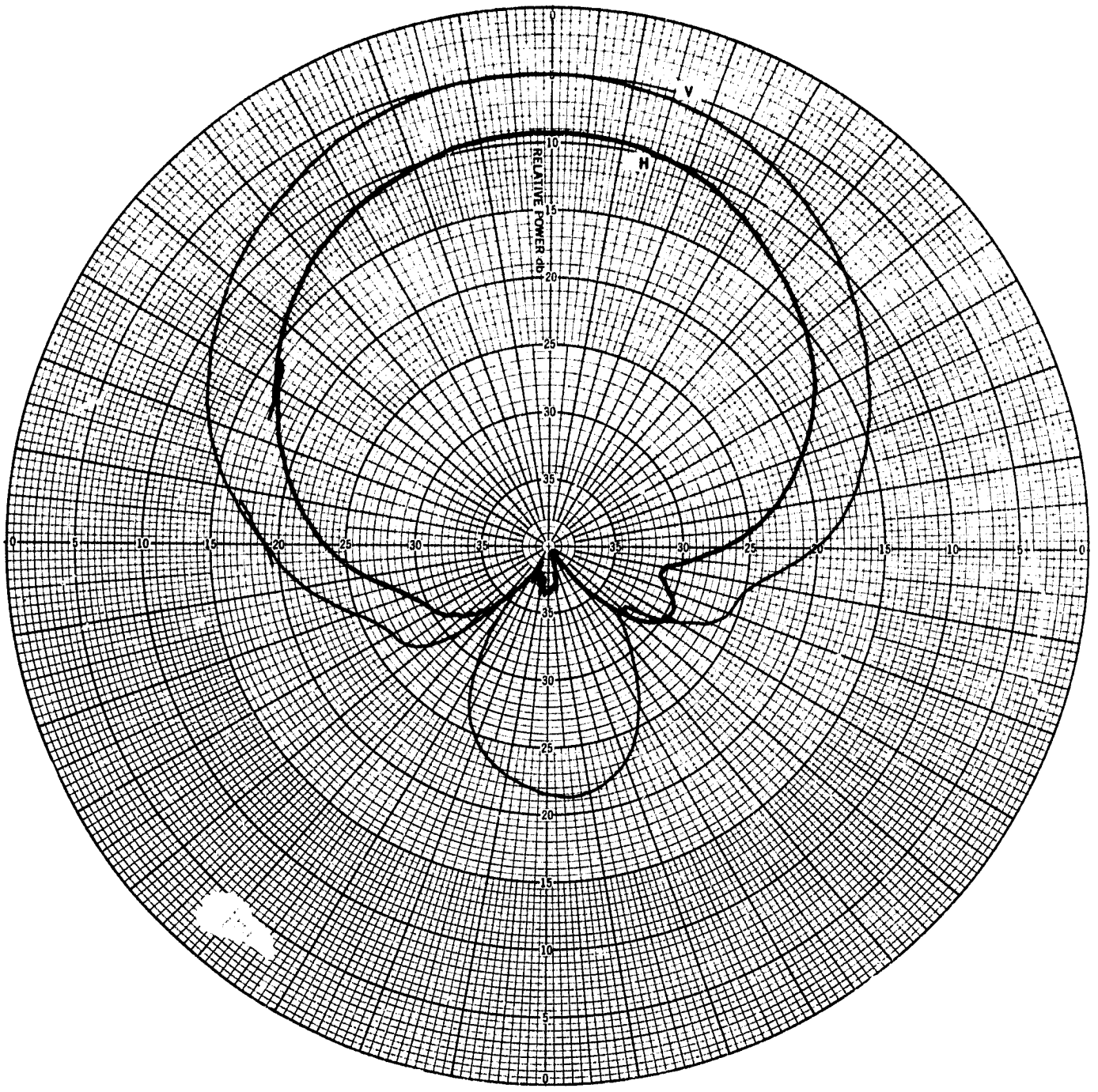

Fig. 10-16

THE JOHNS HOPKINS UNIVERSITY
APPLIED PHYSICS LABORATORY
SILVER SPRING MARYLAND

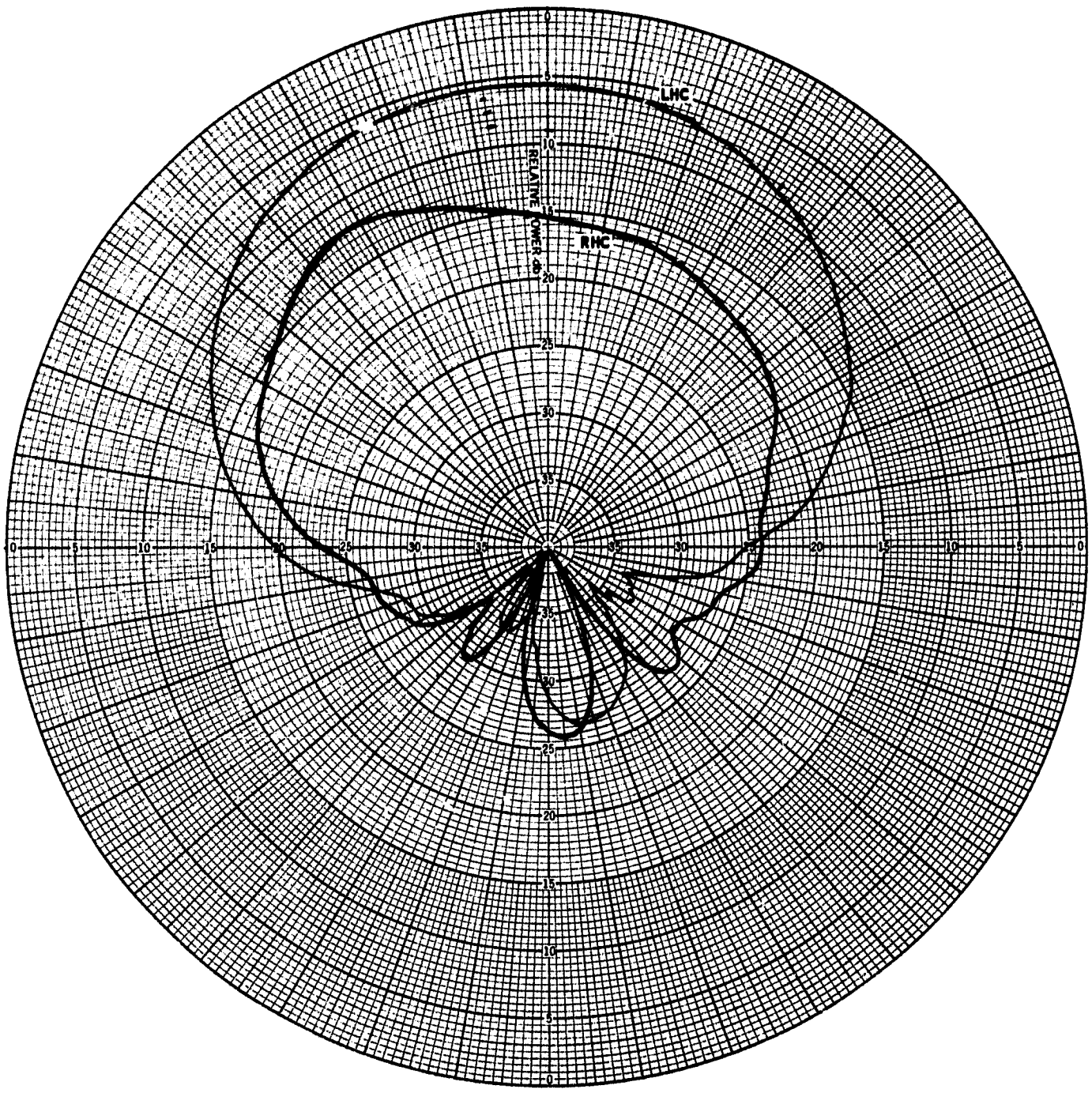

Fig. 10-17

THE JOHNS HOPKINS UNIVERSITY
APPLIED PHYSICS LABORATORY
SILVER SPRING MARYLAND

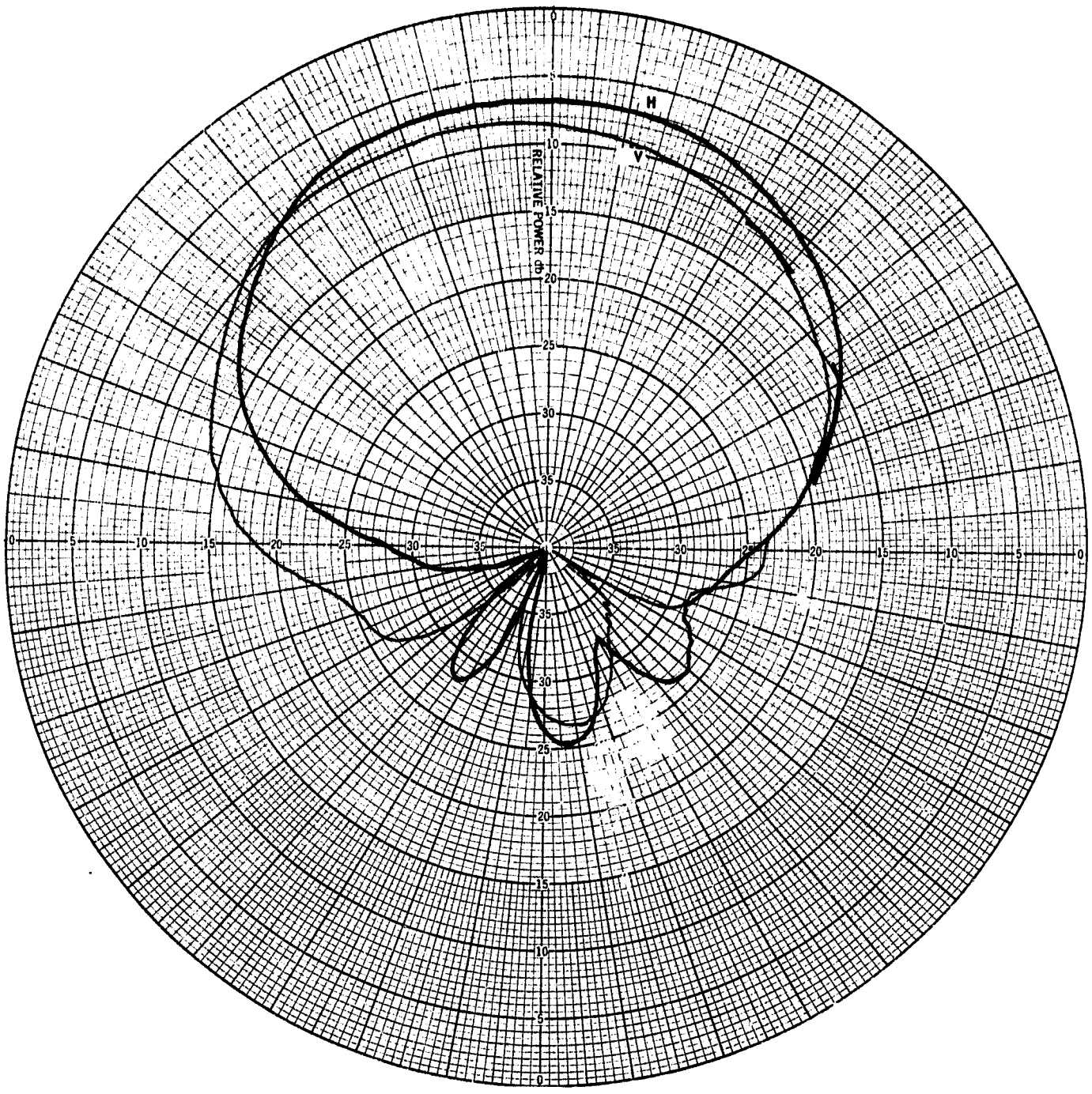

Fig. 10-18

THE JOHNS HOPKINS UNIVERSITY
APPLIED PHYSICS LABORATORY
SILVER SPRING MARYLAND

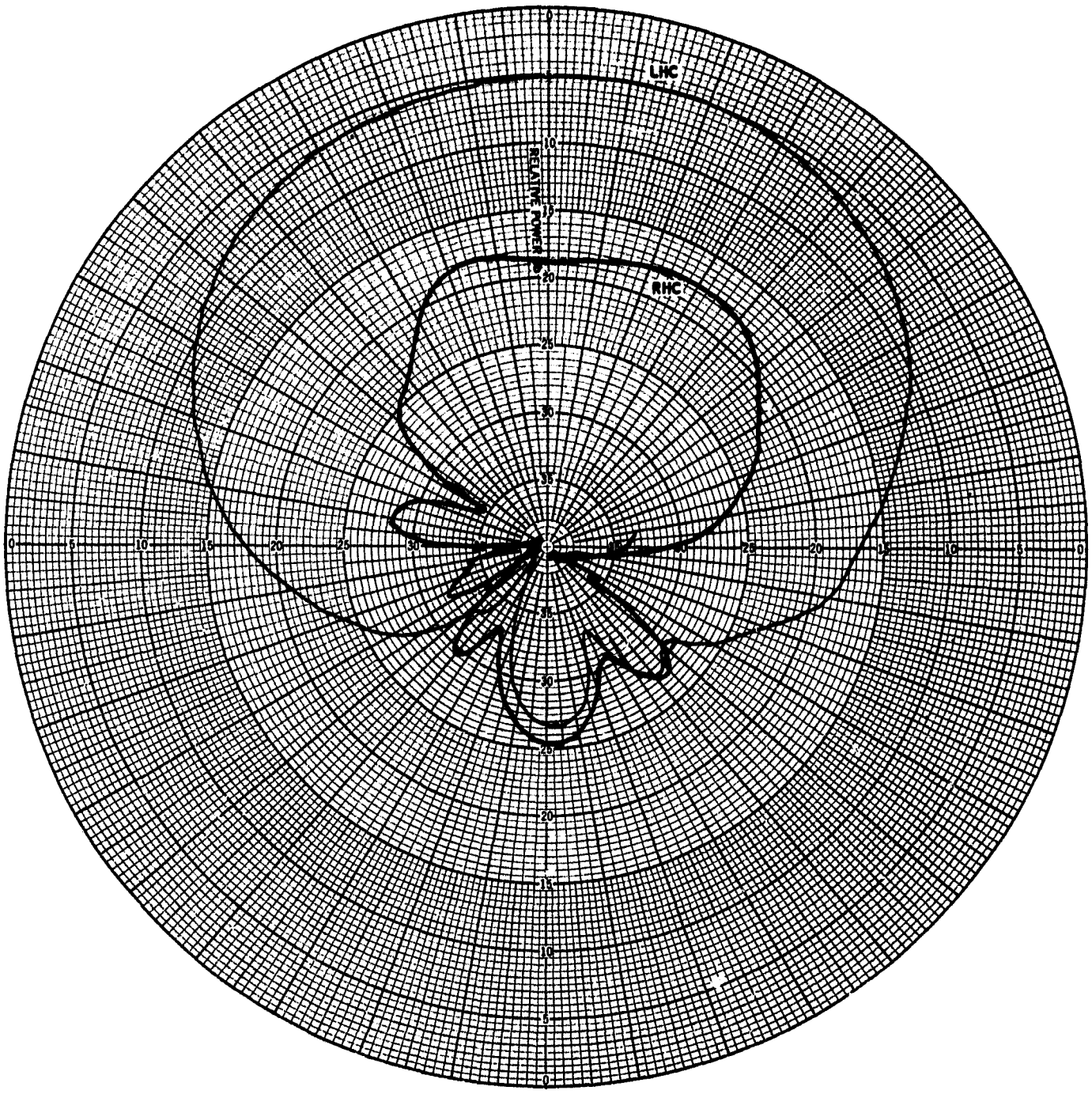

Fig. 10-19

THE JOHNS HOPKINS UNIVERSITY
APPLIED PHYSICS LABORATORY
SILVER SPRING MARYLAND

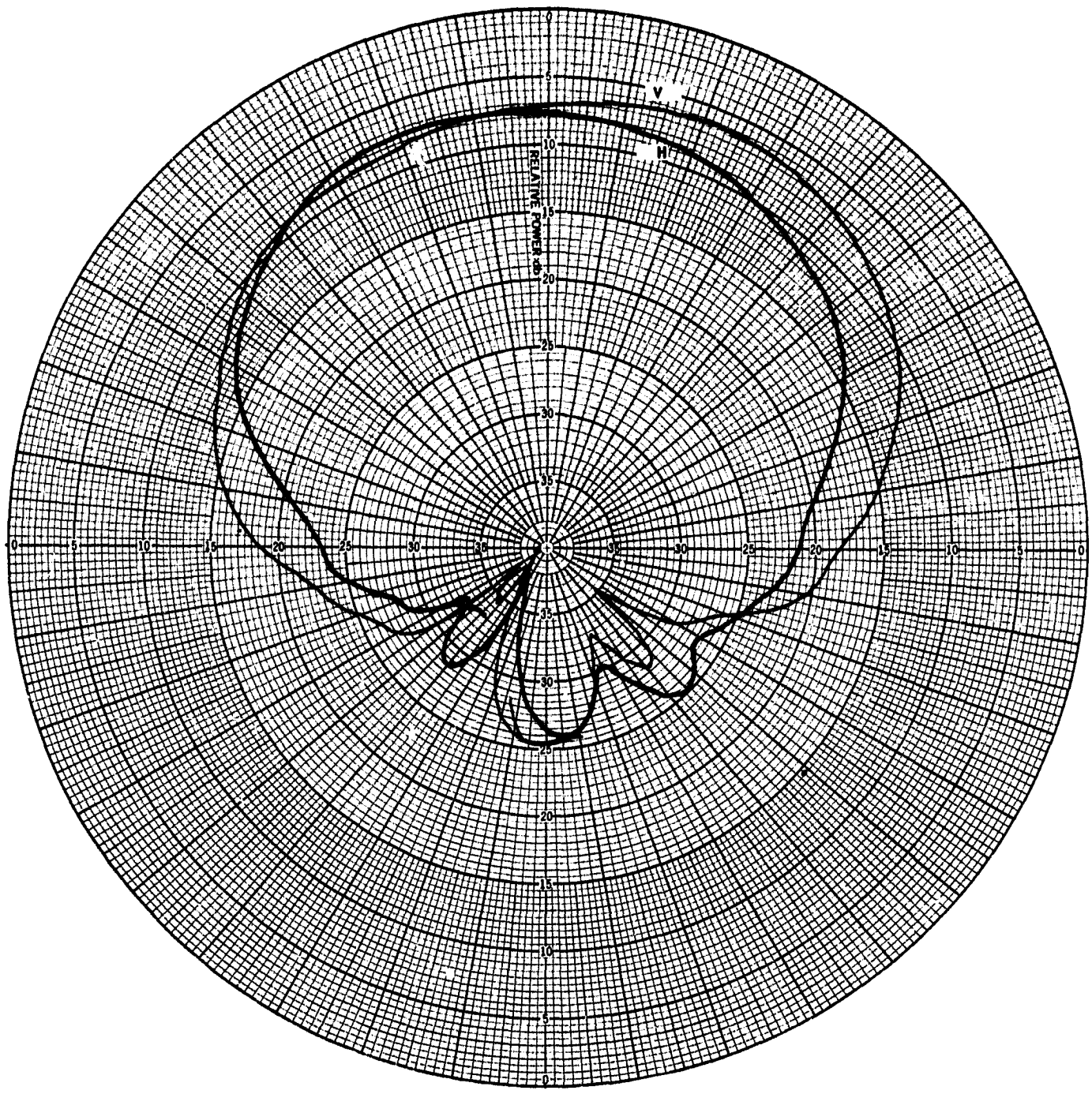

Fig. 10-20

THE JOHNS HOPKINS UNIVERSITY
APPLIED PHYSICS LABORATORY
SILVER SPRING MARYLAND

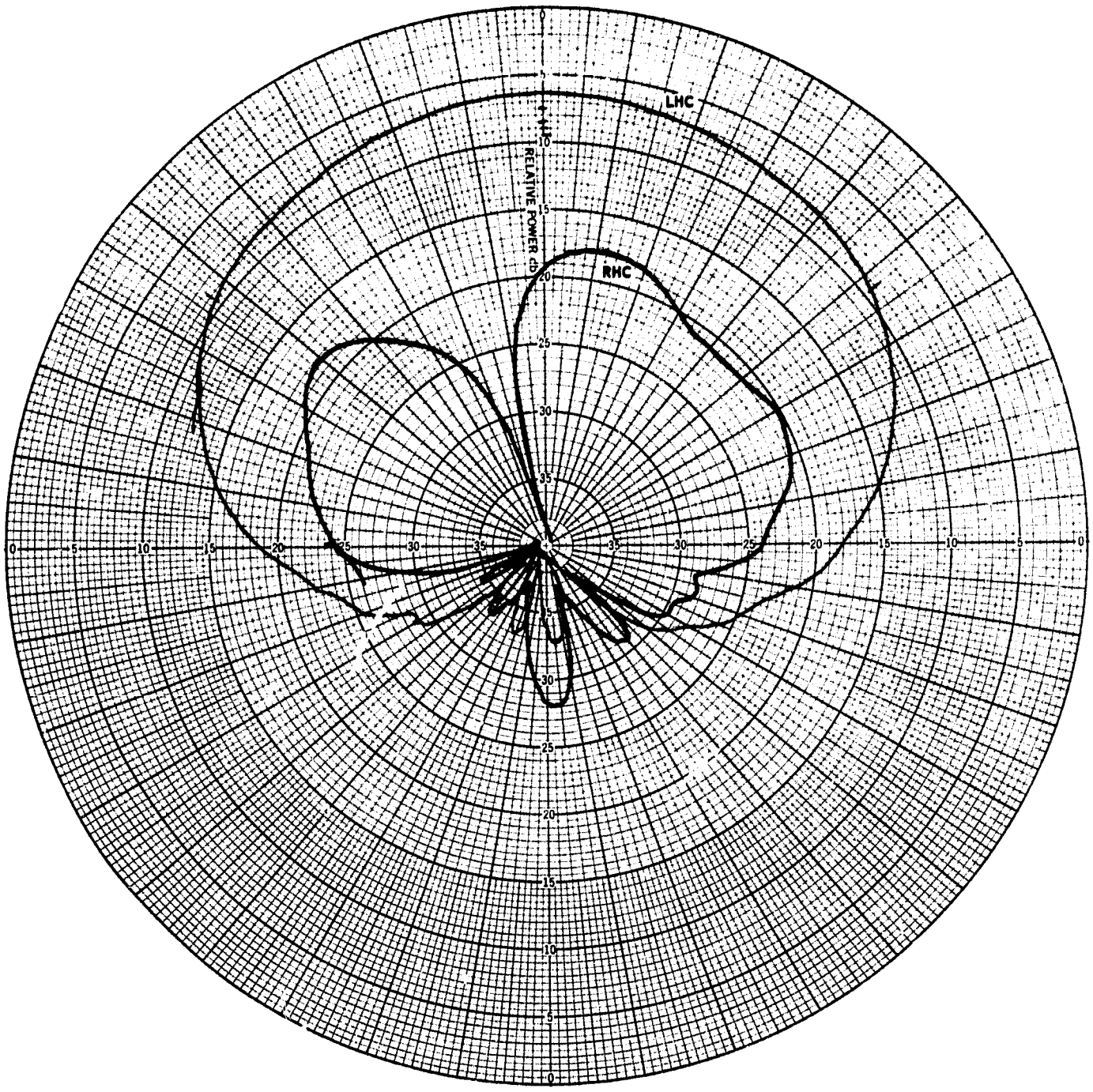

Fig. 10-21

THE JOHNS HOPKINS UNIVERSITY
APPLIED PHYSICS LABORATORY
SILVER SPRING, MARYLAND

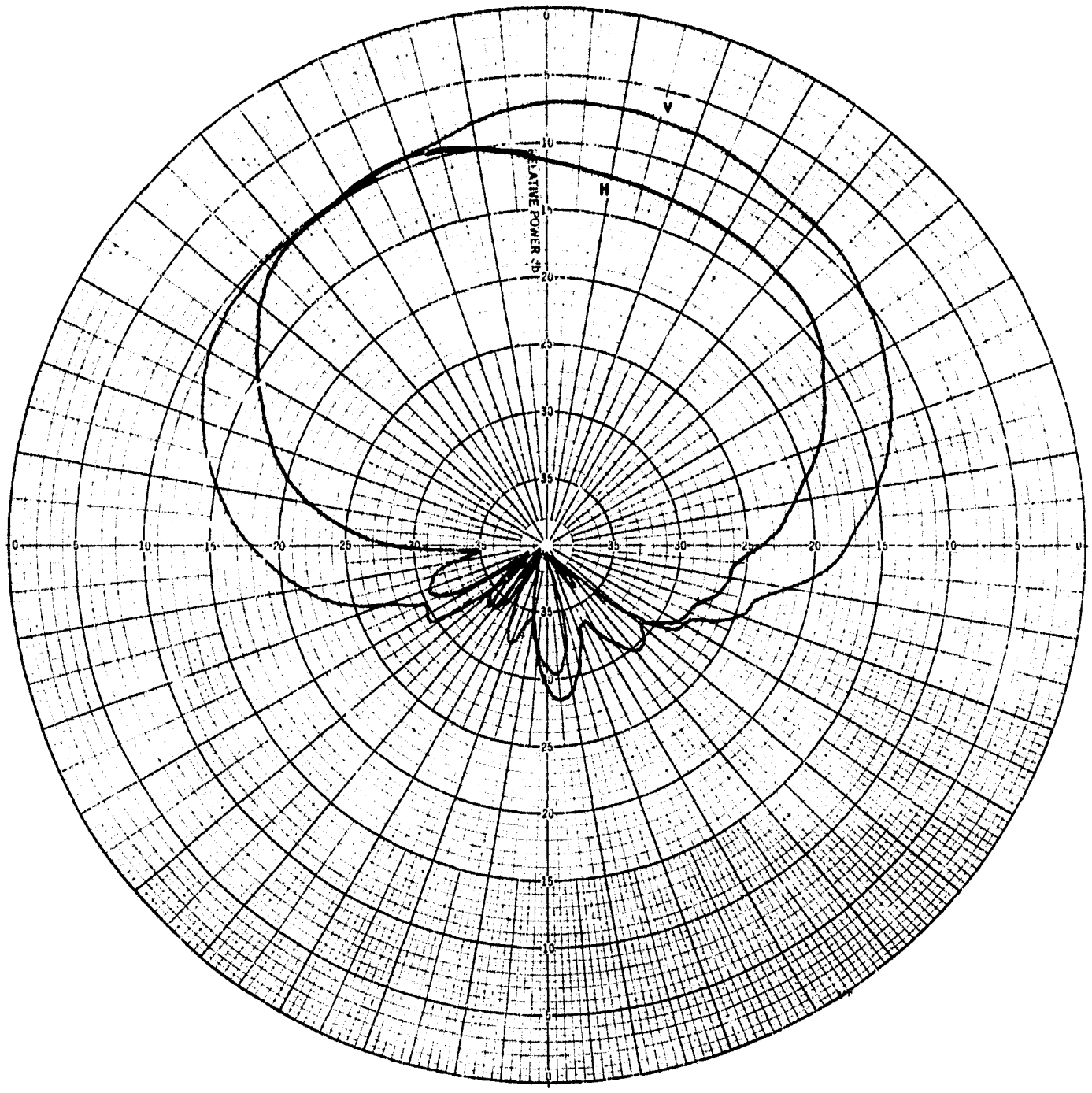

Fig. 10-22

THE JOHNS HOPKINS UNIVERSITY
APPLIED PHYSICS LABORATORY
SILVER SPRING MARYLAND

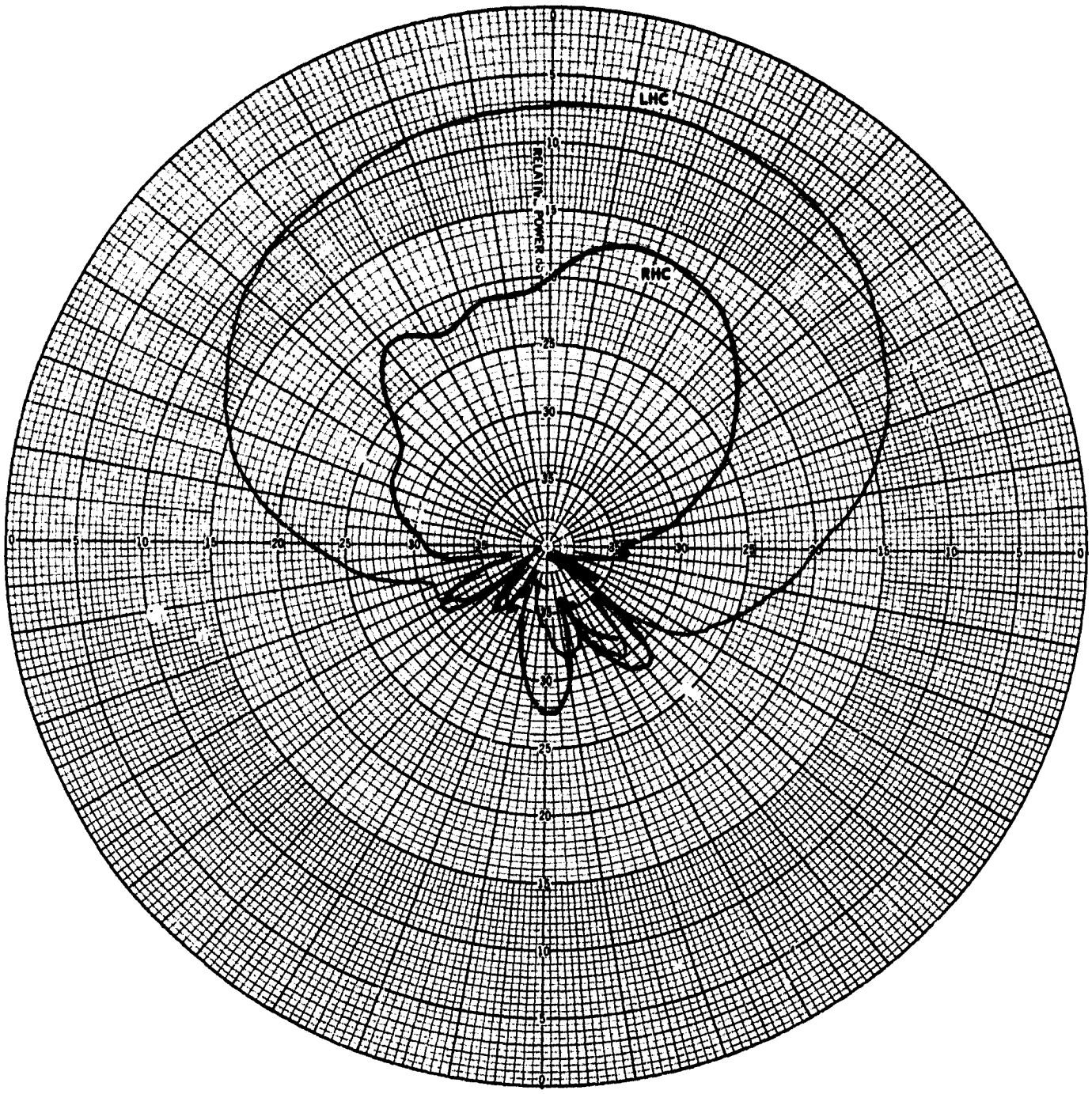

Fig. 10-23

THE JOHNS HOPKINS UNIVERSITY
APPLIED PHYSICS LABORATORY
SILVER SPRING MARYLAND

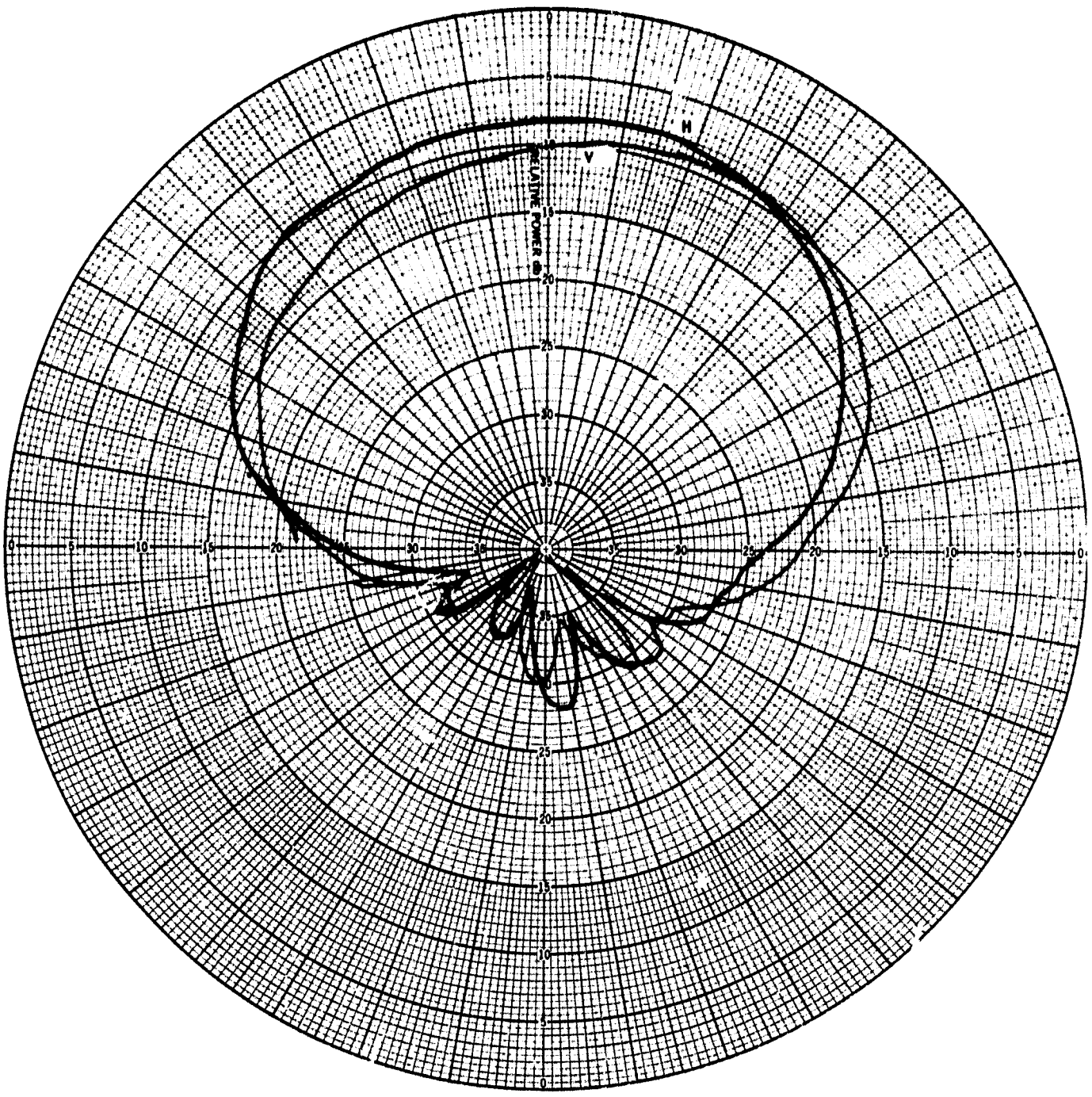

Fig. 10-24

THE JOHNS HOPKINS UNIVERSITY
APPLIED PHYSICS LABORATORY
SILVER SPRING MARYLAND

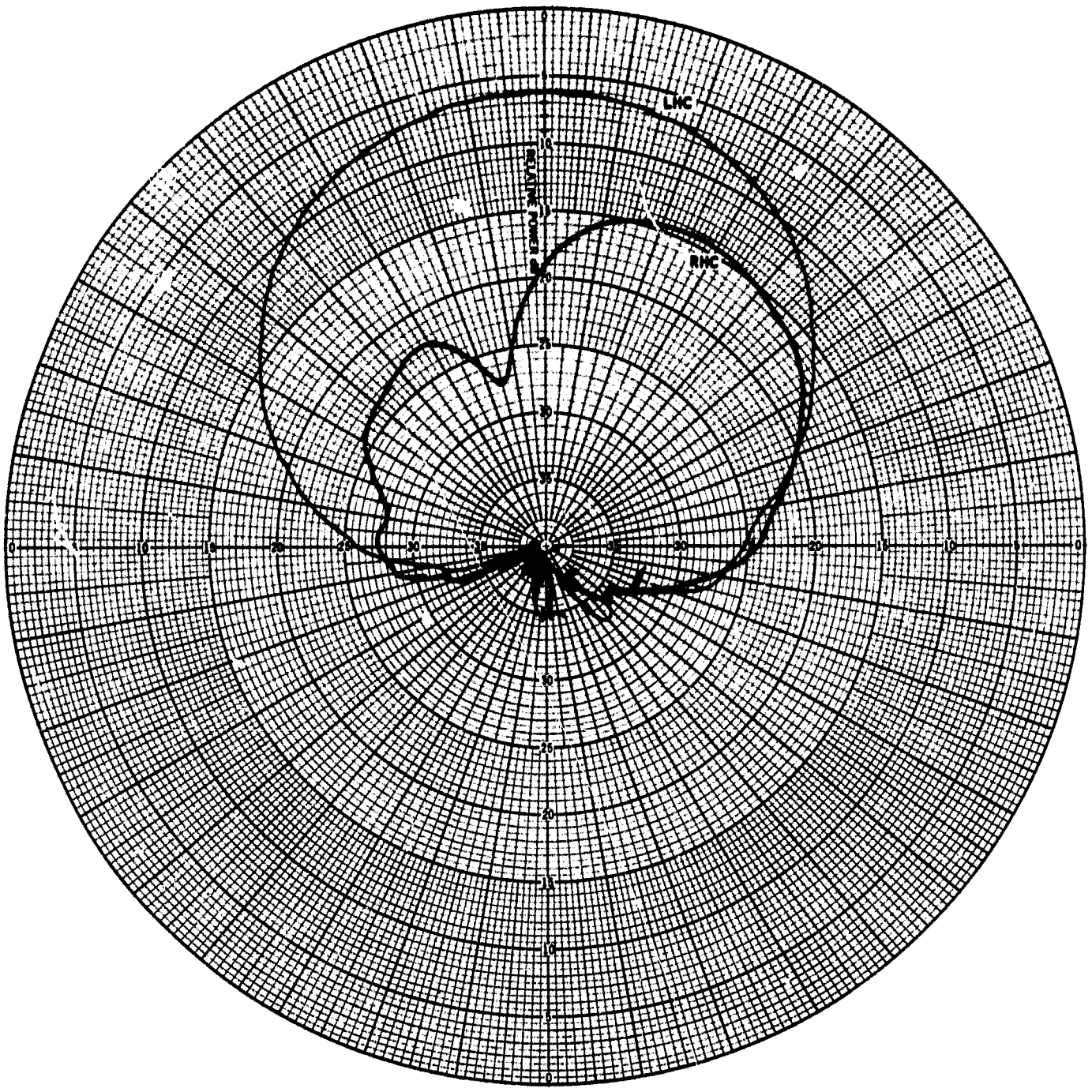

Fig. 10-25

THE JOHNS HOPKINS UNIVERSITY
APPLIED PHYSICS LABORATORY
SILVER SPRING MARYLAND

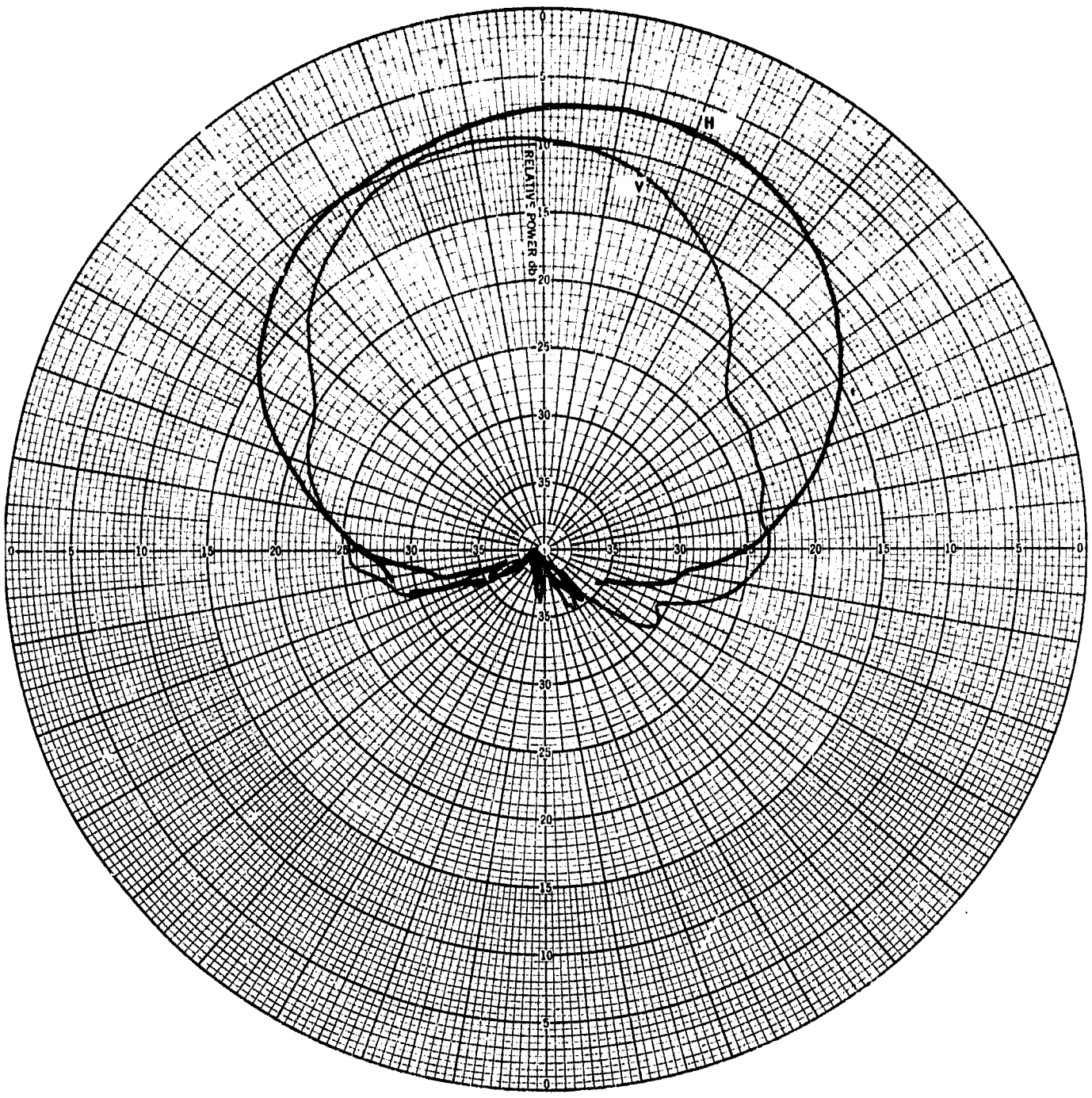

Fig. 10-26

THE JOHNS HOPKINS UNIVERSITY
APPLIED PHYSICS LABORATORY
SILVER SPRING, MARYLAND

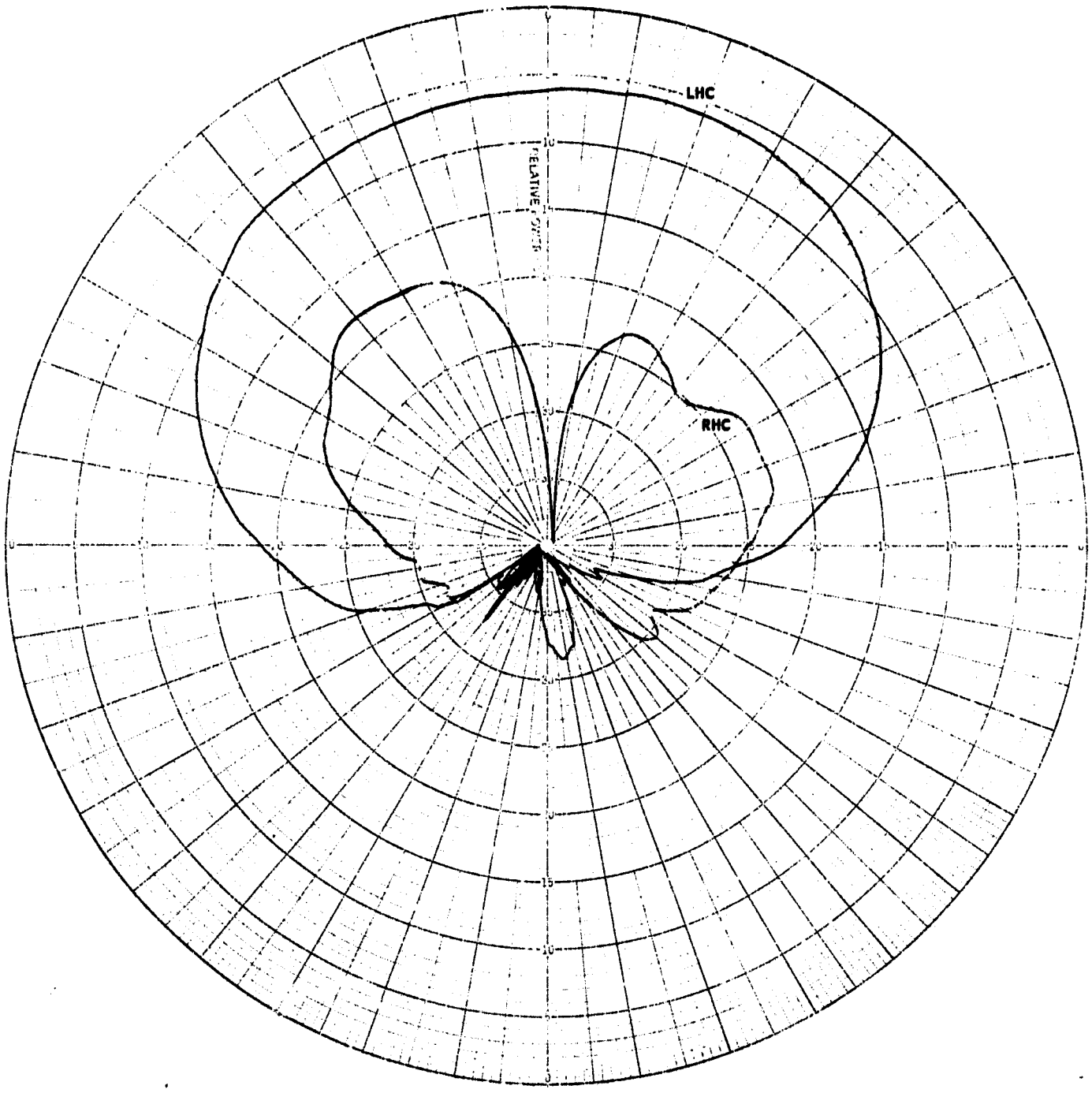

Fig. 10-27

THE JOHNS HOPKINS UNIVERSITY
APPLIED PHYSICS LABORATORY
SILVER SPRING, MARYLAND

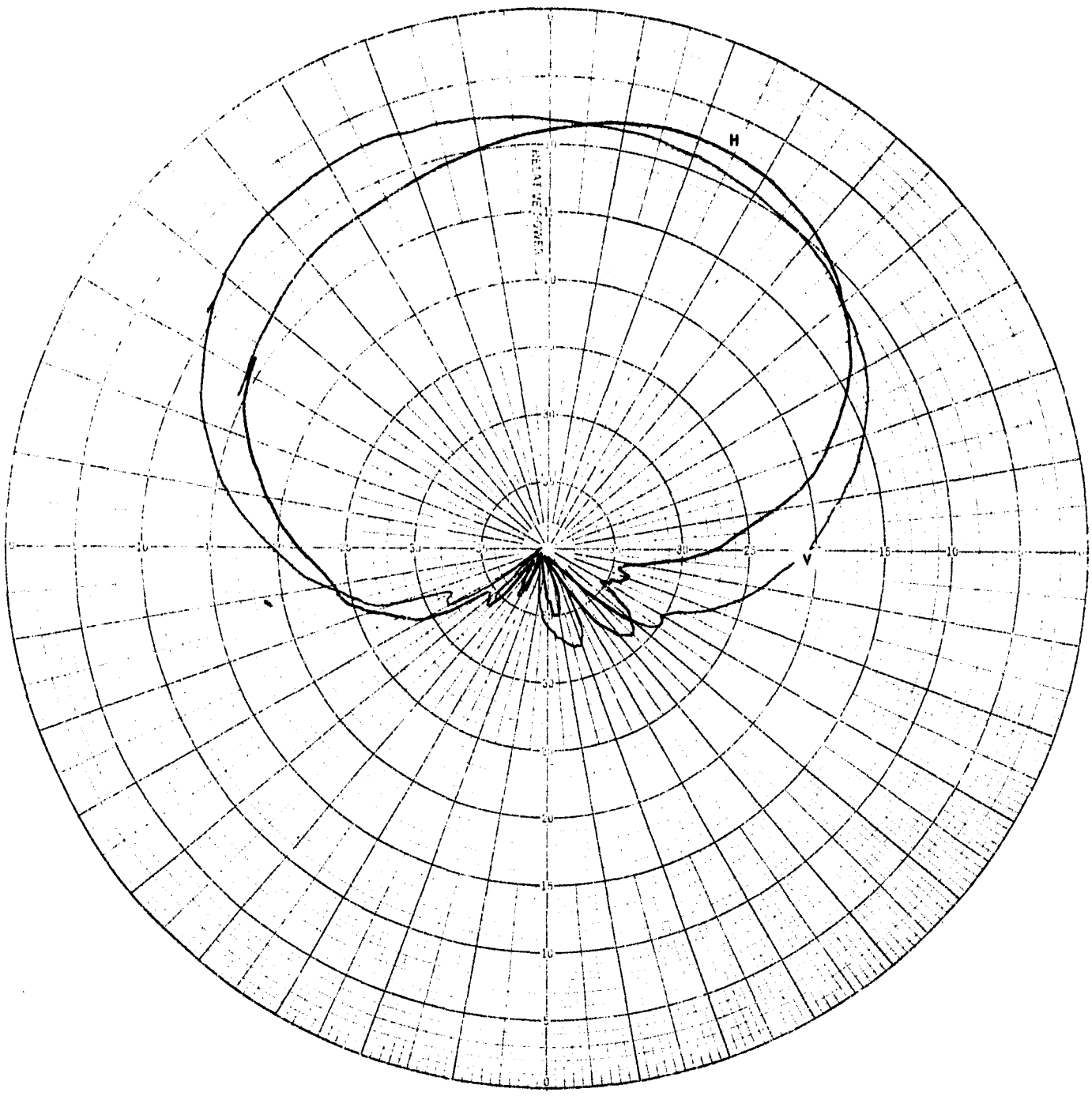

Fig. 10-28

THE JOHNS HOPKINS UNIVERSITY
APPLIED PHYSICS LABORATORY
SILVER SPRING, MARYLAND

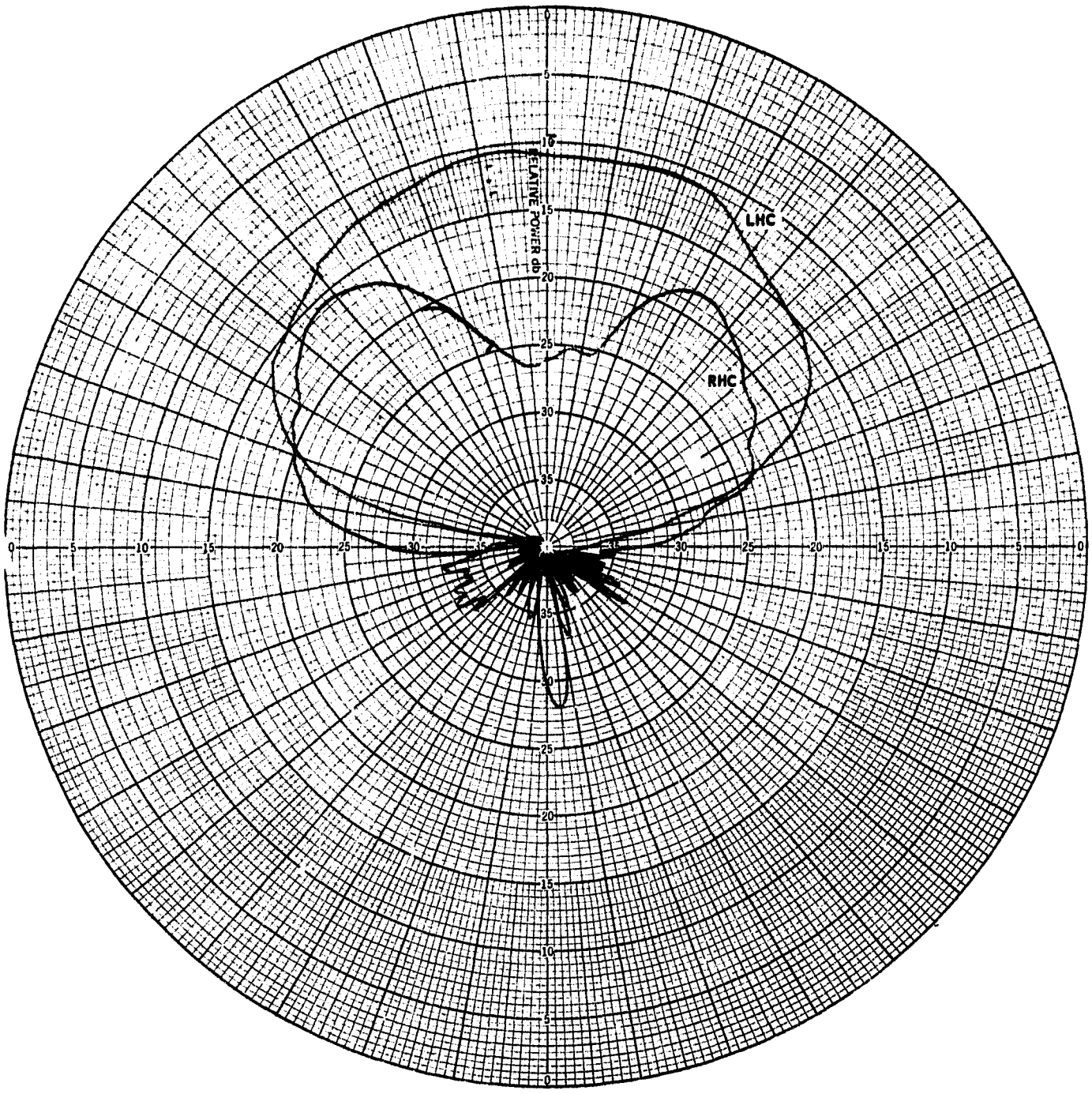

Fig. 10-29

THE JOHNS HOPKINS UNIVERSITY
APPLIED PHYSICS LABORATORY
SILVER SPRING MARYLAND

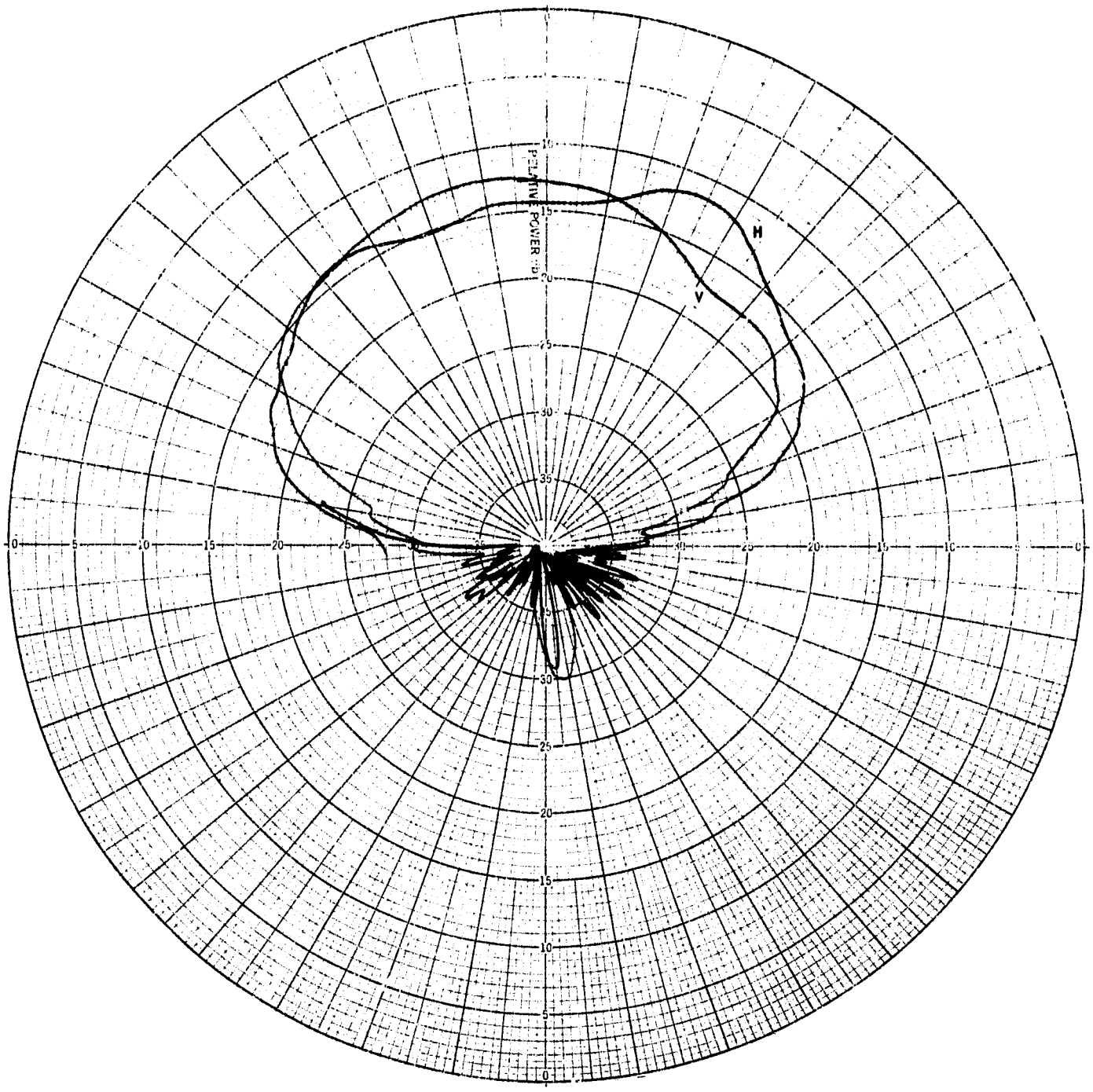

Fig. 10-30

THE JOHNS HOPKINS UNIVERSITY
APPLIED PHYSICS LABORATORY
SILVER SPRING MARYLAND

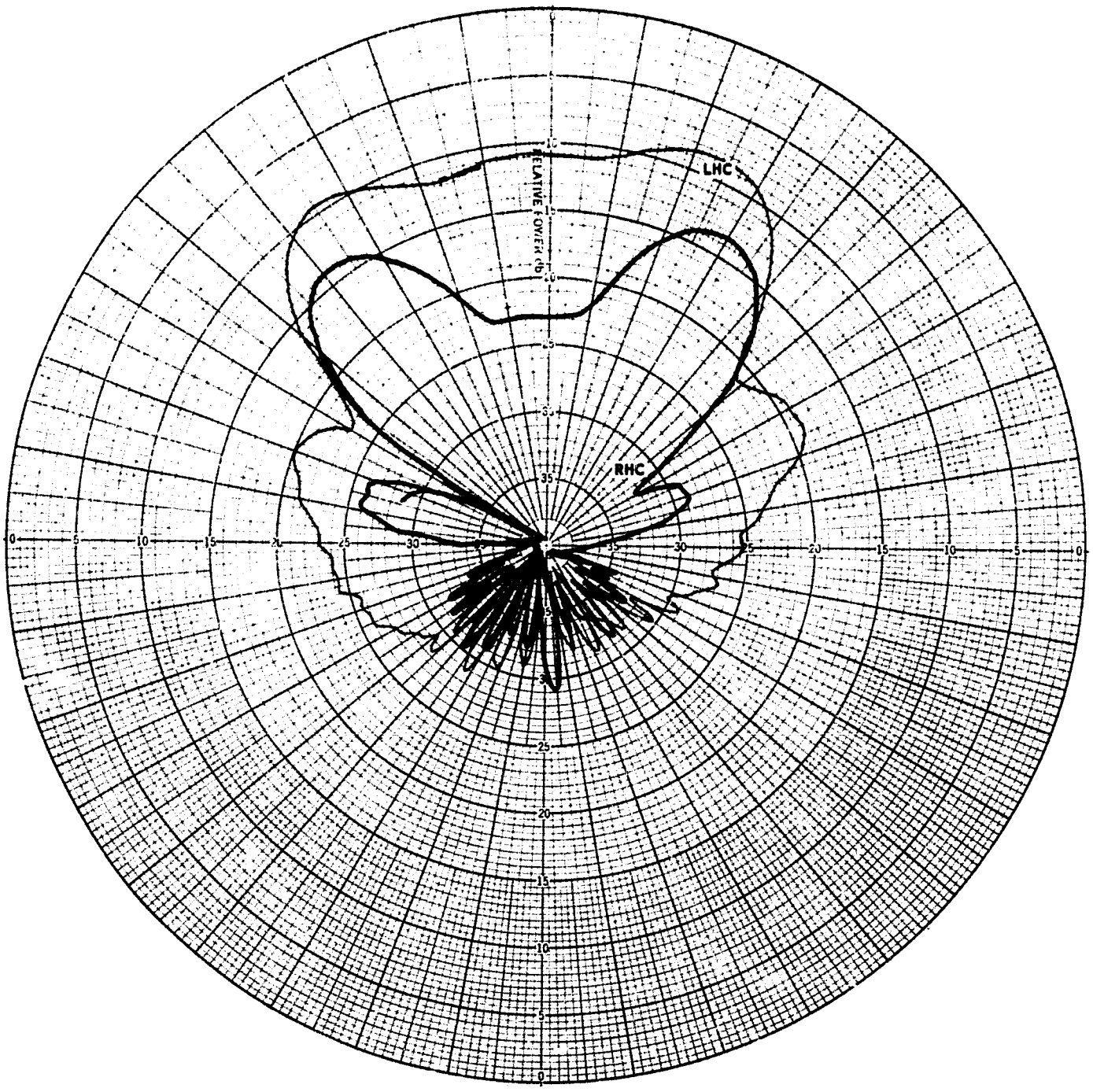

Fig. 10-31

THE JOHNS HOPKINS UNIVERSITY
APPLIED PHYSICS LABORATORY
SILVER SPRING MARYLAND

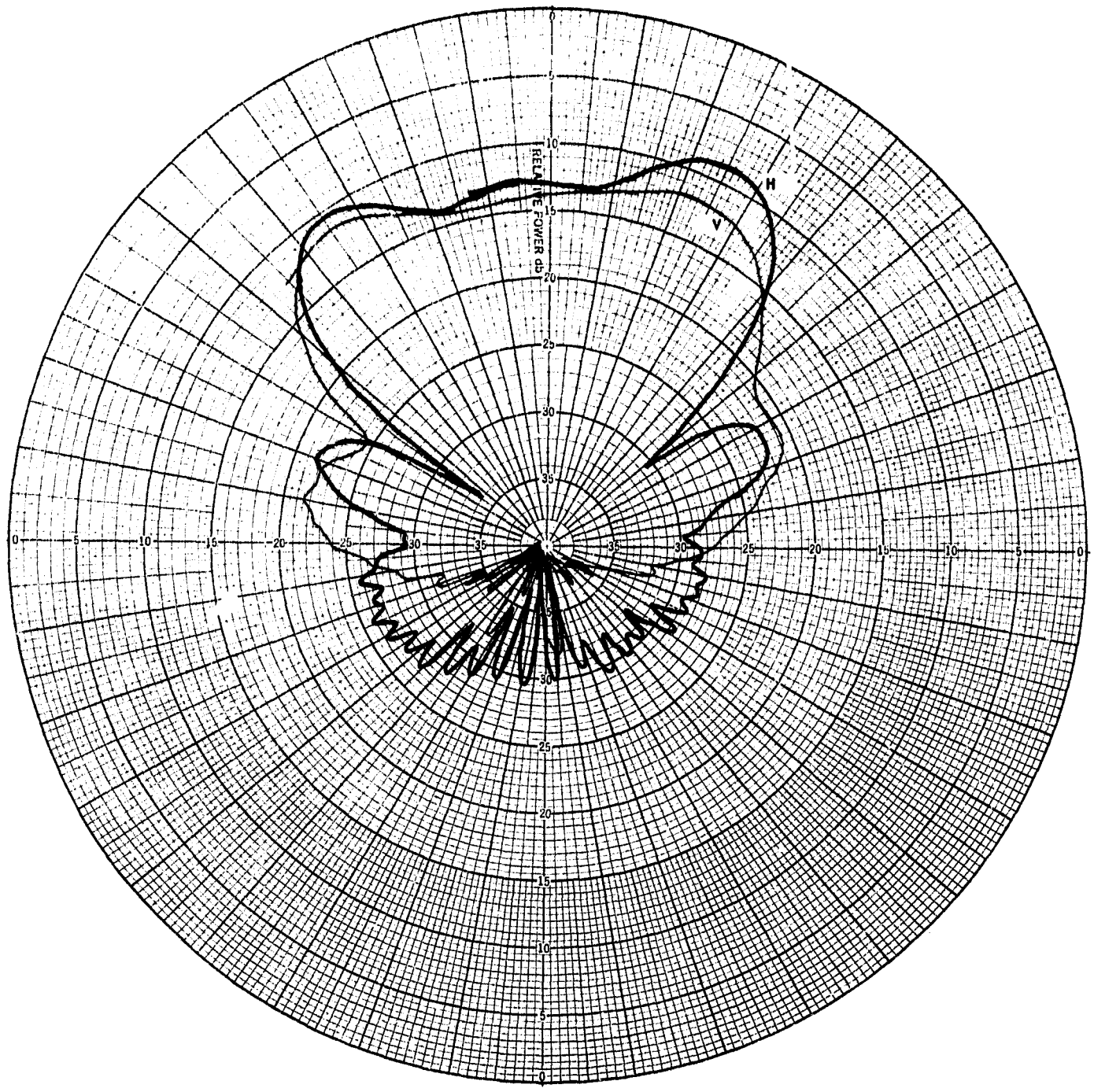

Fig. 10-32

Measured Beamwidth - Figure 11 plots the measured 3 db beamwidth as a function of frequency.

Measured Gain - The gain of the GEOS-B hemisphere is plotted in Figure 12. The matching network loss is included to make this effective antenna gain of the spacecraft.

Measured Axial Ratio - Figure 13 details the axial ratio of the antenna. The axial ratio has been calculated from the radiation patterns by the formula

$$\text{AX Ratio} = \frac{E_R - E_L}{E_R + E_L}$$

Measured Impedance - The input impedance at the feed point of the hemisphere on the RF mockup as a function of frequency is plotted in Figure 14.

IV. MULTIPLEXER AND ANTENNA MATCHING NETWORK

Introduction

This device multiplexes the signals from the spacecraft's six transmitters and two receivers onto the wide band antenna feed cable. It provides isolation between the signal sources and presents a nominally 50-ohm input impedance to each at its operating frequency.

Principle of Operation

Figure 15 is a schematic of the multiplexer. The operation of the directional filter is explained in the next section. It has no effect on the circuit for frequencies other than 972 mcs.

Resonant short circuits and quarter wavelength coaxial lines are used to accomplish frequency selective power division at the branch points. Series tuned circuits are used to short circuit a point on a transmission line to ground at their resonant frequency. The distance from the resonant short circuit to the branch point is adjusted to $\lambda/4$, making the input impedance very high and preventing power flow into the line. The effect of the circuits off resonance will be ignored in the first approximation since their Q is high.

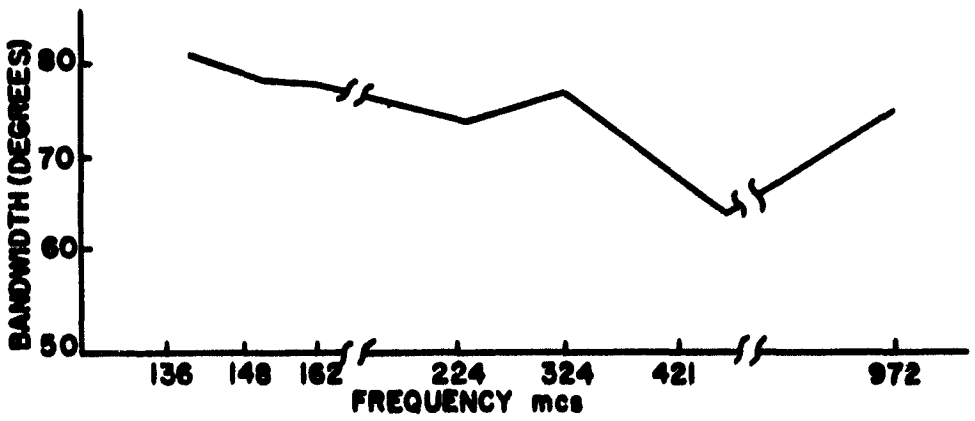

Fig. 11 HEMI SPIRAL BEAMWIDTH

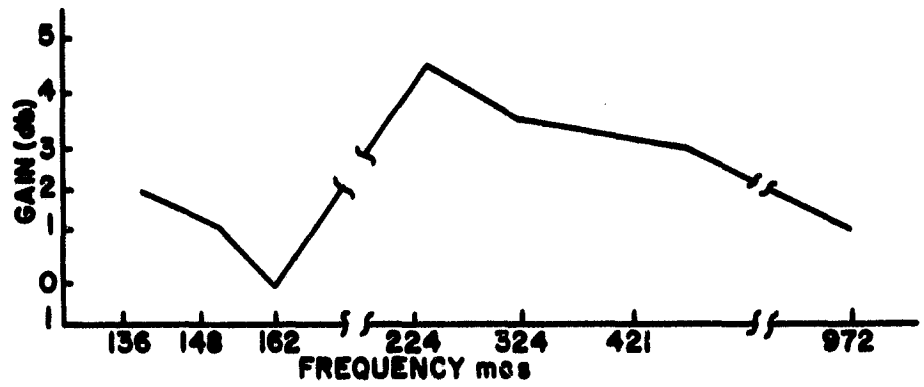

Fig. 12 HEMI SPIRAL GAIN OVER ISOTROPIC
(INCLUDES MATCHING NETWORK LOSS)

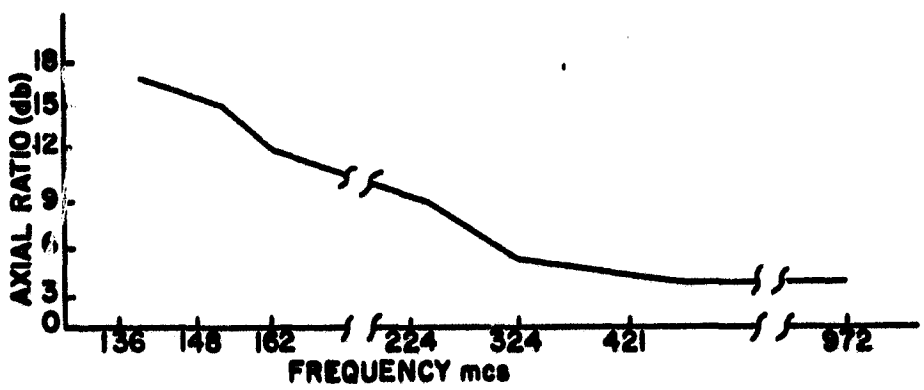

Fig. 13 HEMI SPIRAL AXIAL RATIO

THE JOHNS HOPKINS UNIVERSITY
APPLIED PHYSICS LABORATORY
SILVER SPRING MARYLAND

IMPEDANCE OR ADMITTANCE COORDINATES

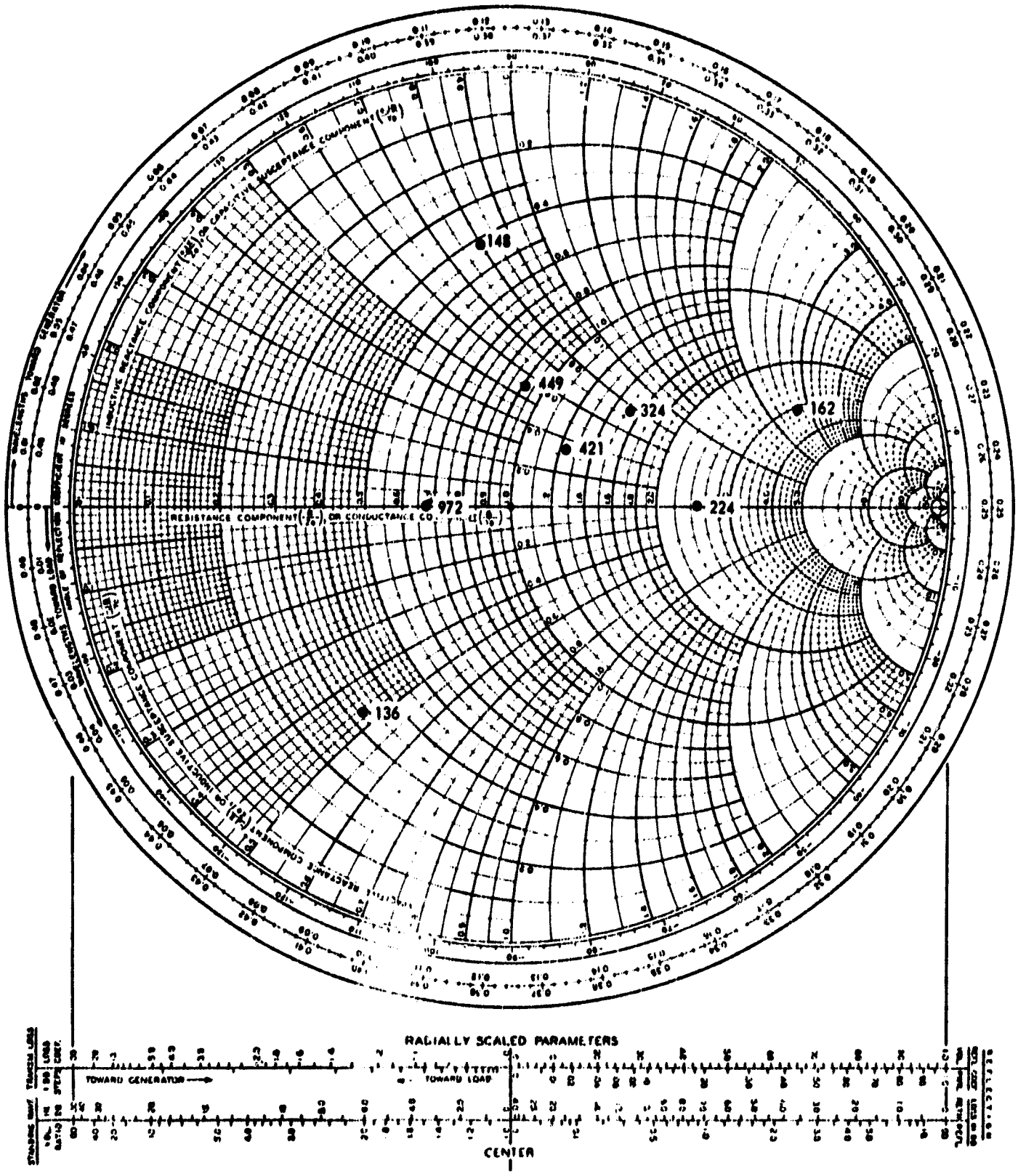

Fig. 14 HEMISPHERICAL SPIRAL IMPEDANCE

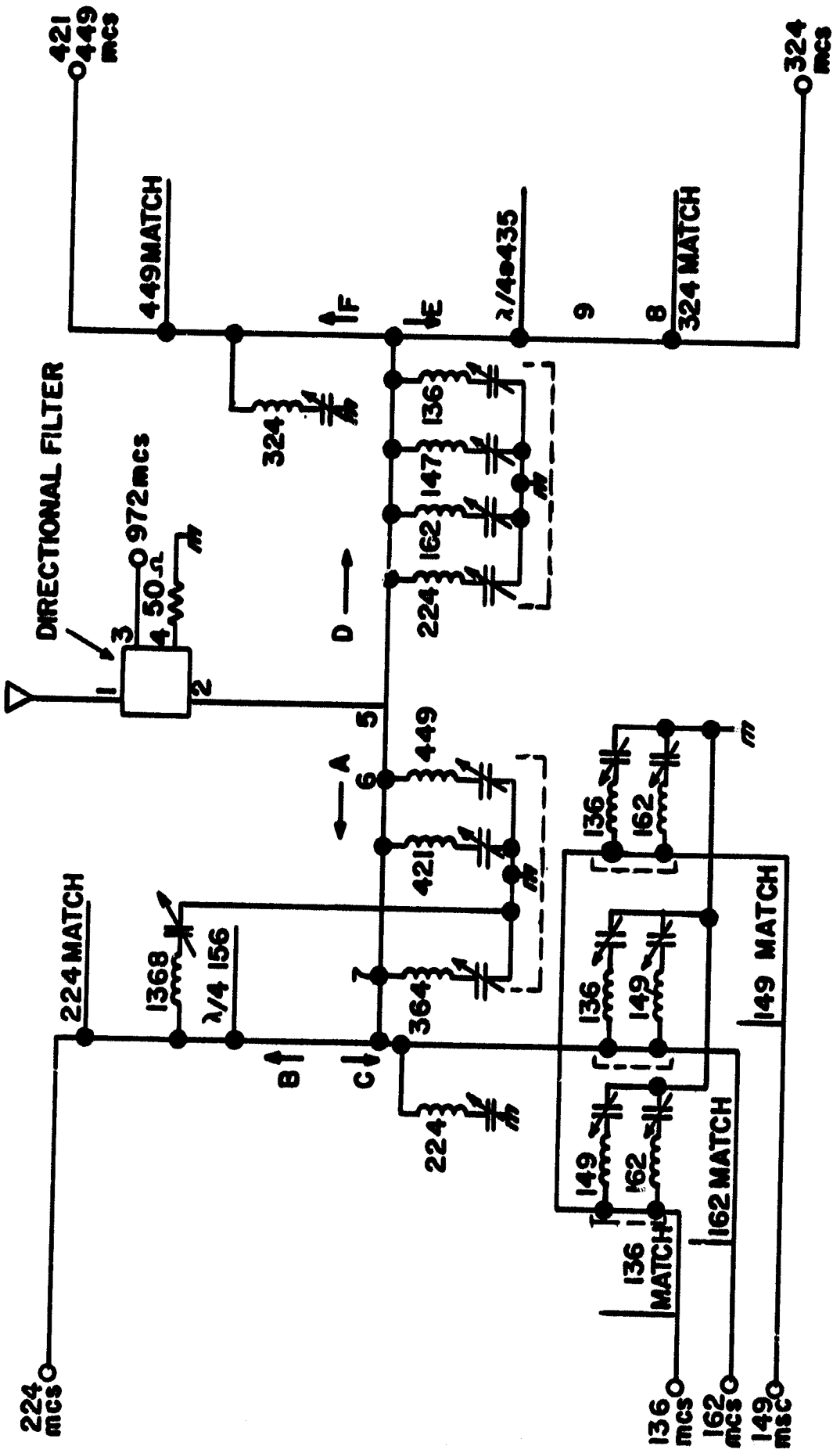

Fig. 15 SCHEMATIC OF MULTIPLEXER

Referring to Figure 15, signals at 449, 421, and 324 mcs, are prevented from flowing in path A by the tuned circuits at 6 and 7. The distance 5 - 6 is one quarter wavelength at 449 mcs, the distance 7 - 5 is one quarter wavelength at 324 mcs. The tuned circuit in path F forces the 324 mcs signal to flow in the path E, the stub (8) and line (9) match the impedance to 50Ω. The stub and $\lambda/4$ line in path E stop 421 and 449 mcs and force it into line F where it is matched at 449 mcs. The 421 mcs signal feeds a receiver and is little effected by an imperfect match. Signals at 136, 148, 162 and 224 mcs are forced into the A path by the tuned circuits in path D. 224 mcs flows into path B where it is matched to 50Ω; 136, 148 and 162 mcs flow into path C where they are divided and separately matched.

The 972 mcs directional filter is a four port device with the frequency response of Figure 16.[12] Arm 4 is isolated from the other three arms. The 972 mcs doppler signal is coupled to the antenna and isolated from the remainder of the matching network. Any other frequency traverses the filter along the 1 - 2 or 2 - 1 path and is isolated from the 972 mcs transmitter. Arms 1 and 2 are perfectly matched at all frequencies.

Principle of Operation - If the coupled and isolated arms of a directional coupler are connected with a ring N wavelengths long, a signal incident at the primary arm of the coupler will cause a resonance in the secondary in the form of a traveling wave circulating about the loop (Figure 17). The process of buildup to resonance is similar to standing wave buildup in a microwave cavity. If two directional couplers are connected in the loop, energy incident at port 1 at the resonant frequency of the loop will be coupled to port 3. Energy at any other frequency will not excite the loop and so will be coupled to port 2. The device behaves as a band pass filter with unloaded Q equal to the Q of the transmission line and loaded Q dependent on the coupling coefficient of the directional couplers.

Multiplexer Mechanical Realization - The tuned circuits and interconnecting lines within a set of dotted lines on the schematic are contained in one filter box. The interconnection cables are nonmagnetic RG 142 U (Times Wire and Calbe Company special cable MI 5199). The mechanical

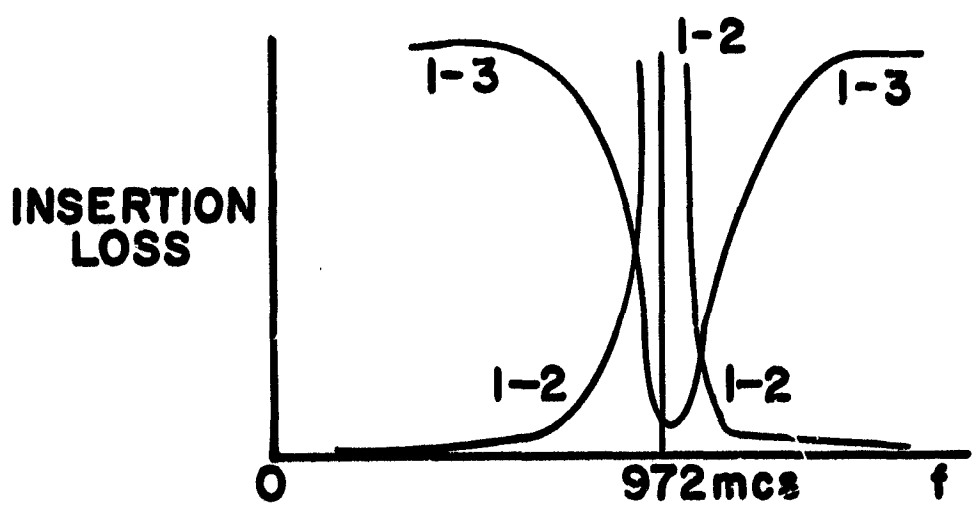

Fig. 16 FREQUENCY RESPONSE OF 972 mcs DIRECTIONAL FILTER

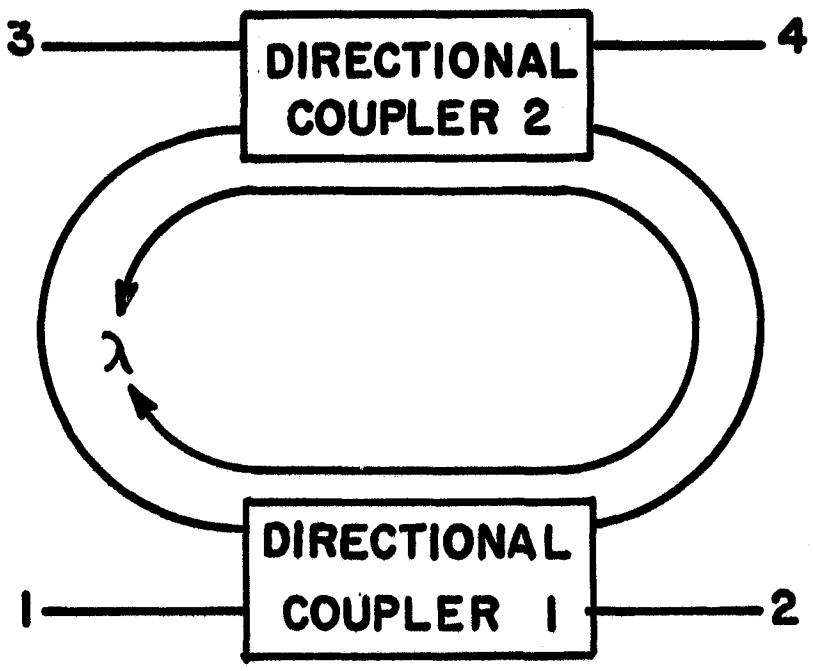

Fig. 17 DIRECTIONAL FILTER SCHEMATIC

constructions are called out on the Assembly Drawing #7211-5500.

Stripline is used to package the GEOS directional filter in a 4" x 3.5" x 3/8" envelope.

The filters are ordered from Hylectronics Corporation to the follcwing specifications:

Mechanical - the dielectric material is teflon fibreglas. The connector pins are soldered to the strip line. The dimensions of the filter will be as called out on Hylectronics Drawing #B 1614* "Model AL-12T Directional Filter".

Electrical

Port 1 to Port 2	Insertion loss -	.25 db max. from 130 to 450 mcs
	VSWR	1.1:1 " " " " " "
Port 3 to Port 1	Insertion loss -	1 db max. at 972 mcs.
		3 db max. at 972 ±2%
	VSWR	1.2:1 max. at 972 mcs.
Port 3 to Port 2	Isolation	20 db min. at 972 mcs.

Thermal - the electrical requirements must be met over the temperature range -7°C to +55°C.

---

* Not a part of this report

THE JOHNS HOPKINS UNIVERSITY
APPLIED PHYSICS LABORATORY
SILVER SPRING, MARYLAND

Multiplexer Fabrication and Test Procedure

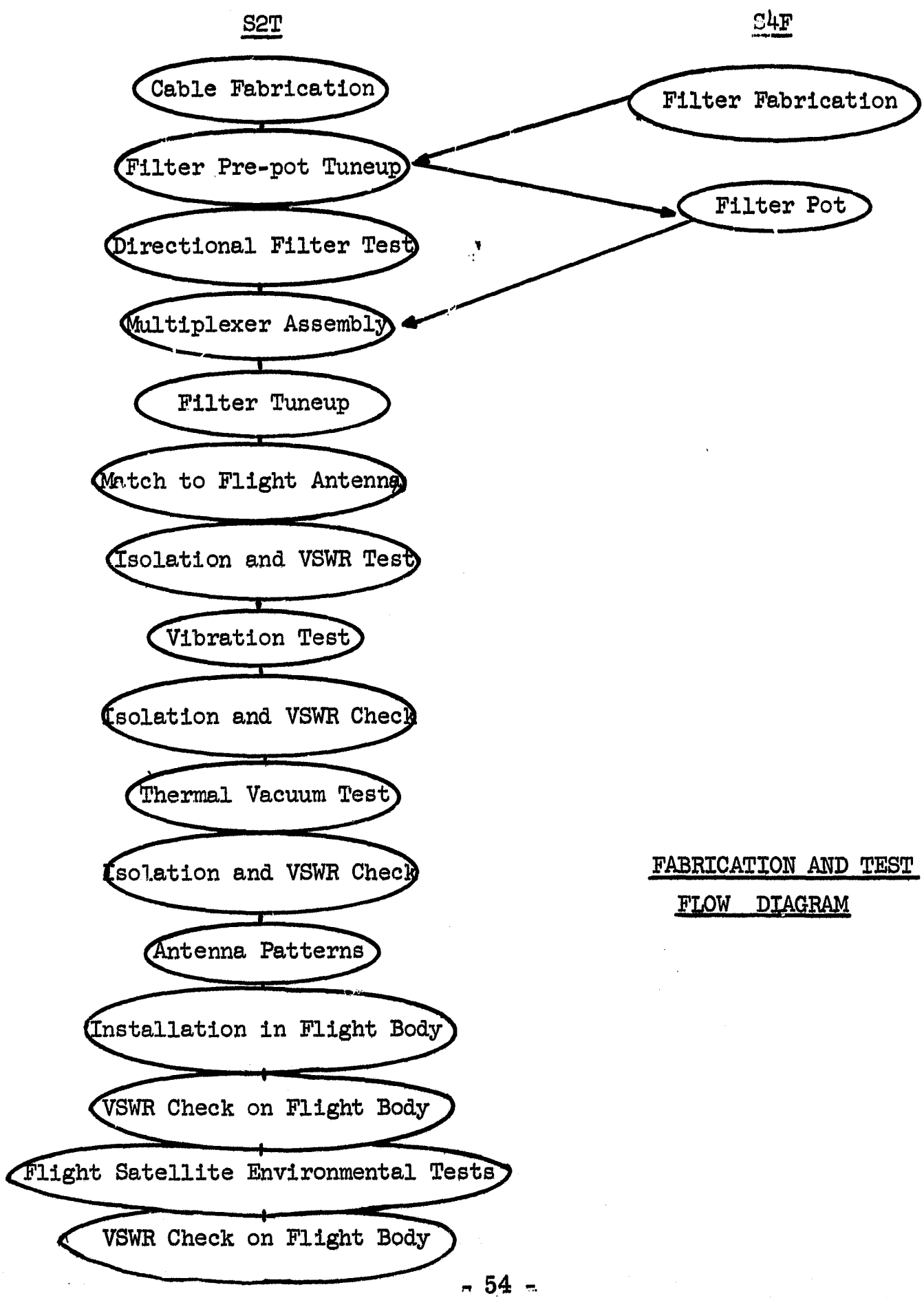

FABRICATION AND TEST
FLOW DIAGRAM

Event Description and Typical Results

Cable Fabrication - Drawing No. 7211-5500 details the electrical lengths of the interconnecting cables.

Filter Pre-pot Tuneup - With the test setup of Figure 18, tune the filter section through its entire range. The filter section must resonate at nearly minimum capacity. Capacitors that have been overheated in soldering often short circuit before reaching the end of travel or are intermittent as they are tuned.

Directional Filter Test - The filter is temperature tested at -7°C and +55°C. Evidence of severe detuning (decreased isolation or increased insertion loss) at low temperature indicates inadequate tension in the screws holding the stripline boards together.

Match to Flight Antenna - Match each port to 50Ω at its resonant frequency.

Isolation and VSWR Test - The test setup of Figure 19 is used to measure isolation, the PRD impedance bridge is used to measure VSWR. Measured VSWR and isolations on GEOS-B:

	Relative Power Out of Port (db)							
Input Port & Frequency	136	148	162	224	324	449 421	972	VSWR
136	---	40	43	47	40	49	53	1.18
148	32	--	40	36	40	52	47	1.22
162	35	32	--	44	37	48	45	1.26
224	42	48	45	--	43	48	48	1.12
324	55	47	41	42	--	60	60	1.06
421	60	60	56	60	27	--	52	2.2
449	49	51	48	58	36	--	48	1.05
972	40	52	50	40	40	46	--	1.30

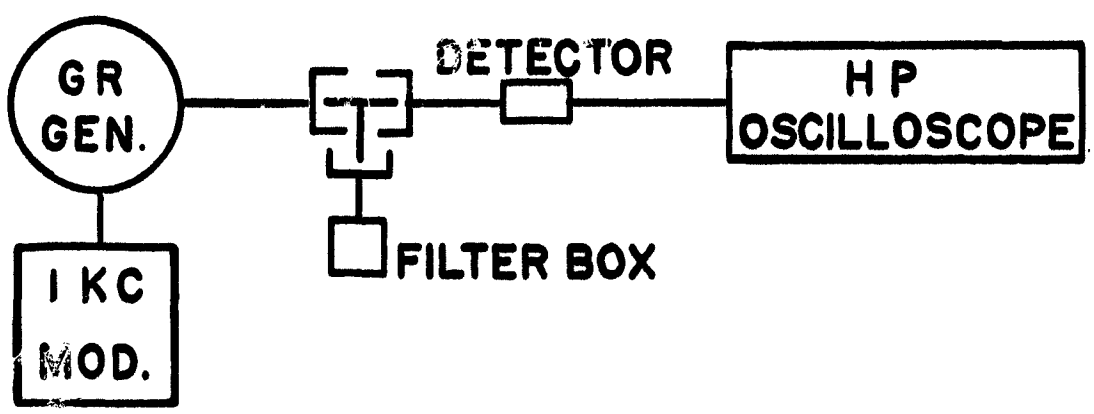

Fig. 18 FILTER PRE-POT TUNEUP, TEST SETUP

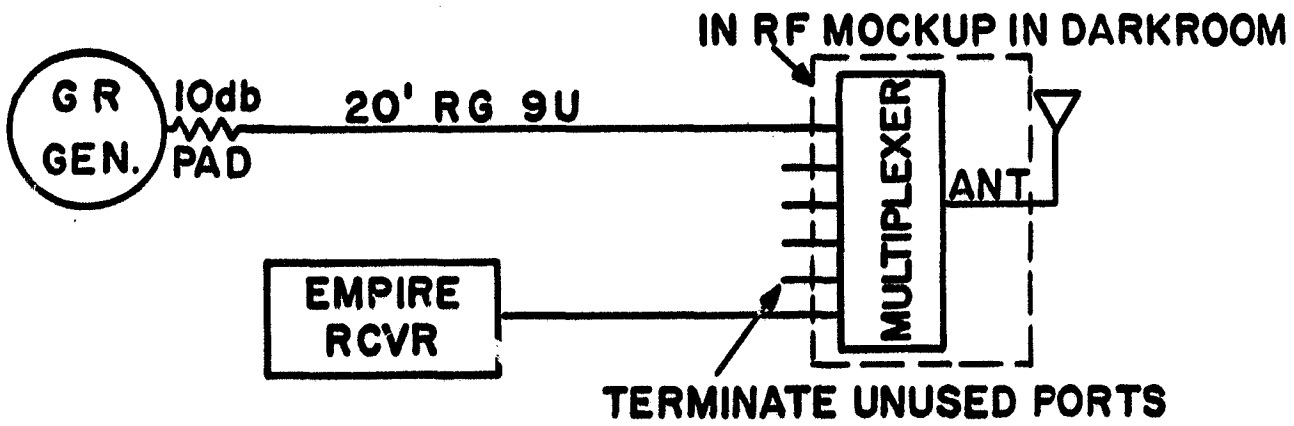

Fig. 19 ISOLATION AND VSWR TEST SETUP

Measurement During Vibration Test - During the test the generator in Figure 20 is varied to the frequency of each port in turn. The output of the port is monitored for evidence of intermittent operation.

Measurement During Thermal Vacuum Tests - The VSWR is measured with a 50Ω termination in place of the antenna. Little change occurred with temperature variations.

Post Environmental Checks - Little change in VSWR or isolation was observed after environmental tests.

Checks on the Flight Satellite - Little change was observed in the VSWR when installed on the flight satellite or after satellite level environmental tests.

V. S-BAND ANTENNA

A balanced equiangular spiral projected onto a cone provides an antenna for the Range transponder. This antenna is discussed extensively in the literature, for the sake of brevity, this bibliography is presented in place of a technical discussion:

DYSON, I. D. (1959). The unidirectional equiangular spiral antenna. IRE Trans. Antennas Propagation AP-7, 329-334.

DYSON, J. D. and MAYES, P. E. (1961). New Circularly Polarized Frequency-Independent Antennas with Conical Beam Batterns. IRE Trans. Antennas Propagation AP-9 334-342.

DYSON, J. D. (1965). The Characteristics and Design of the Conical Log-Spiral Antenna. IEEE Trans. Antennas Propagation AP-13.

Measured Radiation Patterns

S-band radiation patterns were recorded using the S2T antenna range and the coordinate system already discussed and are included as Figure 21. Table II lists the pattern numbers for the various angles and frequencies.

Frequency	Omnidirectional Level on the Charts
1705	15 db
2270	18 db

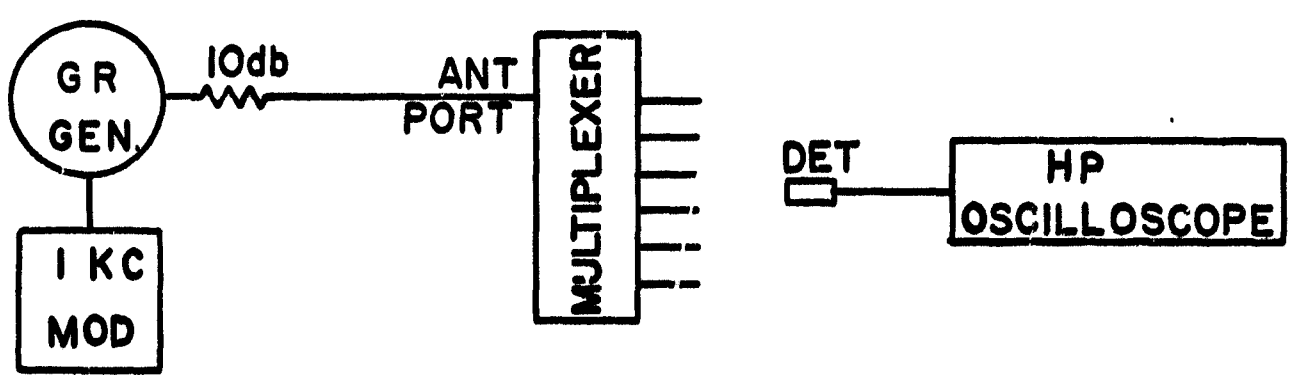

Fig. 20 MEASUREMENT DURING VIBRATION TEST

THE JOHNS HOPKINS UNIVERSITY
APPLIED PHYSICS LABORATORY
SILVER SPRING, MARYLAND

Fig. 21 S-BAND MEASURED RADIATION PATTERNS

THE JOHNS HOPKINS UNIVERSITY
APPLIED PHYSICS LABORATORY
SILVER SPRING MARYLAND

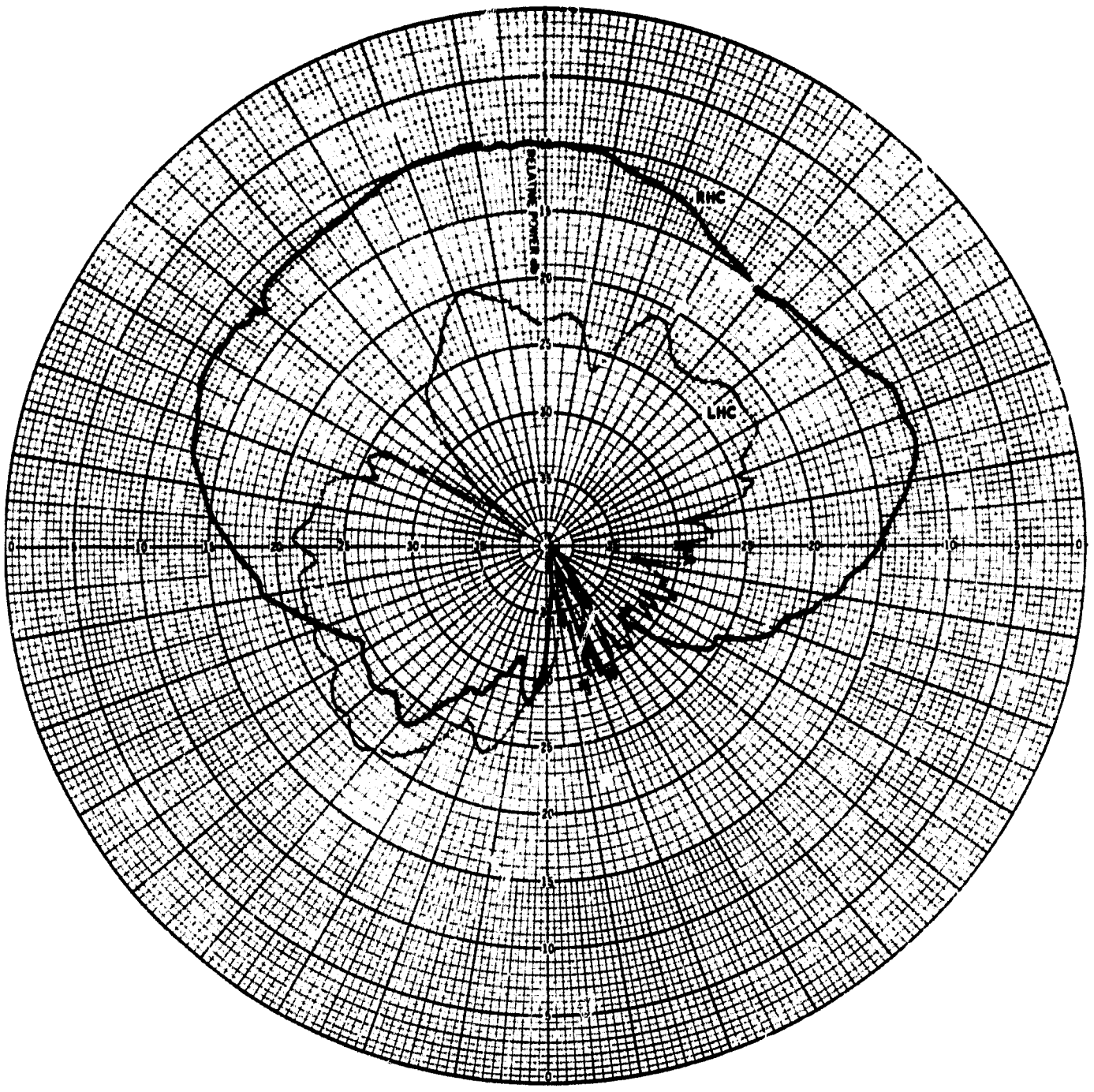

Fig. 21-1

THE JOHNS HOPKINS UNIVERSITY
APPLIED PHYSICS LABORATORY
SILVER SPRING, MARYLAND

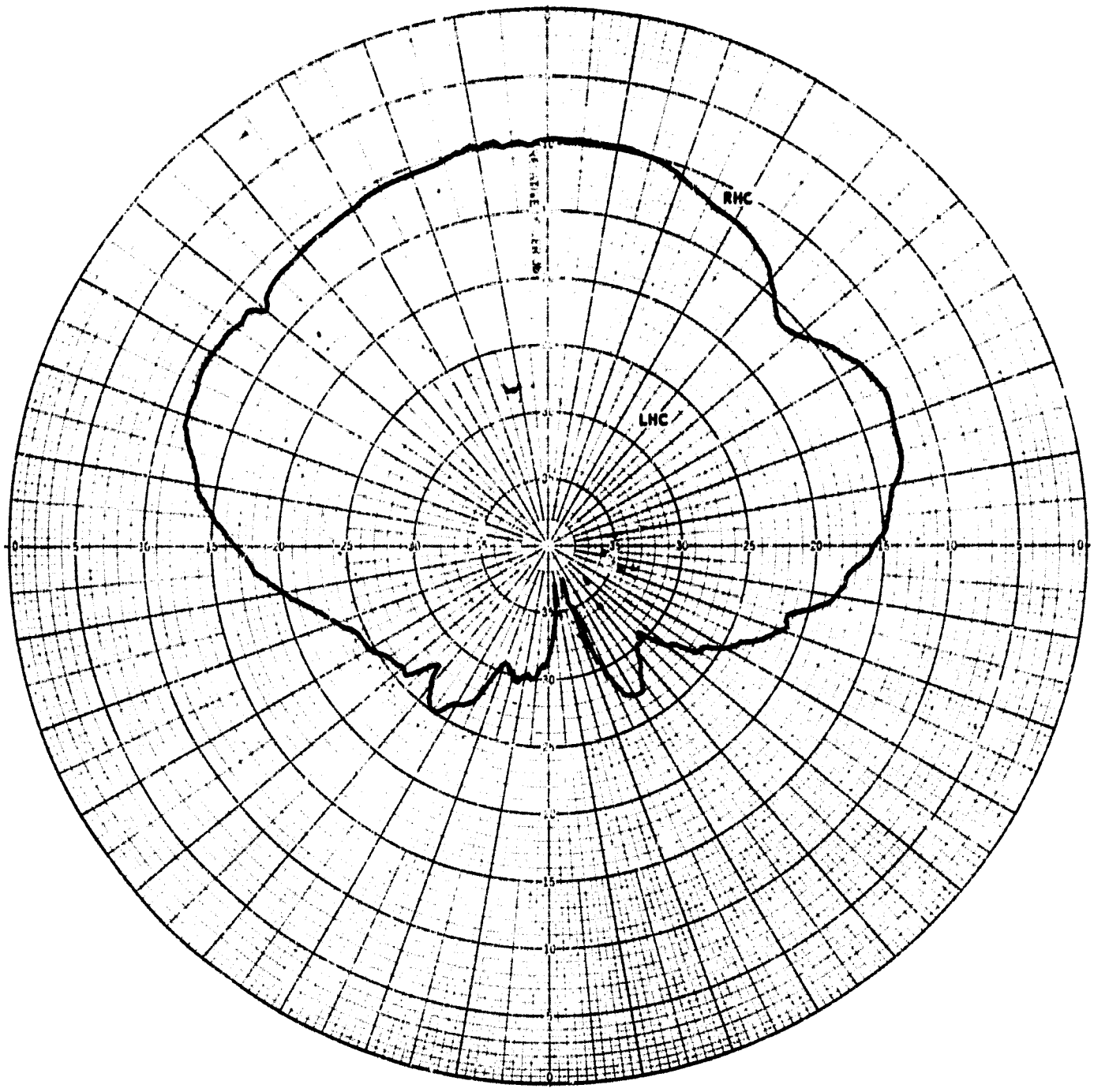

Fig. 21-2

THE JOHNS HOPKINS UNIVERSITY
APPLIED PHYSICS LABORATORY
SILVER SPRING MARYLAND

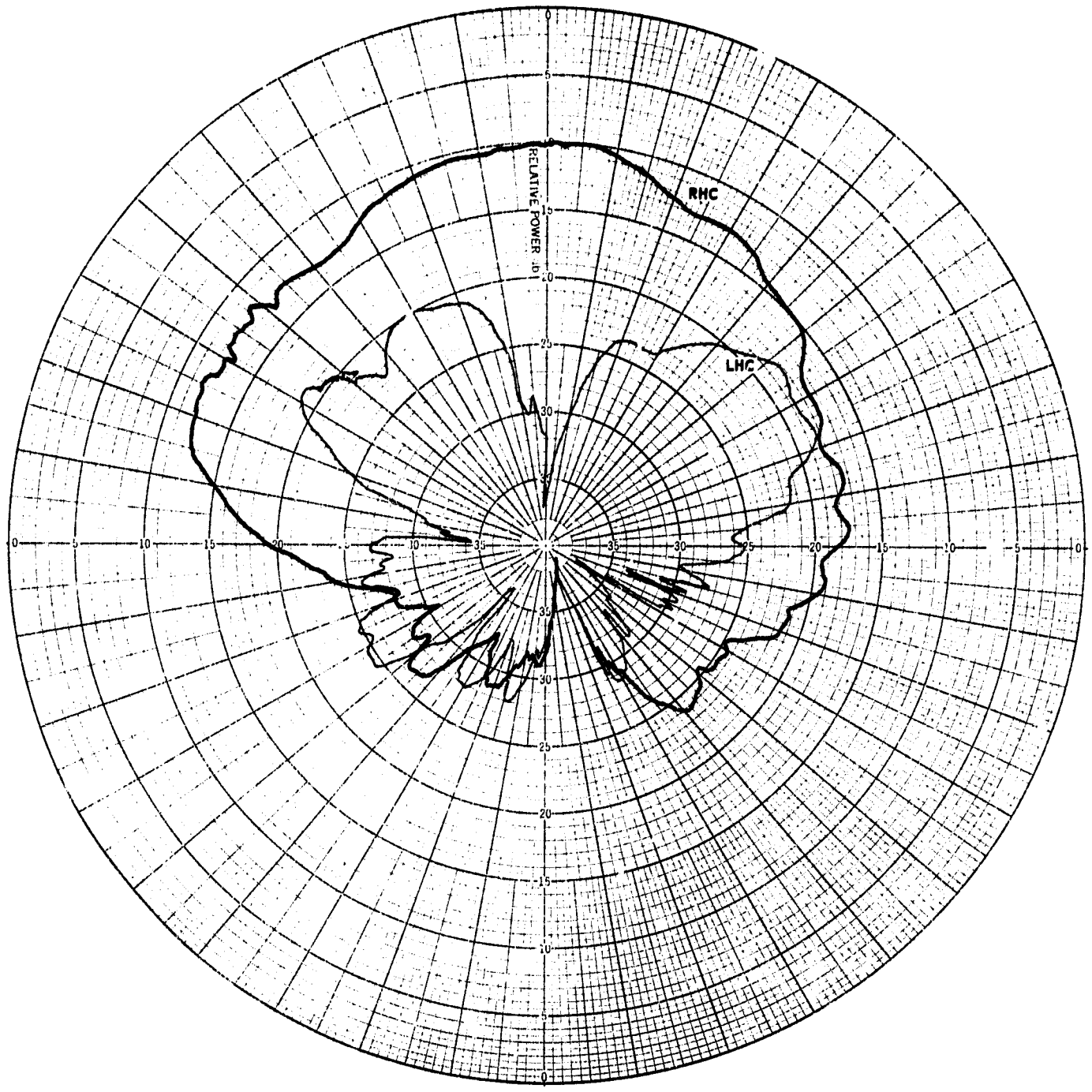

Fig. 21-3

THE JOHNS HOPKINS UNIVERSITY
APPLIED PHYSICS LABORATORY
SILVER SPRING MARYLAND

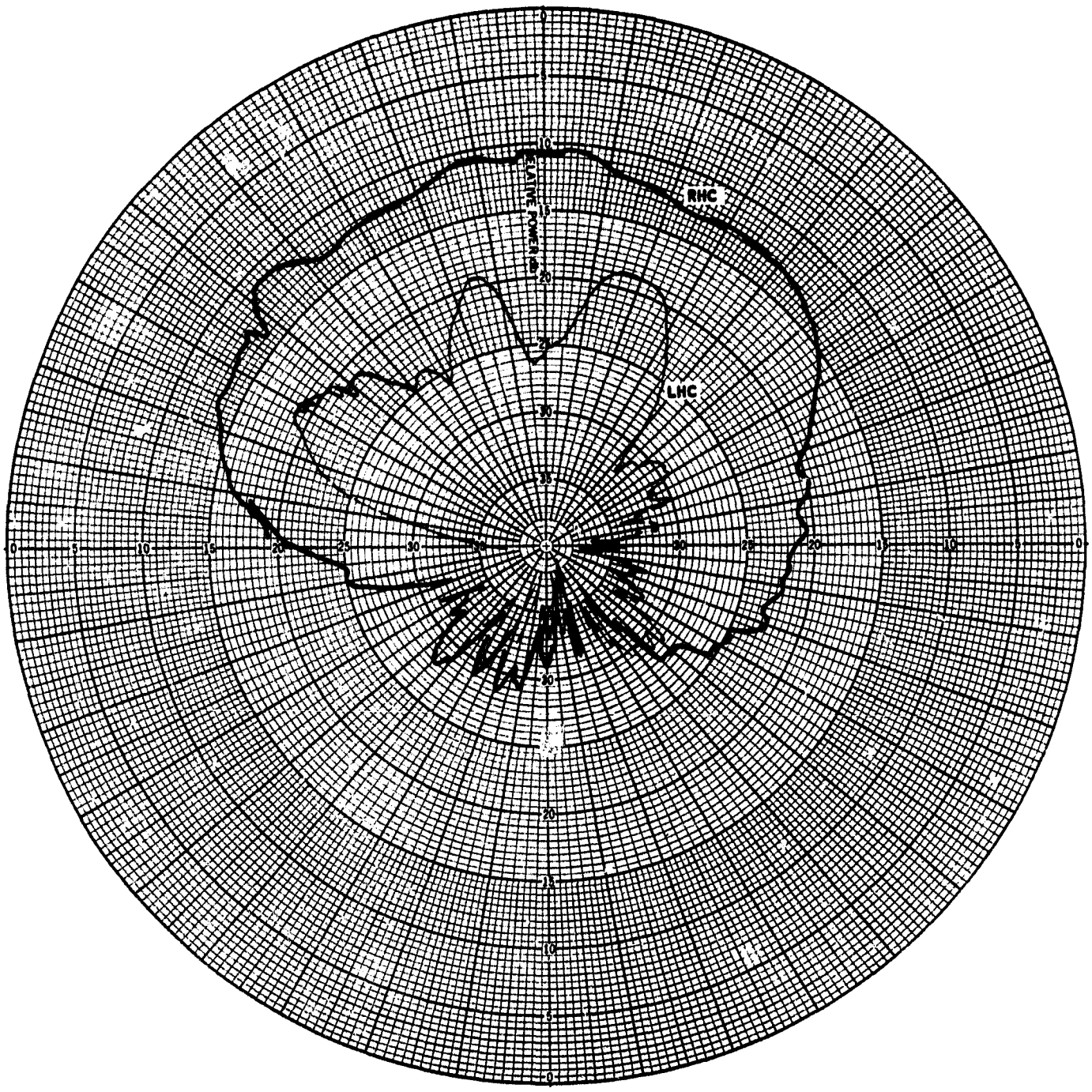

Fig. 21-4

THE JOHNS HOPKINS UNIVERSITY
APPLIED PHYSICS LABORATORY
SILVER SPRING MARYLAND

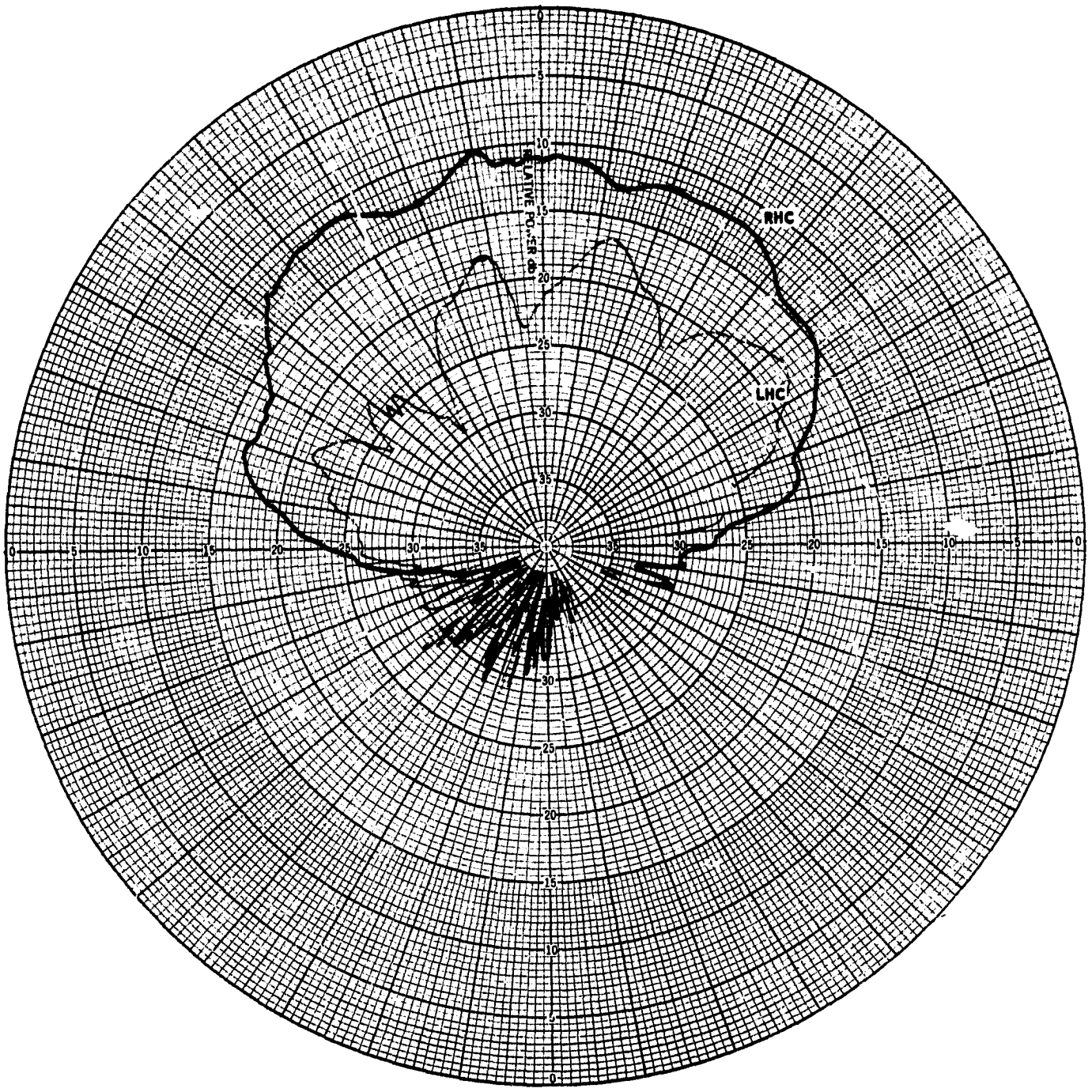

Fig. 21-5

THE JOHNS HOPKINS UNIVERSITY
APPLIED PHYSICS LABORATORY
SILVER SPRING MARYLAND

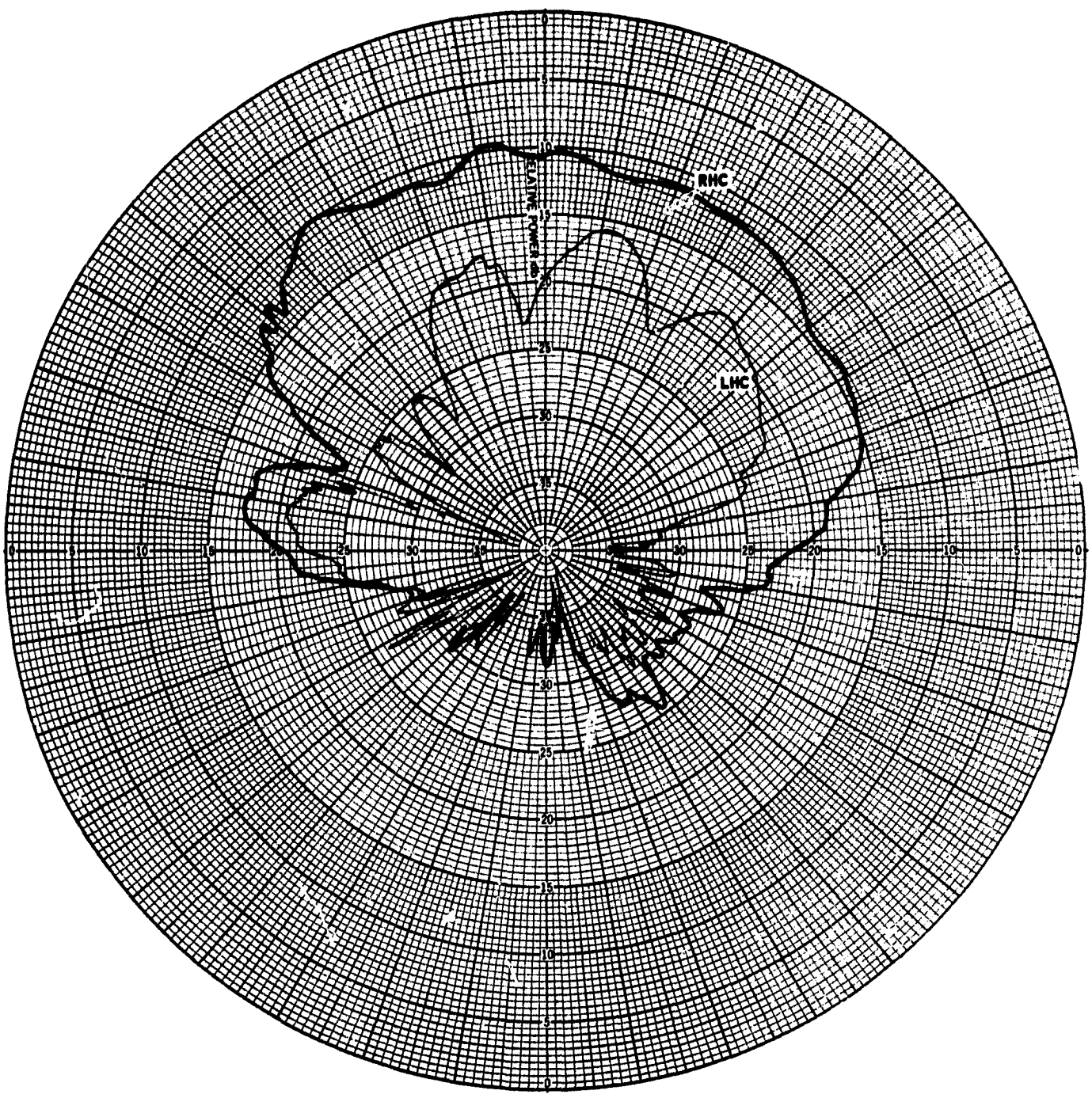

Fig. 21-6

THE JOHNS HOPKINS UNIVERSITY
APPLIED PHYSICS LABORATORY
SILVER SPRING MARYLAND

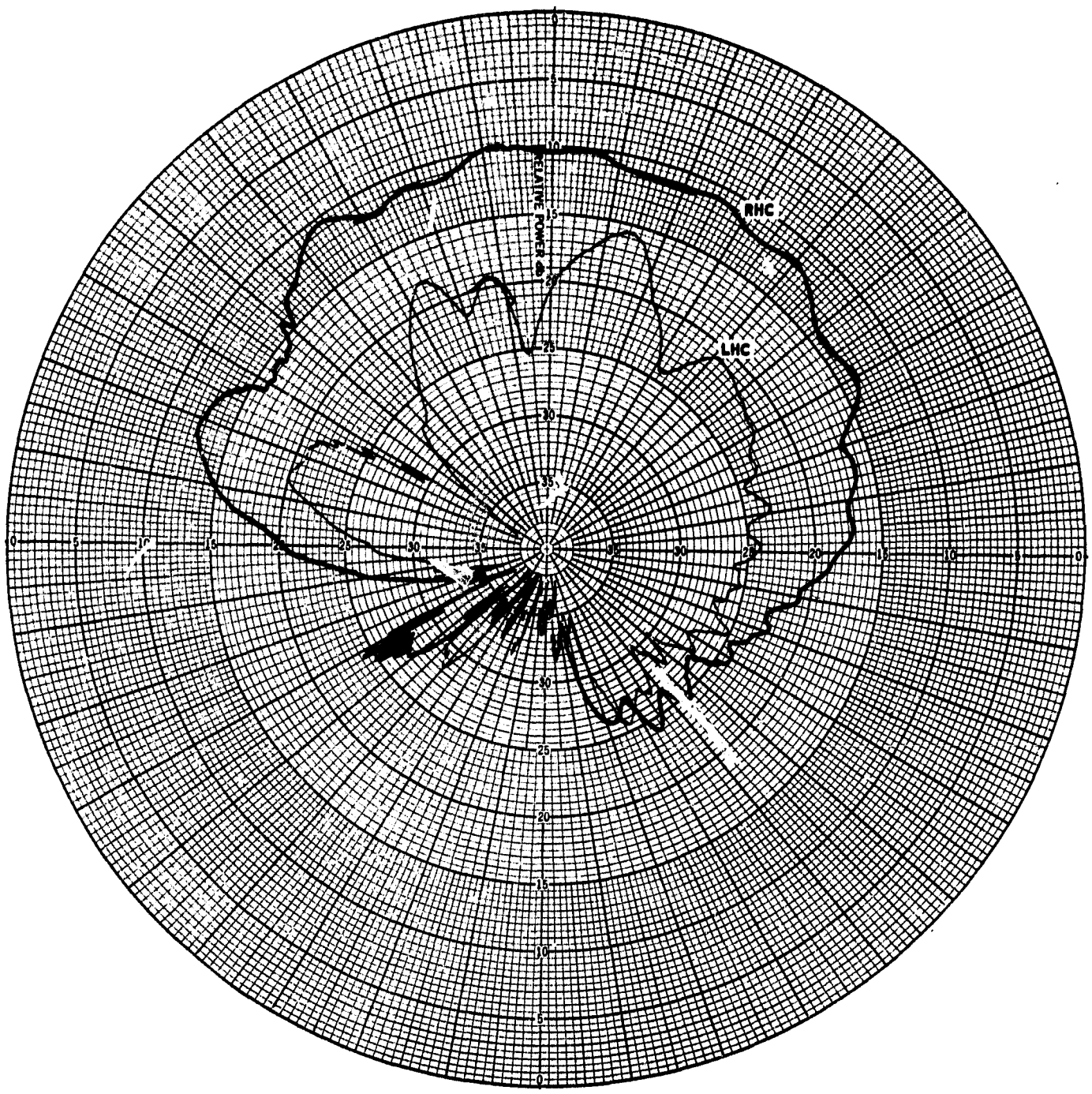

Fig. 21-7

THE JOHNS HOPKINS UNIVERSITY
APPLIED PHYSICS LABORATORY
SILVER SPRING MARYLAND

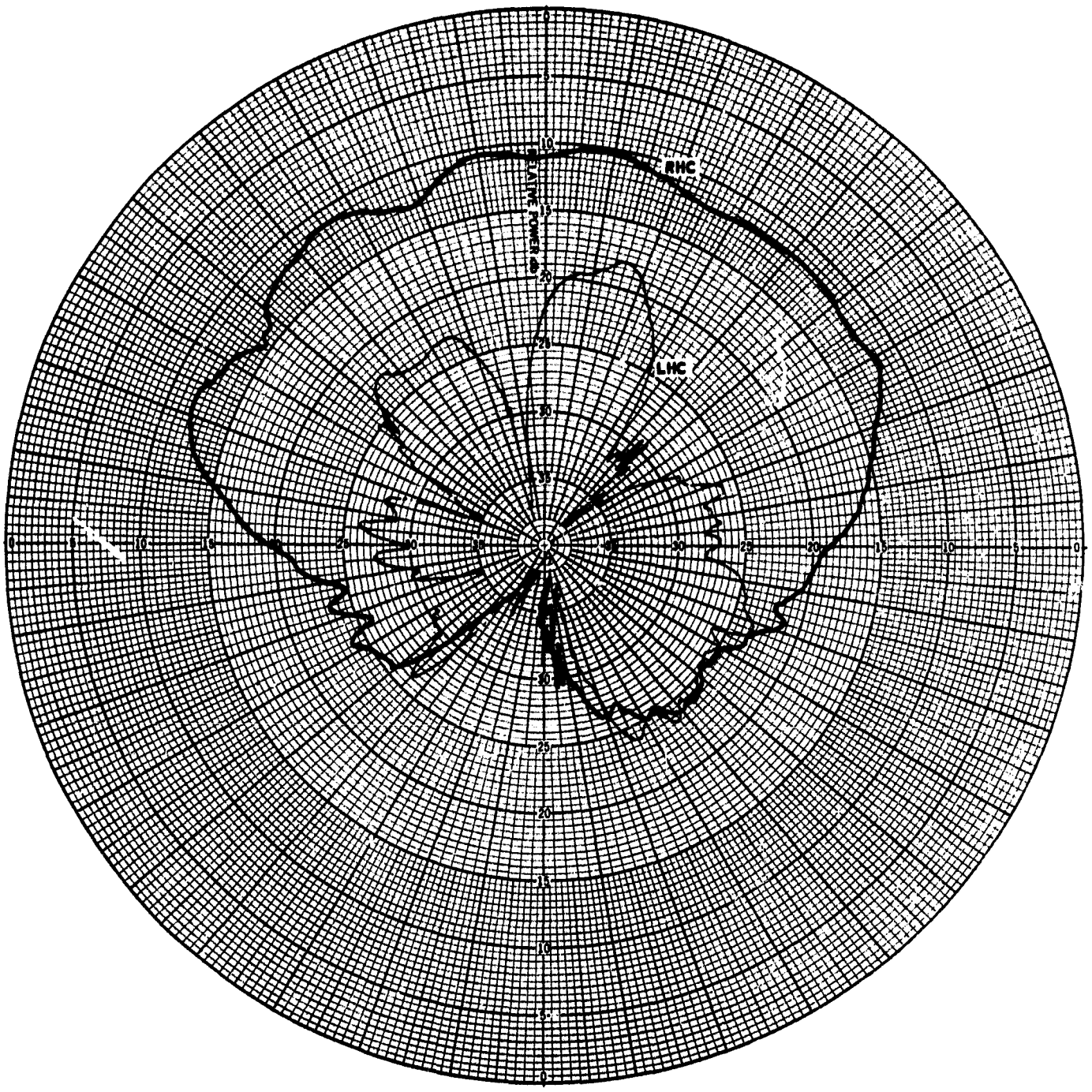

Fig. 21-8

THE JOHNS HOPKINS UNIVERSITY
APPLIED PHYSICS LABORATORY
SILVER SPRING MARYLAND

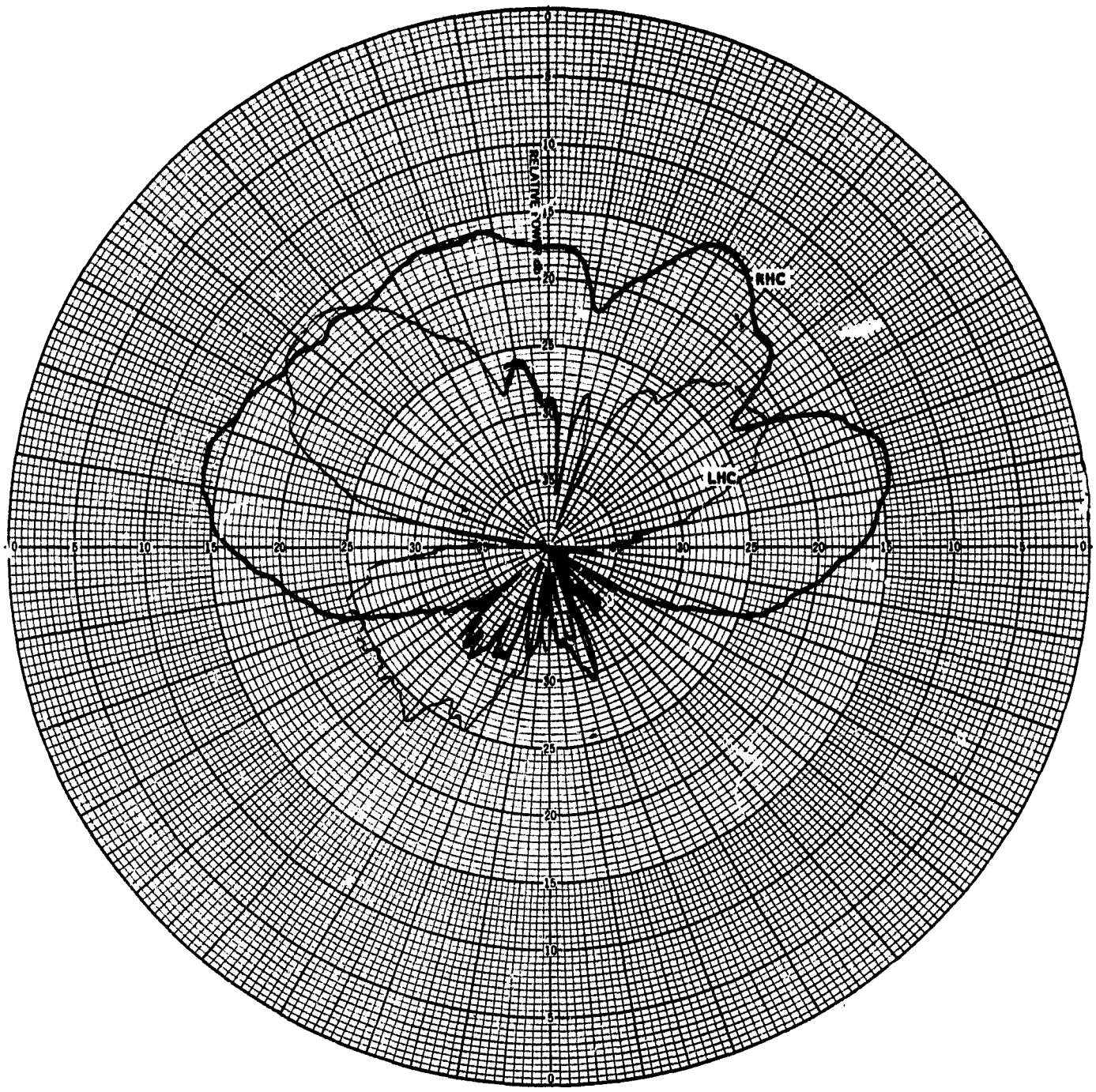

Fig. 21-9

THE JOHNS HOPKINS UNIVERSITY
APPLIED PHYSICS LABORATORY
SILVER SPRING, MARYLAND

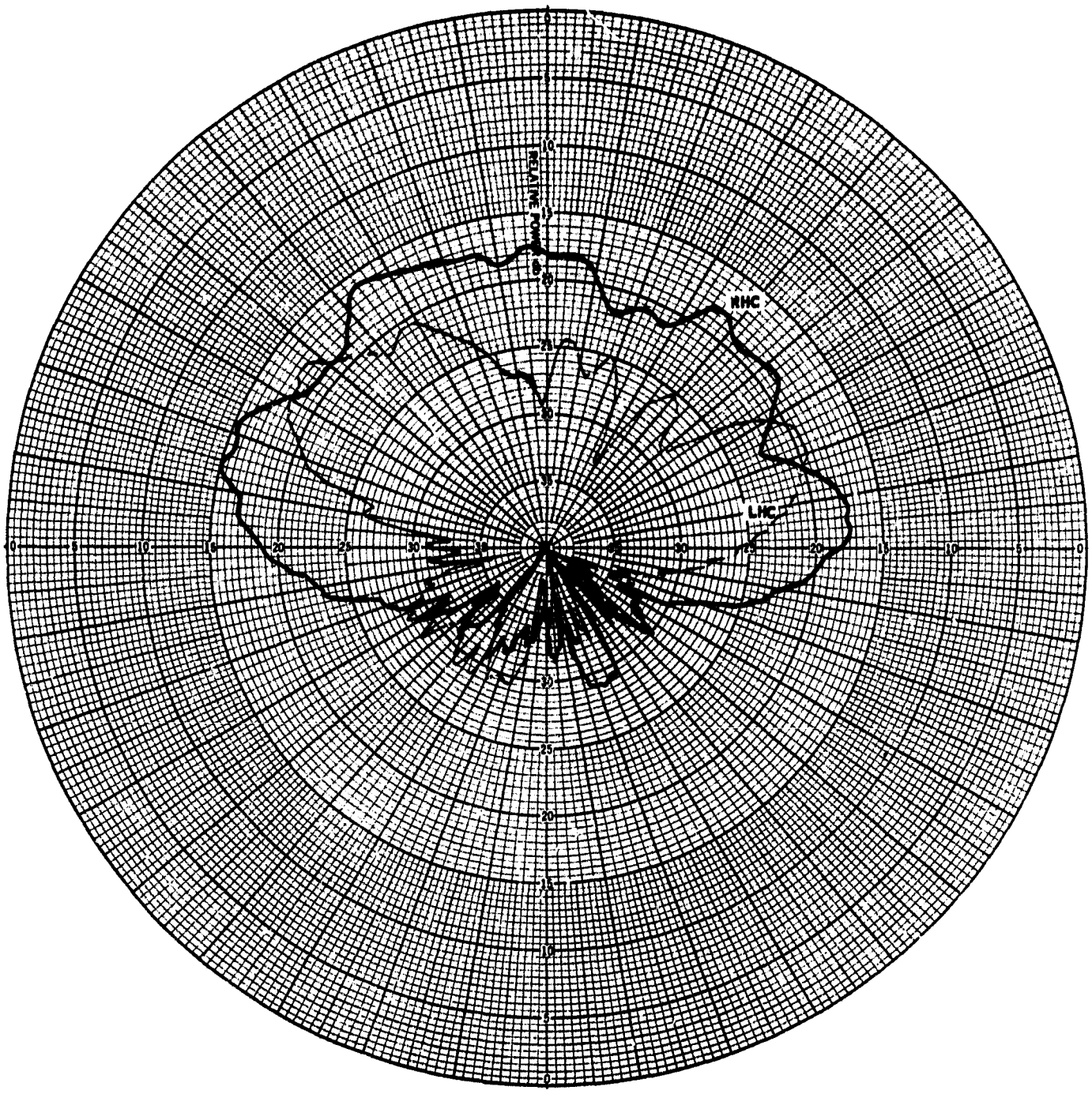

Fig. 21-10

THE JOHNS HOPKINS UNIVERSITY
APPLIED PHYSICS LABORATORY
SILVER SPRING MARYLAND

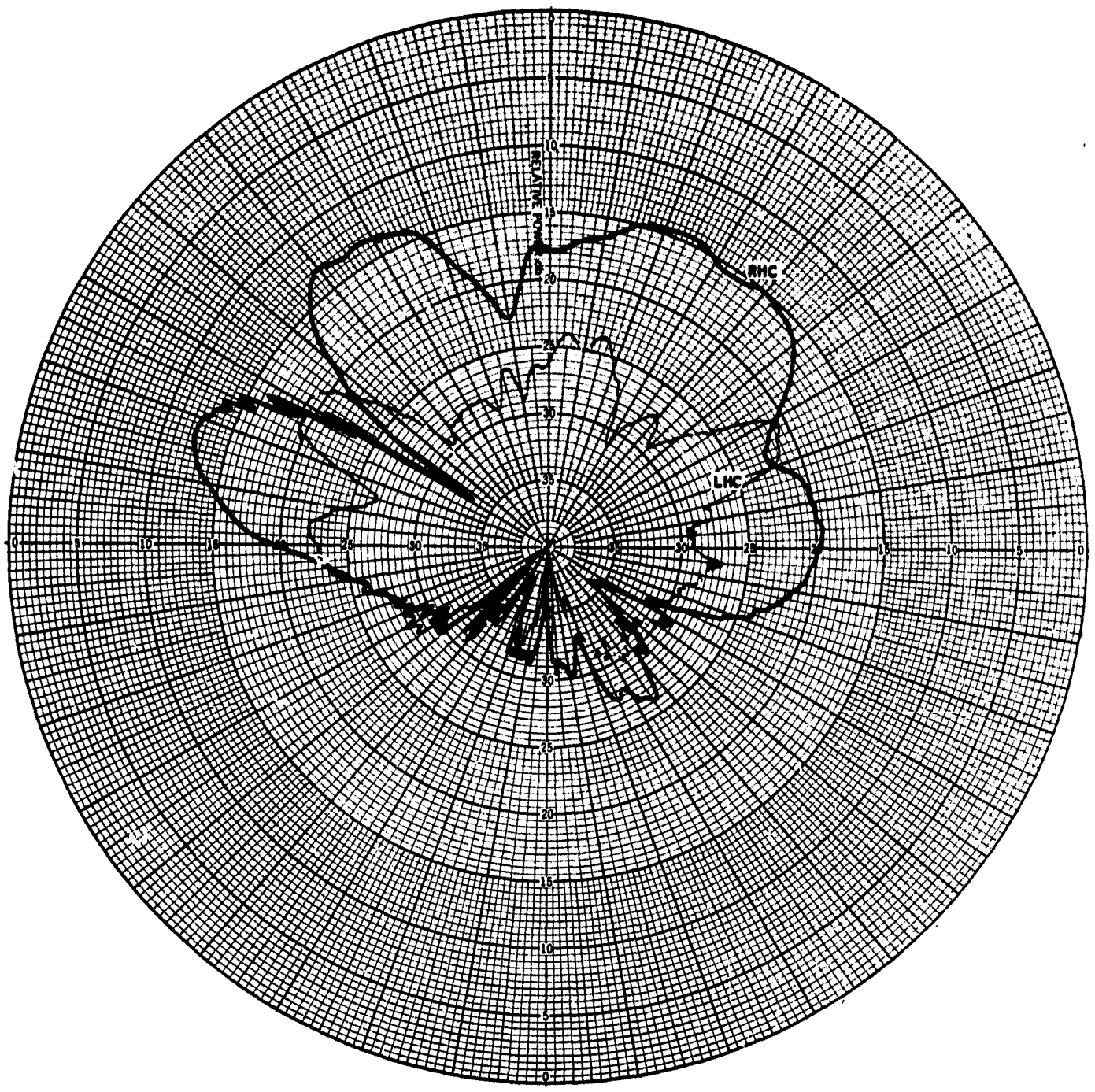

Fig. 21-11

THE JOHNS HOPKINS UNIVERSITY
APPLIED PHYSICS LABORATORY
SILVER SPRING, MARYLAND

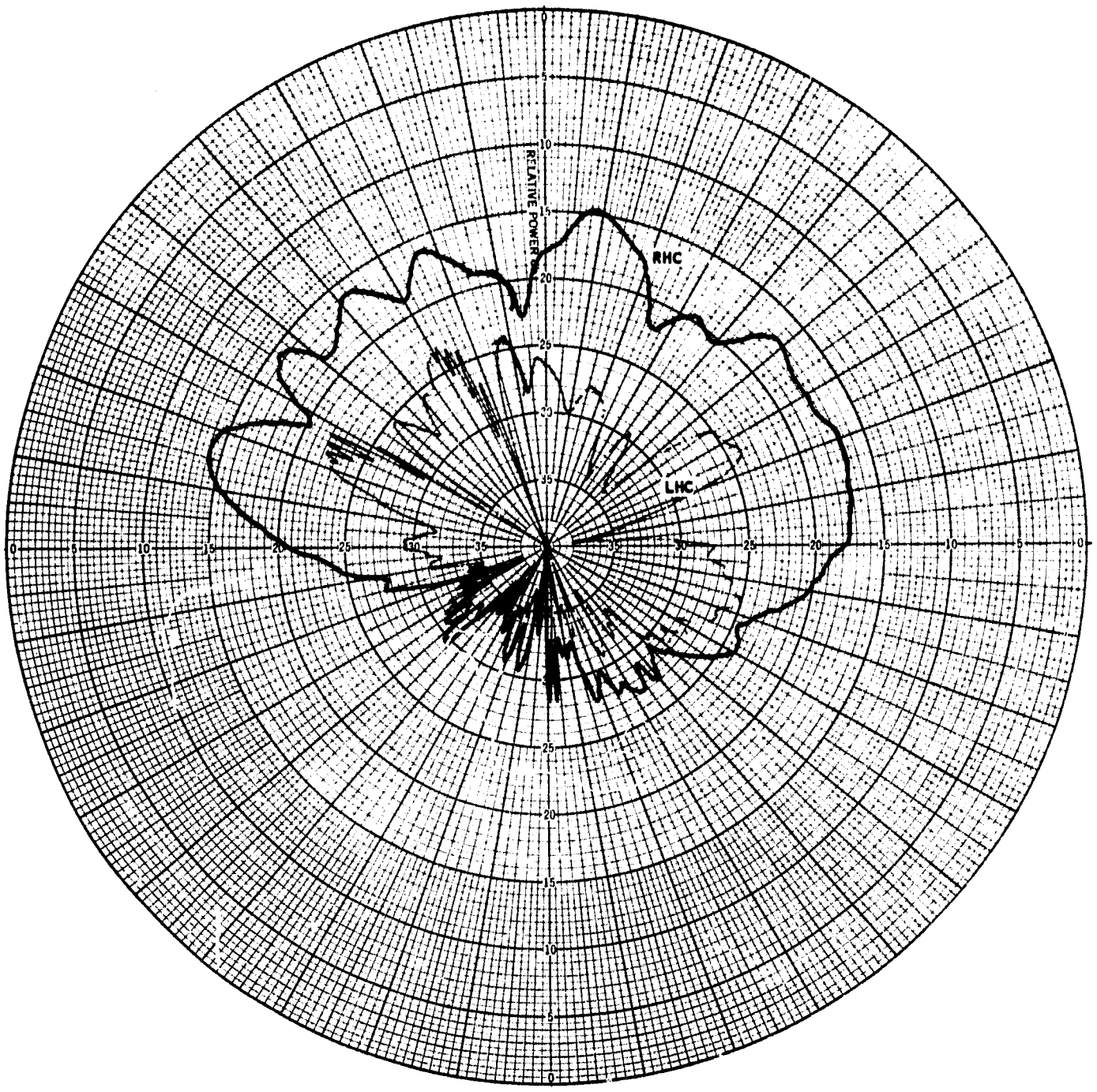

Fig. 21-12

THE JOHNS HOPKINS UNIVERSITY
APPLIED PHYSICS LABORATORY
SILVER SPRING MARYLAND

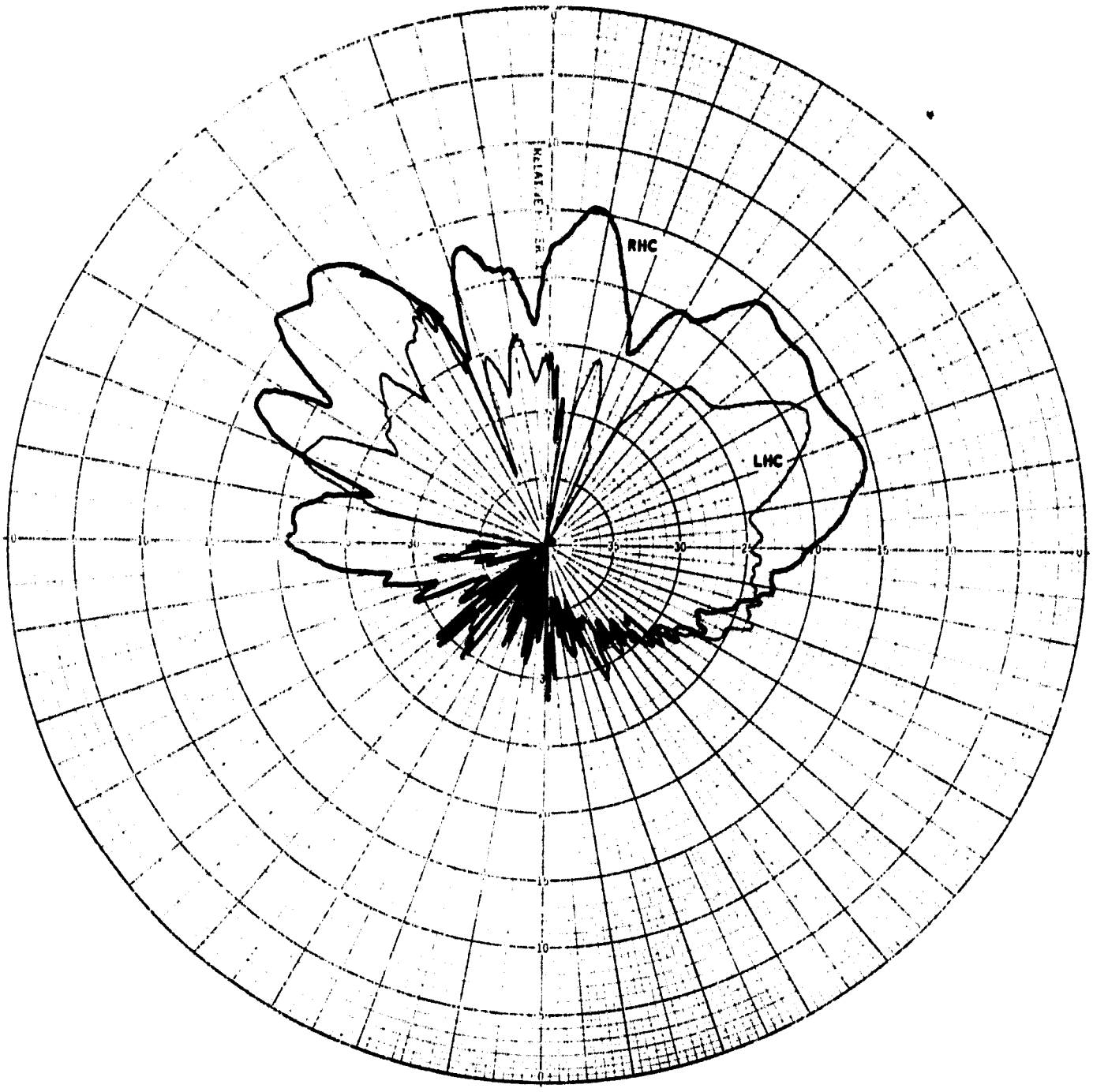

Fig. 21-13

THE JOHNS HOPKINS UNIVERSITY
APPLIED PHYSICS LABORATORY
SILVER SPRING, MARYLAND

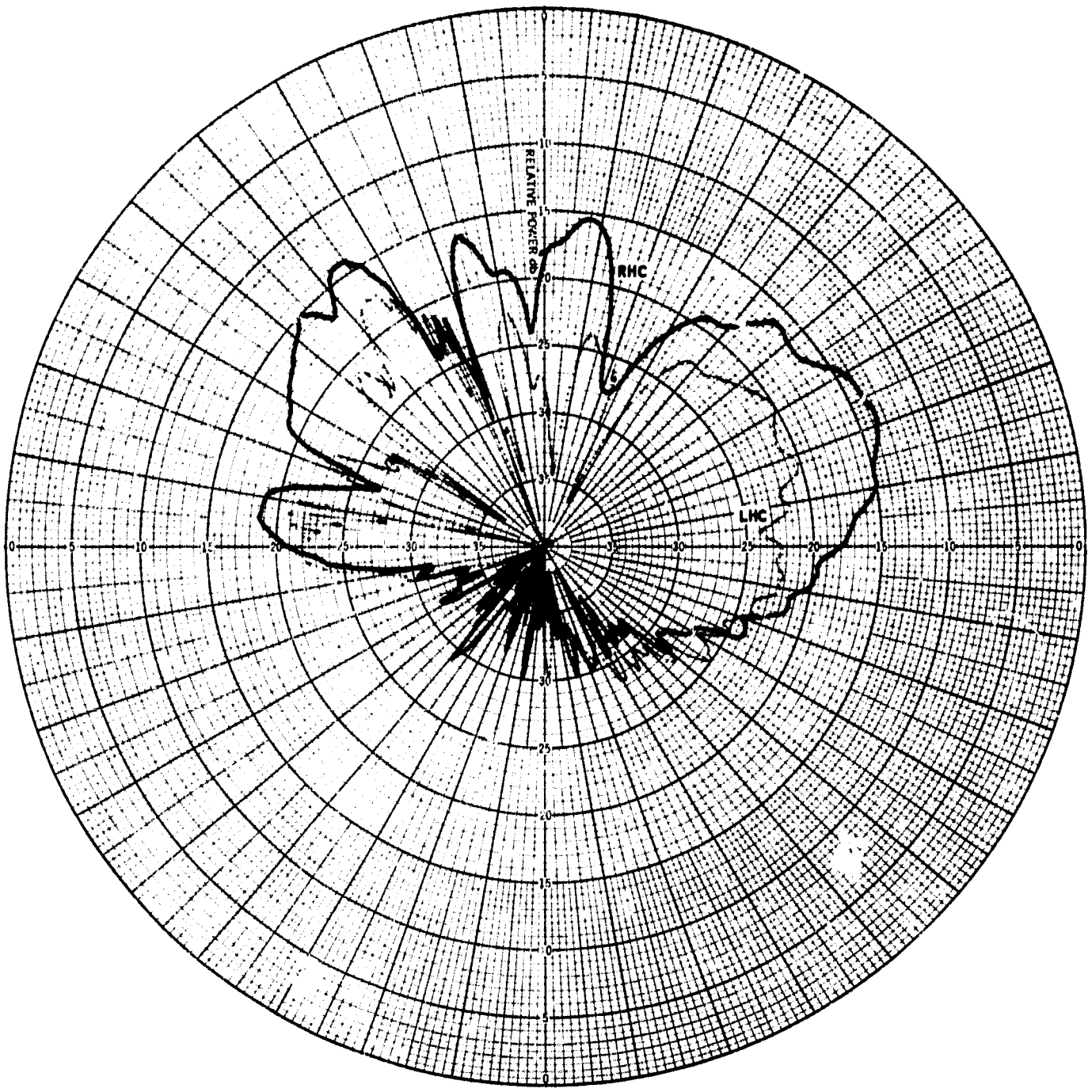

Fig. 21-14

THE JOHNS HOPKINS UNIVERSITY
APPLIED PHYSICS LABORATORY
SILVER SPRING MARYLAND

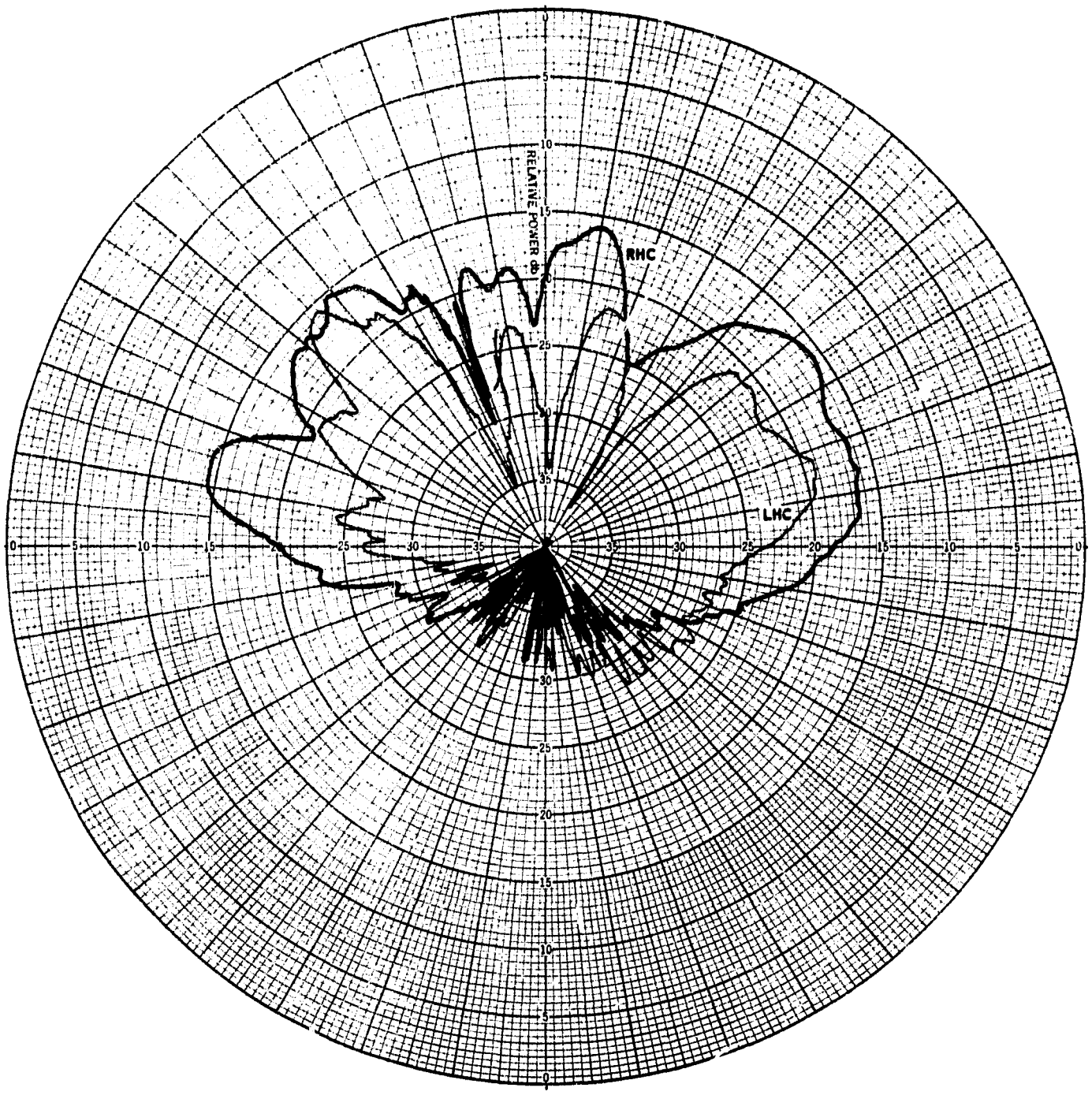

Fig. 21-15

THE JOHNS HOPKINS UNIVERSITY
APPLIED PHYSICS LABORATORY
SILVER SPRING MARYLAND

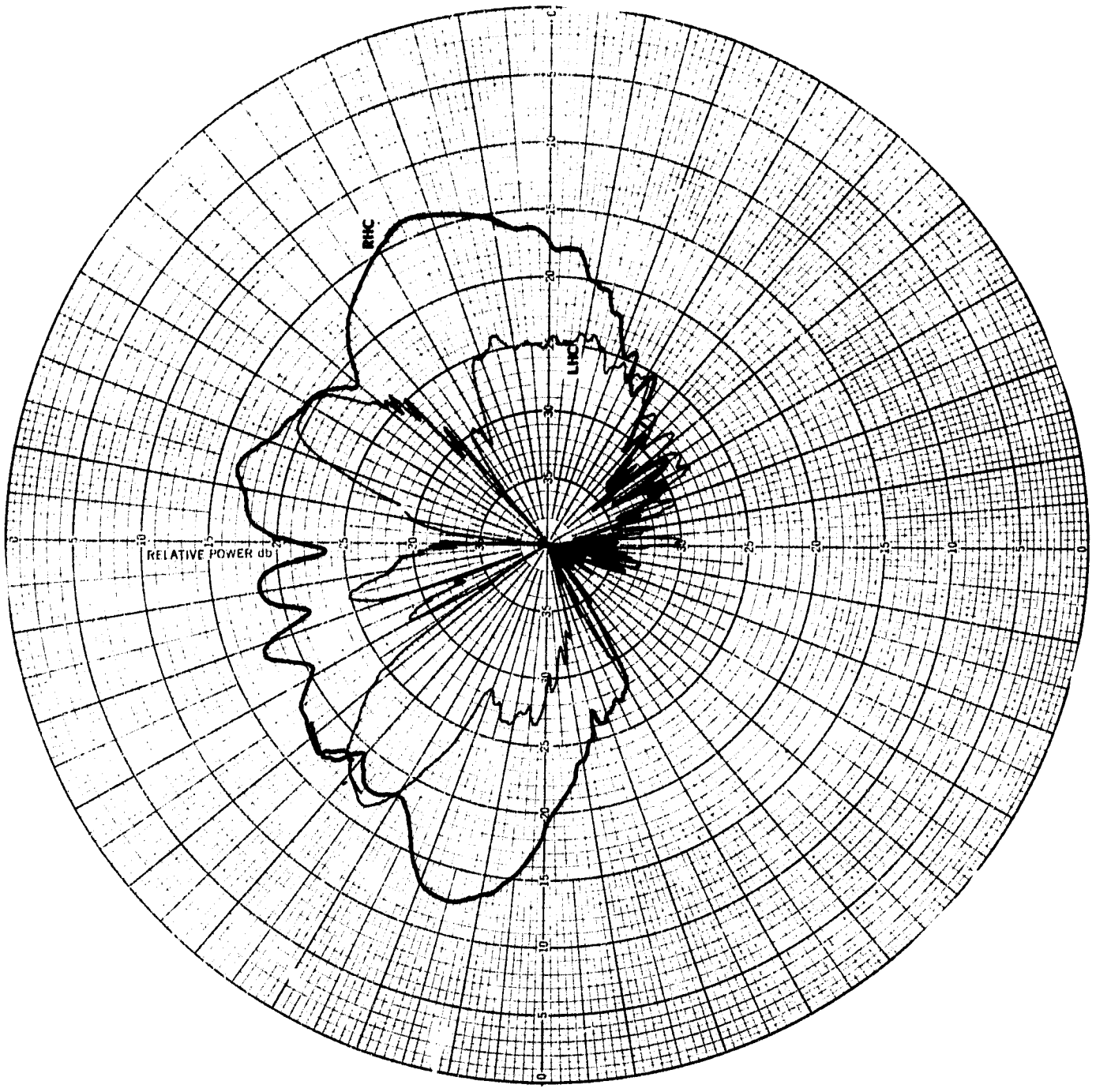

Fig. 21-16

TABLE II

	Frequency	
	1705 mcs	2270 mcs
ϕ = 0	1	9
22.5	2	10
45	3	11
67.5	4	12
90	5	13
112.5	6	14
135	7	15
157.5	8	16

Measured VSWR

The VSWRs of the S-band antennas mounted on the RF mockup are

Frequency	VSWR
1705 mcs	1.28:1
2270 mcs	1.30:1

Flight Qualifications Tests

The tests performed to flight qualify the S-band antennas are exactly similar to those used for the C-band antennas.

VI. C-BAND CAVITY MOUNTED HELICAL ANTENNAS

Each C-band transponder feeds a right hand circular helix mounted in a dielectrically loaded cavity. The antennas are mounted on the body as shown in Drawing No. 7211-0005. Litton Systems, Inc., Amecon Division of Silver Spring, Maryland developed and manufactures the antenna.

Mechanical Details

The antennas as received from Litton are modified by milling the upper flange and drilling mounting holes according to Drawing No. 7211-1300. The

face of the quartz window is painted with two coats of "GEOS" paint for thermal protection. The construction of the antenna is best described by its x-ray (Figure 22).

Principle of Operation

The name "cavity mounted helix" is a misnomer that suggests association with the axial mode helical antenna. Several characteristics of the cavity mounted helix, for example the independence of beamwidth and axial length, make it more coherent to consider it an open ended circular waveguide. The following sections justify this model for the operation of the antenna.

The cutoff wavelengths for circular electric modes in a dielectrically loaded pipe (13) are given by

$$fc = \frac{k \quad c}{2\pi\sqrt{\epsilon_r}a}$$

where k = roots of $J_1'(2\pi a/\lambda)$

J_1' = derivative of the first order Bessel function

a = pipe radius

c = velocity of light in vacuum

For the silver plated quartz cylinder of the antenna,

$$\sqrt{\epsilon_r} = 1.94, \quad a = .5" = 1.27 \text{ cm}$$

For the dominant mode ($TE1_{11}$), k = 1.841 and

fc = 3600 mcs

For the next higher modes TM_{01}, fc = 4650 mcs

TE_{21} fc = 5900 mcs

At the GEOS C-band frequencies, the quartz loaded cavity will support the dominant TE_{11} mode and the higher order TM_{01} mode.

Mode Generation

A helical antenna operating in the axial mode will generate a circularly polarized TE_{11} mode wave when placed in a circular guide[14]. The TM_{01} mode will not be excited to any significant degree. The dimensions of the helix imbedded in the quartz dielectric ($D = 1.01\lambda$) cause it to operate in the

THE JOHNS HOPKINS UNIVERSITY
APPLIED PHYSICS LABORATORY
SILVER SPRING MARYLAND

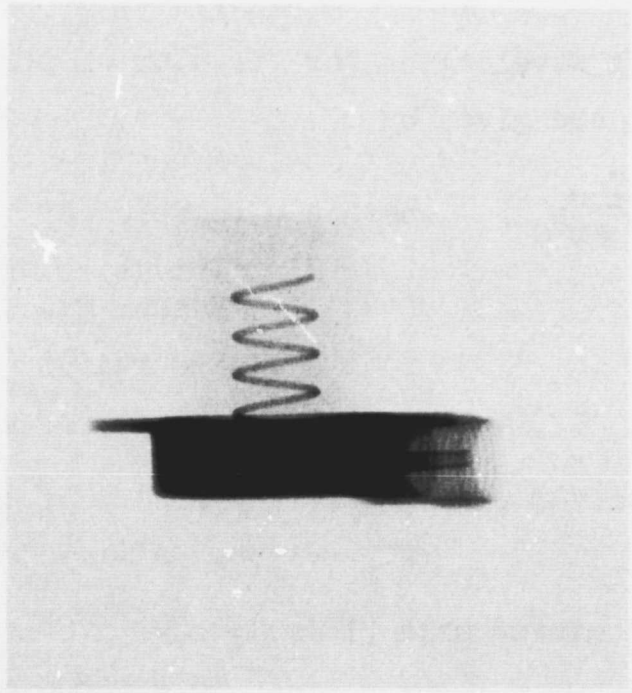

Fig. 22 X-RAY OF CONSTRUCTION OF ANTENNA

axial mode.

Characteristics of the Cavity Mounted Helix

The radiation pattern of the cavity helix is independent of the number of turns provided it is greater than 2. The input impedance is nominally 50Ω over its range of operation. The cavity helix has nearly a decade bandwidth corresponding to axial mode operation of the helix.

GEOS-B C-Band Antenna Measured Data

Measured VSWR - The VSWR of the antennas when mounted on the RF mockup was less than 1.3:1 at both frequencies.

Measured Radiation Patterns - The radiation patterns (Figure 23) of the antennas mounted on the RF mockup were taken on the S2T-4 antenna range (Figure 8), using the standard spherical coordinate system (Figure 9). Table III lists the pattern numbers for a particular antenna, frequency and angle. The isotropic level falls at 10db on the charts.

TABLE III. Antenna Serial Number

	1153 (Inboard)		1237 (Outboard)	
	Frequency		Frequency	
	5690 mcs	5765 mcs	5690 mcs	5765 mcs
$\phi = 0$	1	9	17	25
22.5	2	10	18	26
45	3	11	19	27
67.5	4	12	20	28
90	5	13	21	29
112.5	6	14	22	30
135	7	15	23	31
157.5	8	16	24	32

Fig. 23 C-BAND MEASURED RADIATION PATTERNS

THE JOHNS HOPKINS UNIVERSITY
APPLIED PHYSICS LABORATORY
SILVER SPRING MARYLAND

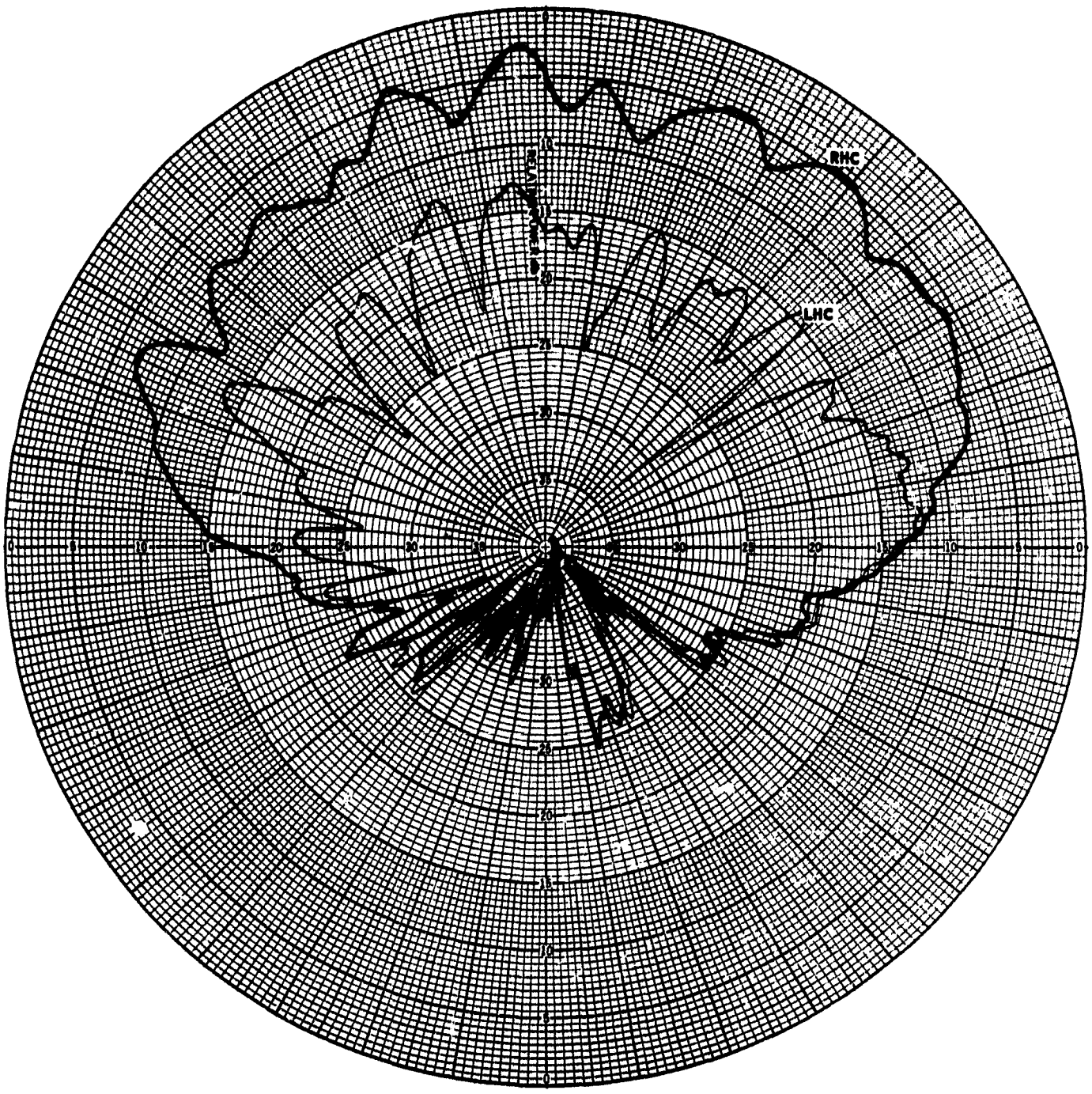

Fig. 23-1

THE JOHNS HOPKINS UNIVERSITY
APPLIED PHYSICS LABORATORY
SILVER SPRING MARYLAND

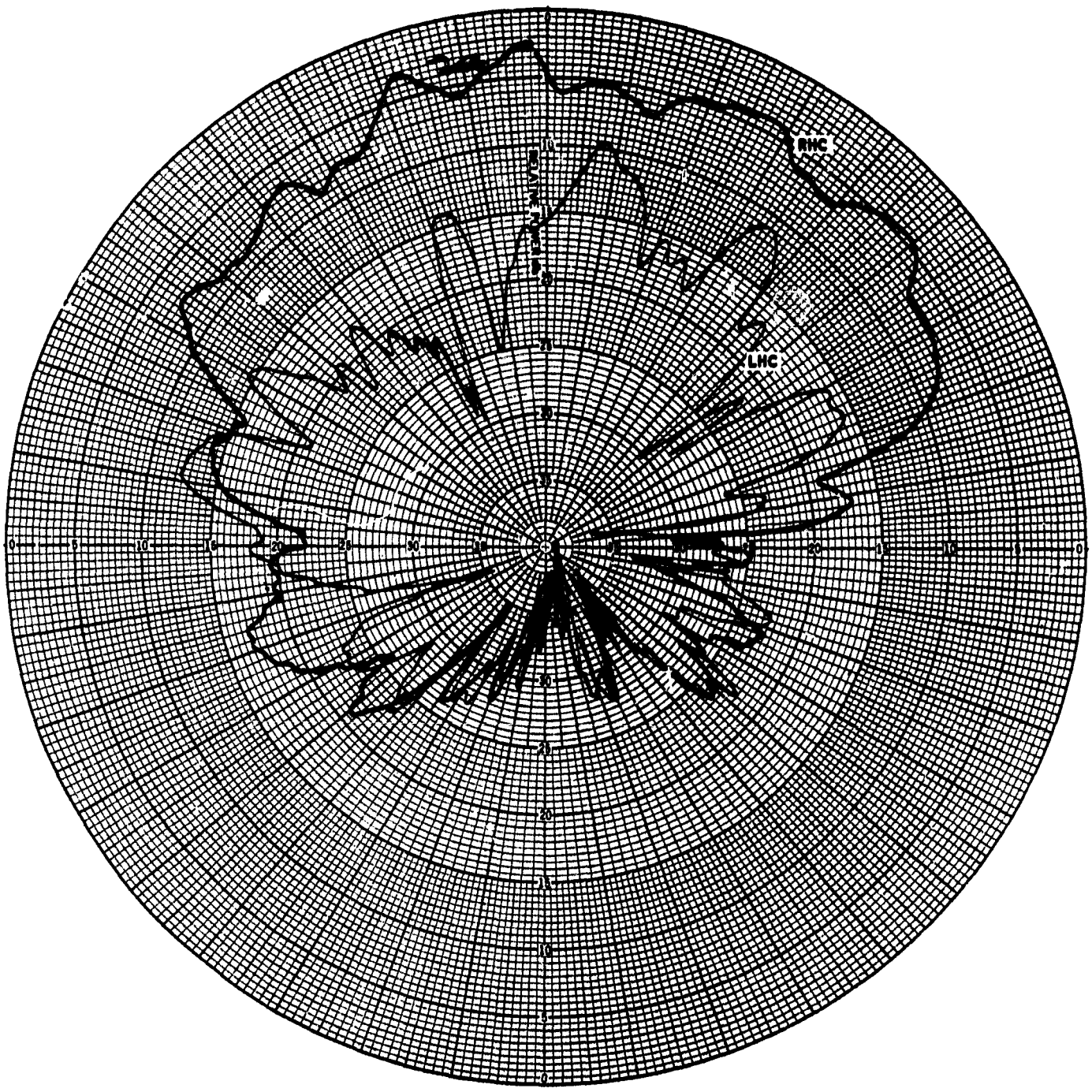

Fig. 23-2

THE JOHNS HOPKINS UNIVERSITY
APPLIED PHYSICS LABORATORY
SILVER SPRING MARYLAND

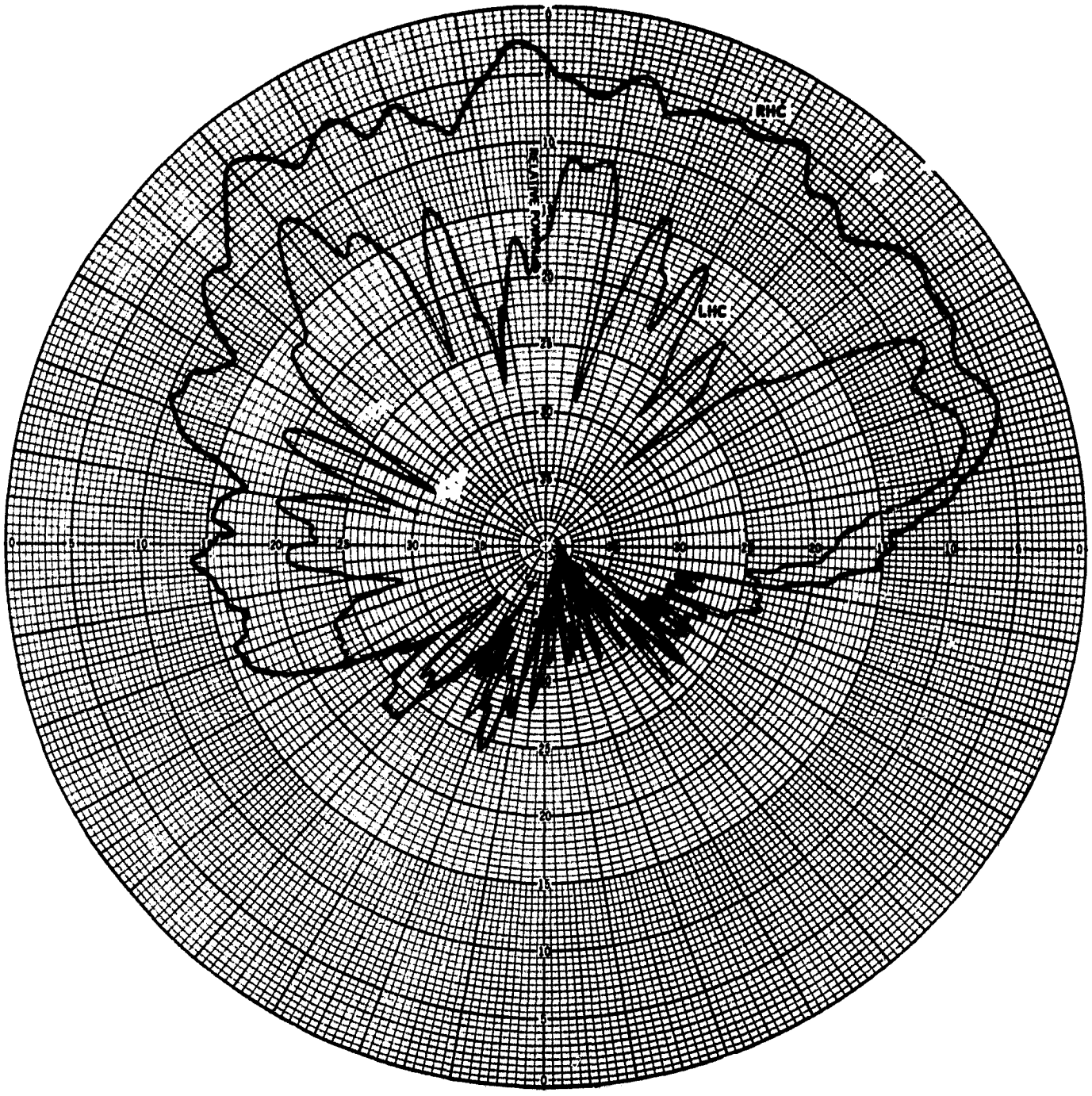

Fig. 23-3

THE JOHNS HOPKINS UNIVERSITY
APPLIED PHYSICS LABORATORY
SILVER SPRING MARYLAND

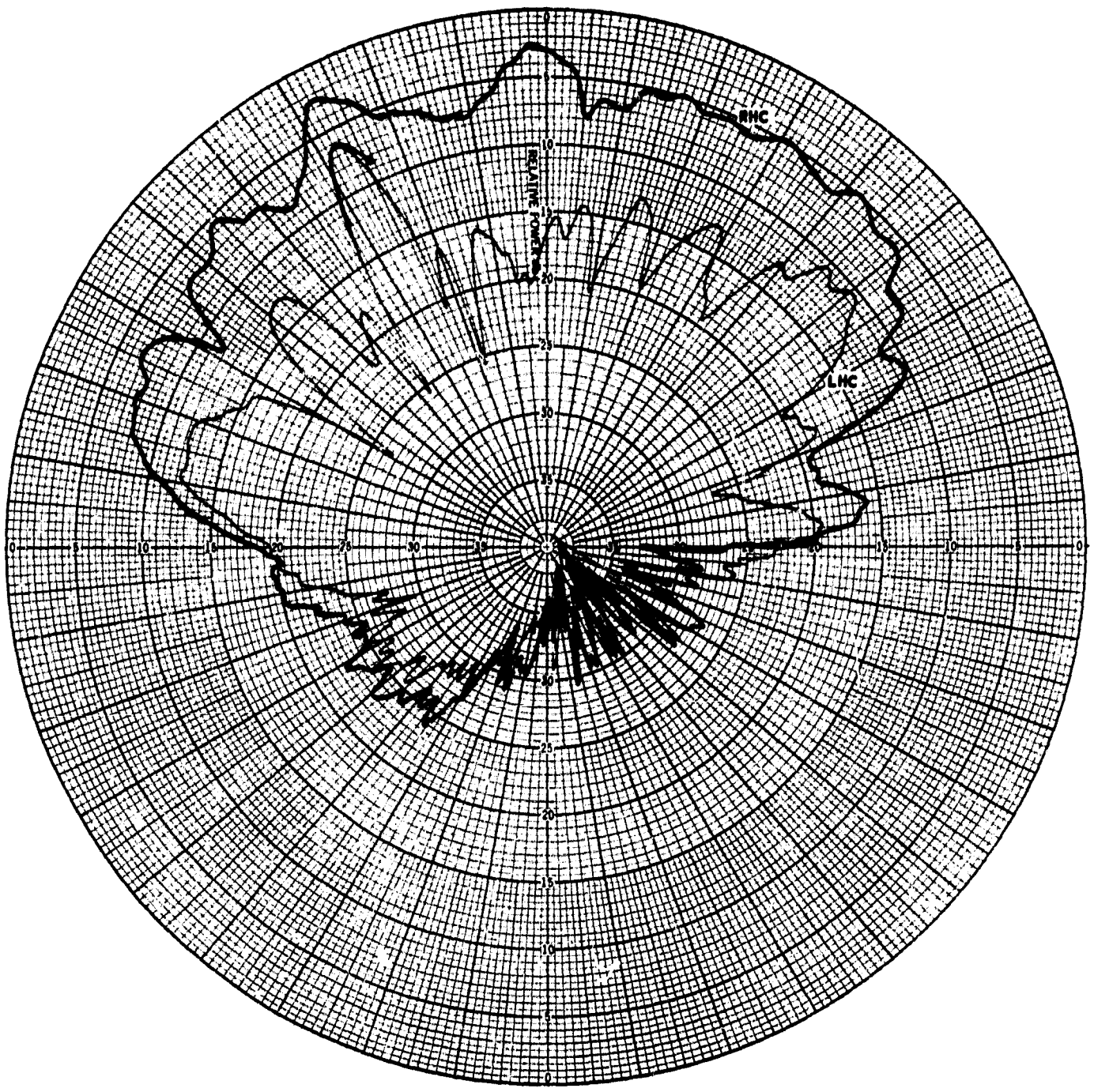

Fig. 23-4

THE JOHNS HOPKINS UNIVERSITY
APPLIED PHYSICS LABORATORY
SILVER SPRING MARYLAND

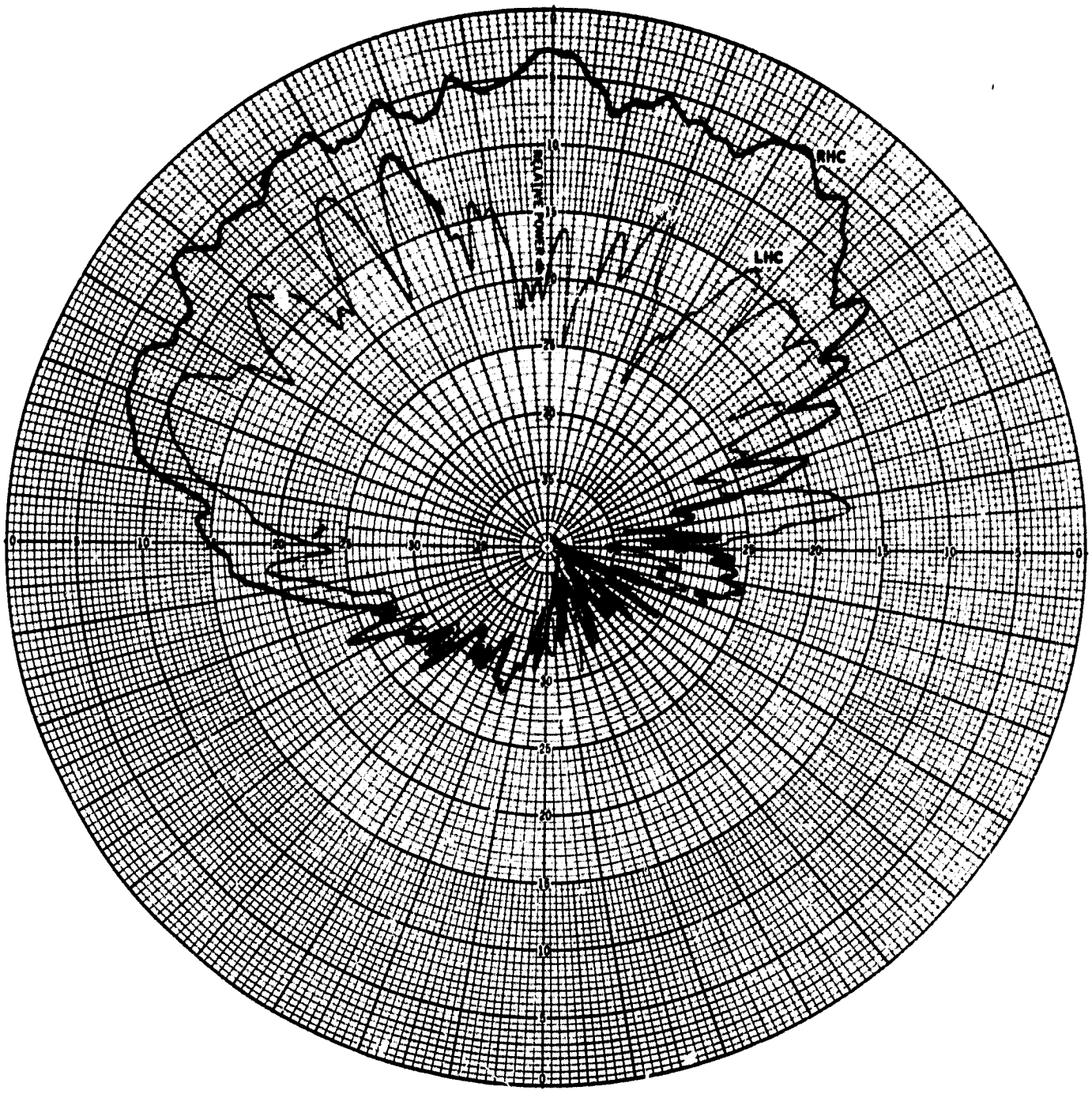

Fig. 23-5

THE JOHNS HOPKINS UNIVERSITY
APPLIED PHYSICS LABORATORY
SILVER SPRING MARYLAND

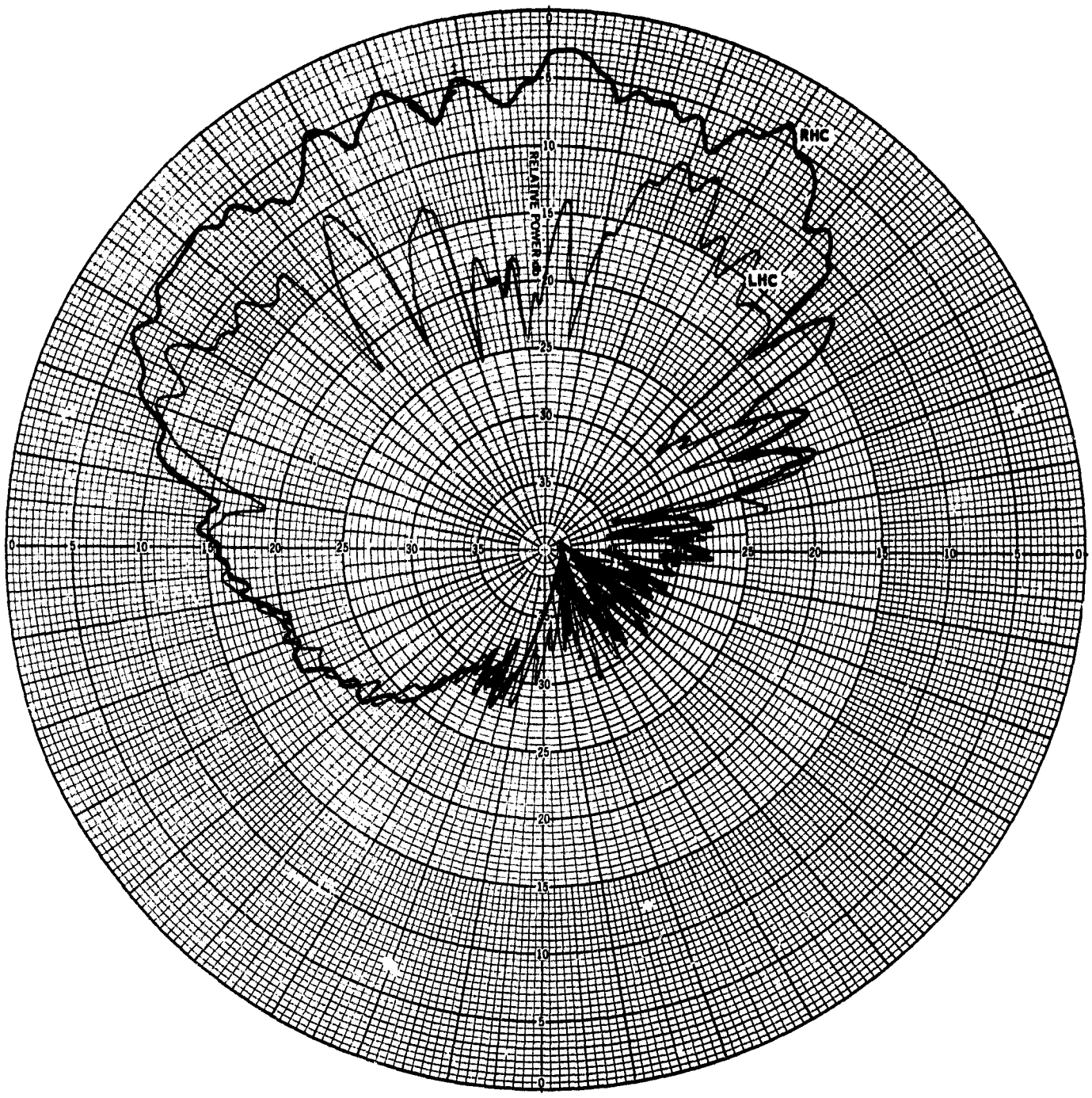

Fig. 23-6

THE JOHNS HOPKINS UNIVERSITY
APPLIED PHYSICS LABORATORY
SILVER SPRING MARYLAND

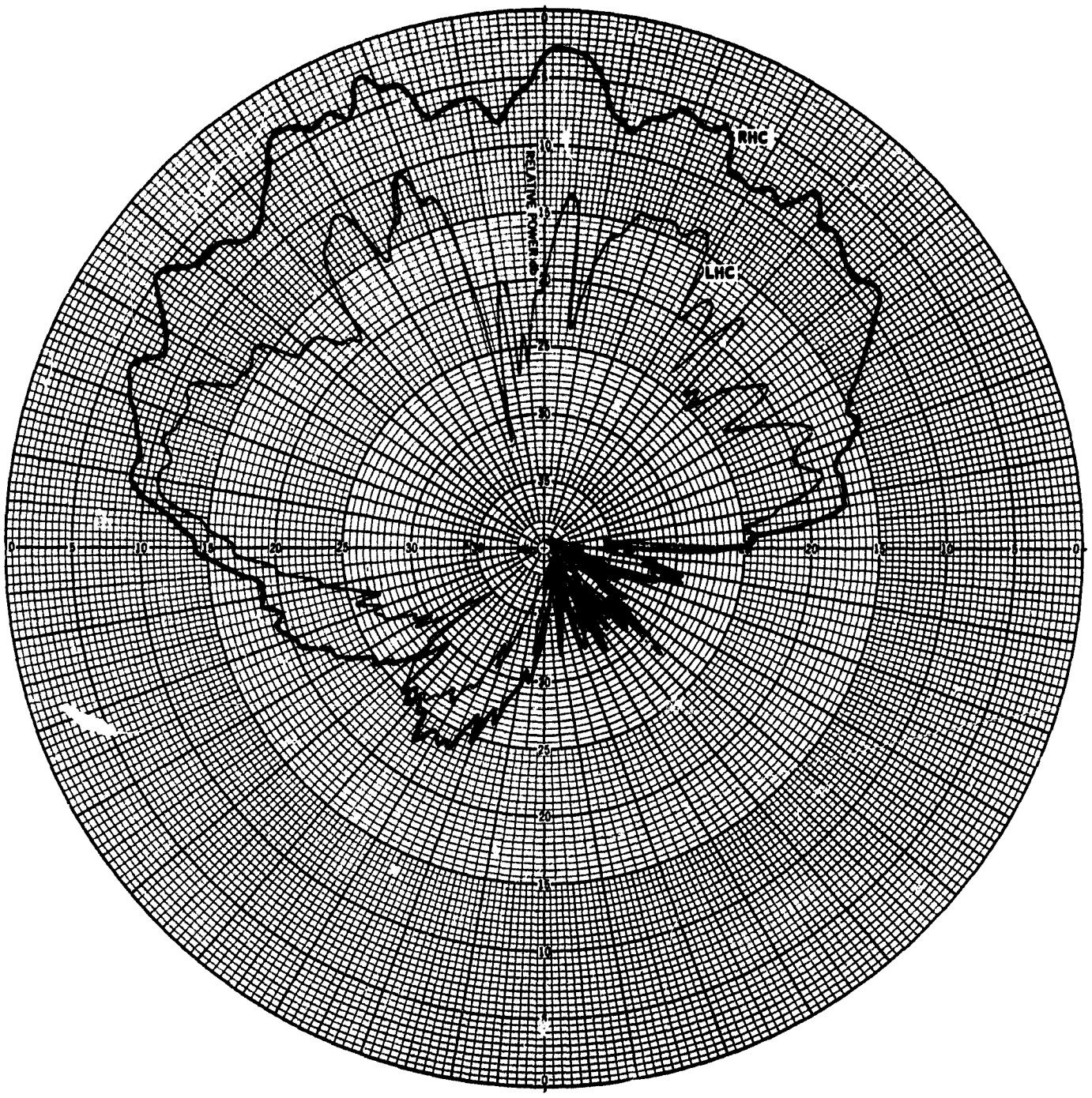

Fig. 23-7

THE JOHNS HOPKINS UNIVERSITY
APPLIED PHYSICS LABORATORY
SILVER SPRING, MARYLAND

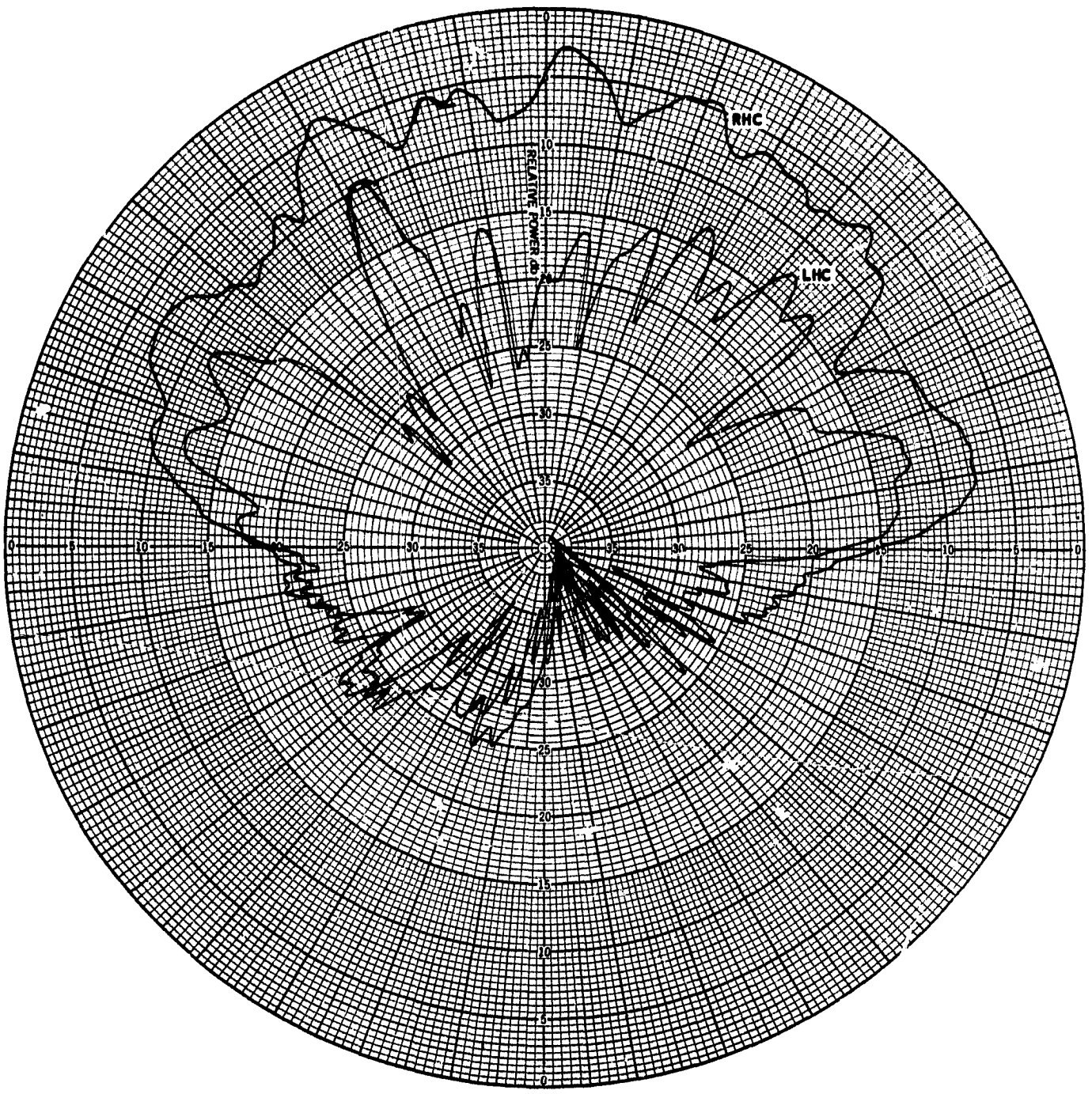

Fig. 23-8

THE JOHNS HOPKINS UNIVERSITY
APPLIED PHYSICS LABORATORY
SILVER SPRING MARYLAND

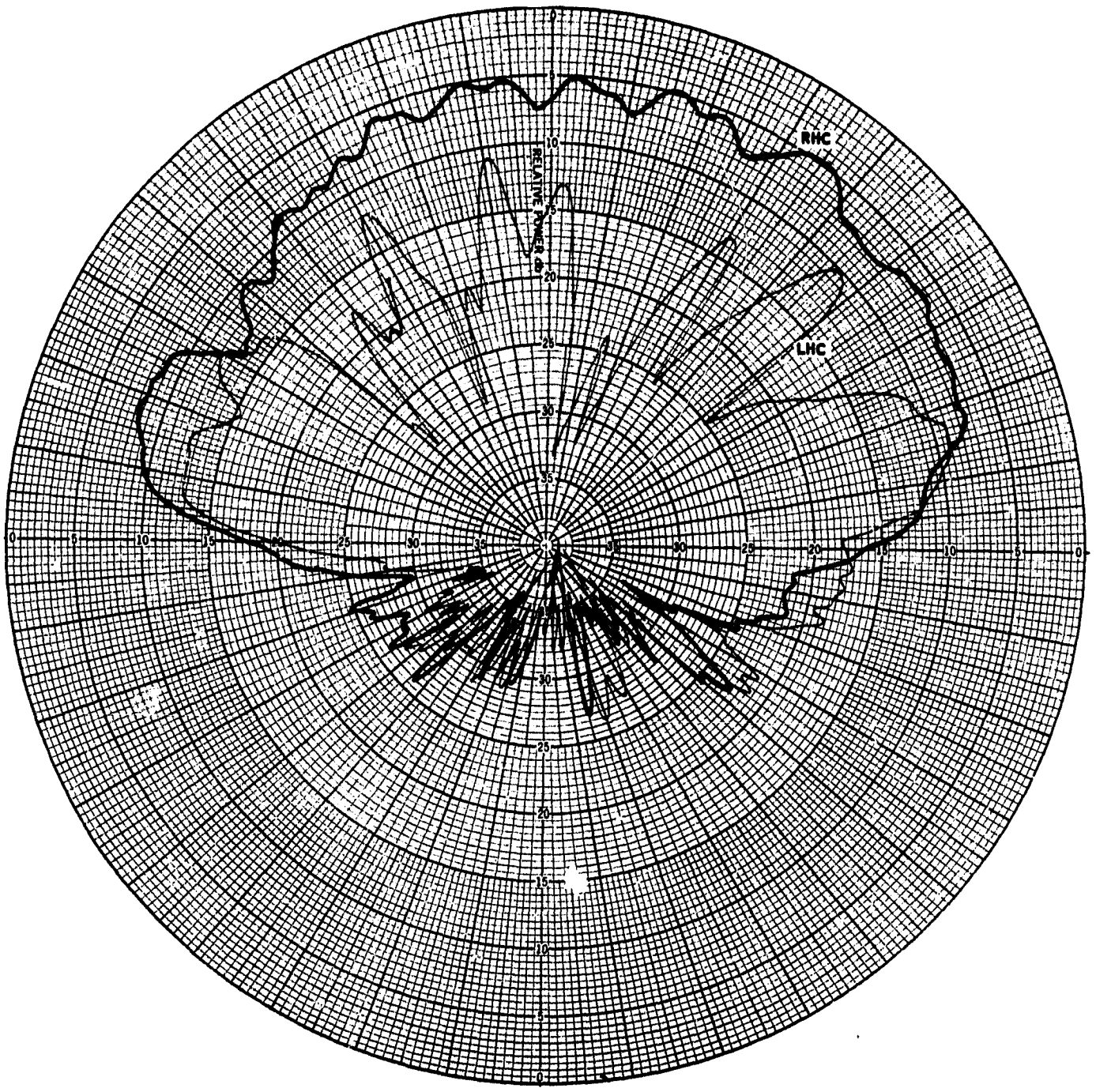

Fig. 23-9

THE JOHNS HOPKINS UNIVERSITY
APPLIED PHYSICS LABORATORY
SILVER SPRING, MARYLAND

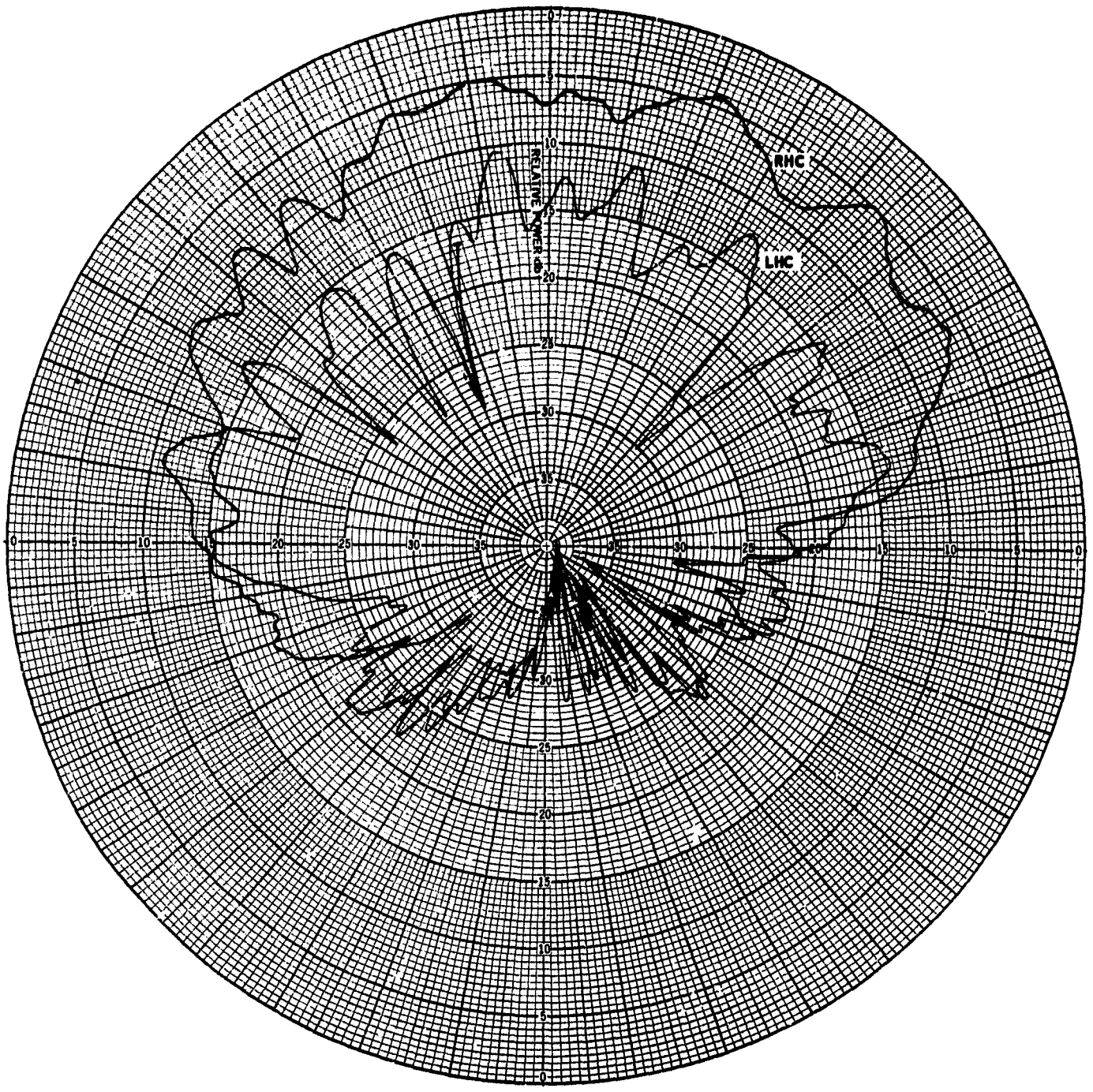

Fig. 23-10

THE JOHNS HOPKINS UNIVERSITY
APPLIED PHYSICS LABORATORY
SILVER SPRING MARYLAND

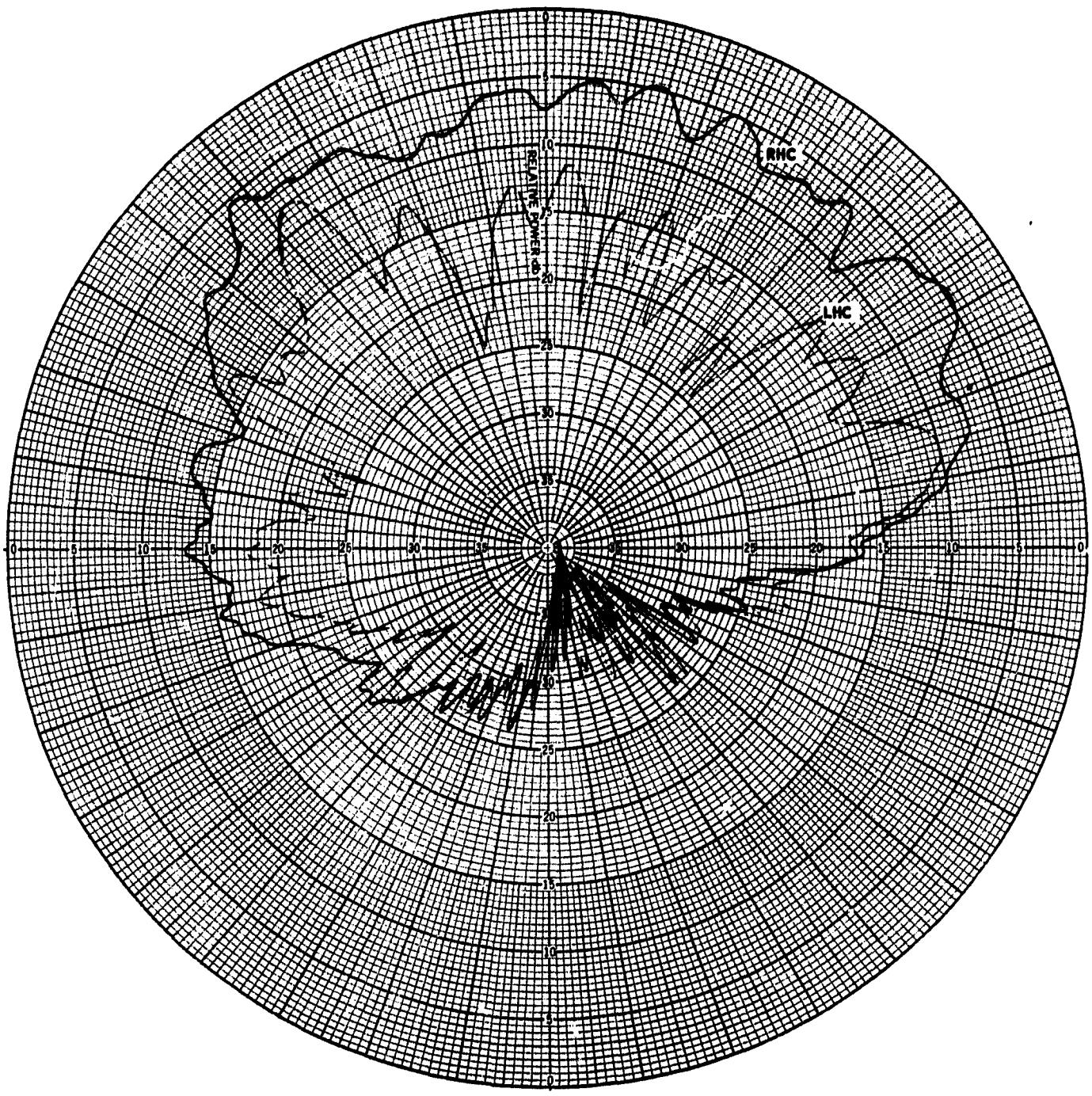

Fig. 23-11

THE JOHNS HOPKINS UNIVERSITY
APPLIED PHYSICS LABORATORY
SILVER SPRING MARYLAND

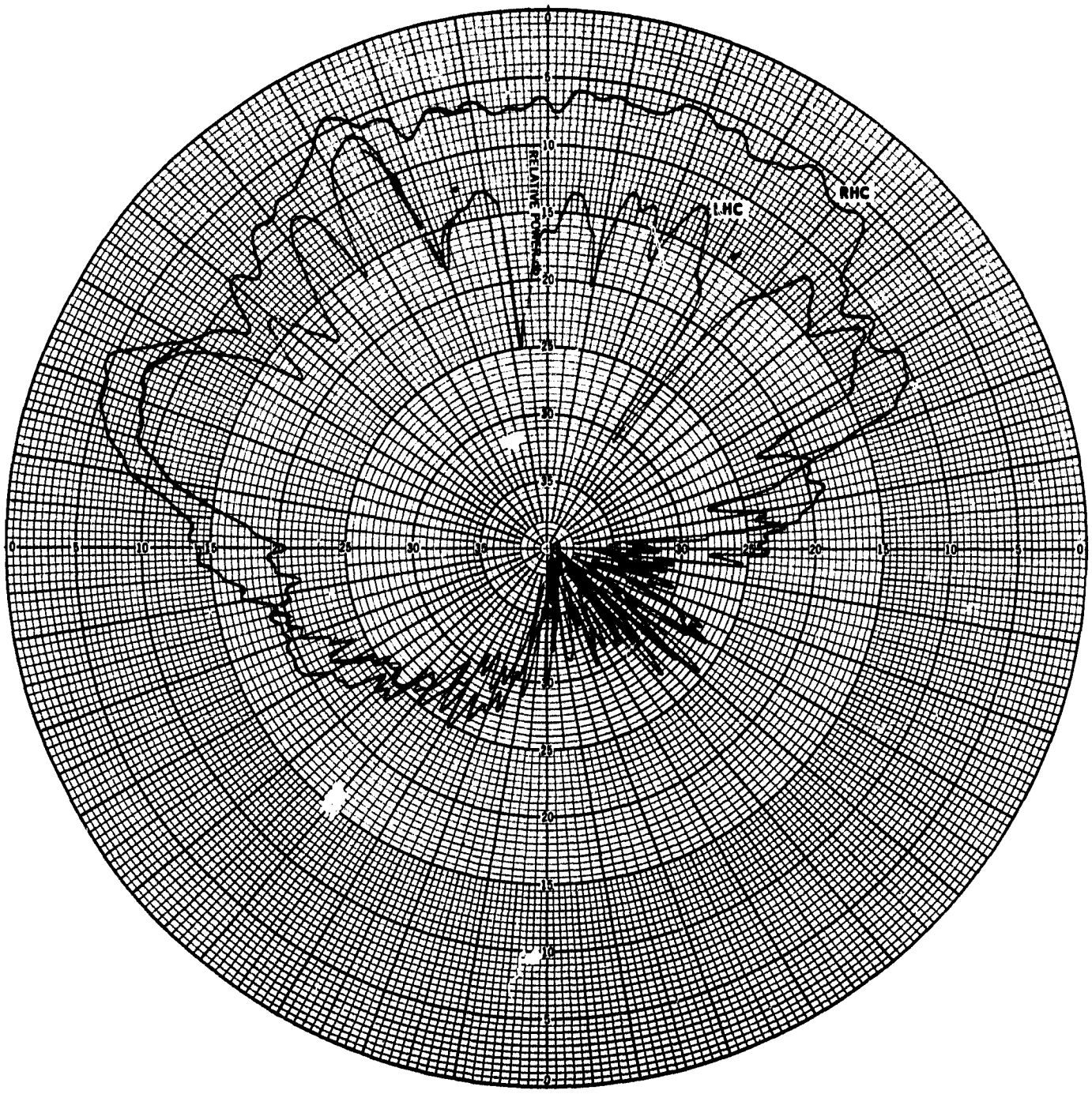

Fig. 23-12

THE JOHNS HOPKINS UNIVERSITY
APPLIED PHYSICS LABORATORY
SILVER SPRING MARYLAND

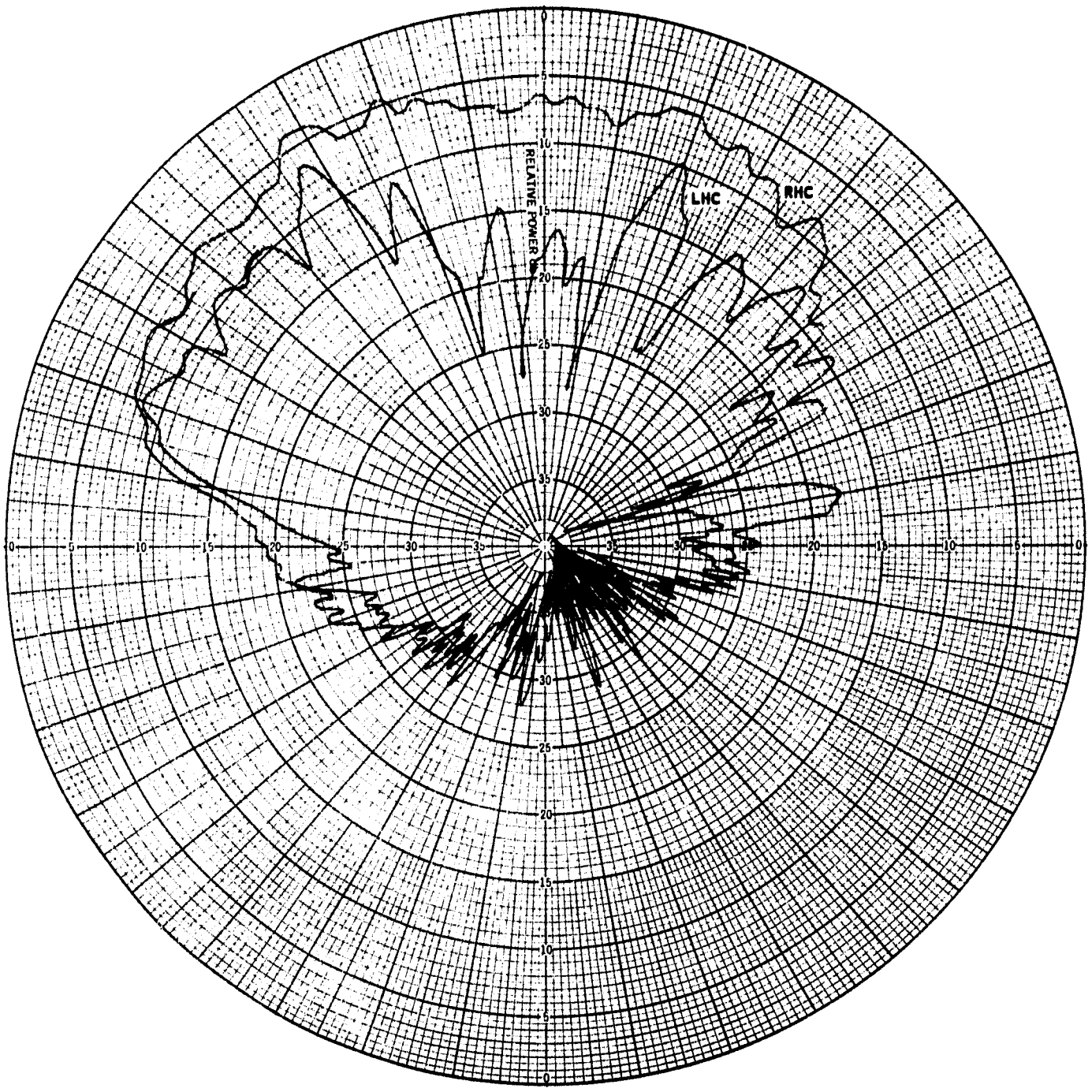

Fig. 23-13

THE JOHNS HOPKINS UNIVERSITY
APPLIED PHYSICS LABORATORY
SILVER SPRING MARYLAND

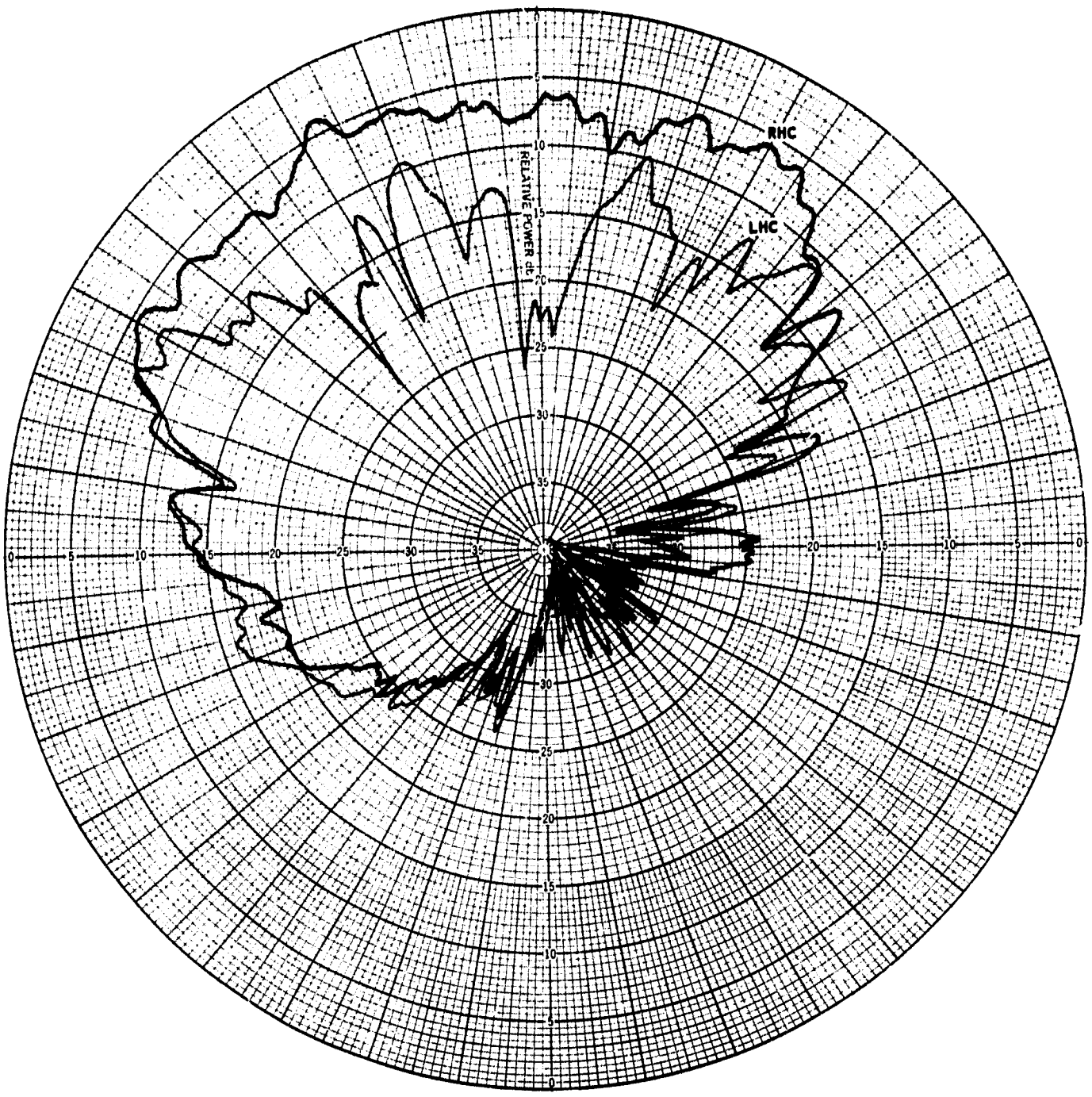

Fig. 23-14

THE JOHNS HOPKINS UNIVERSITY
APPLIED PHYSICS LABORATORY
SILVER SPRING MARYLAND

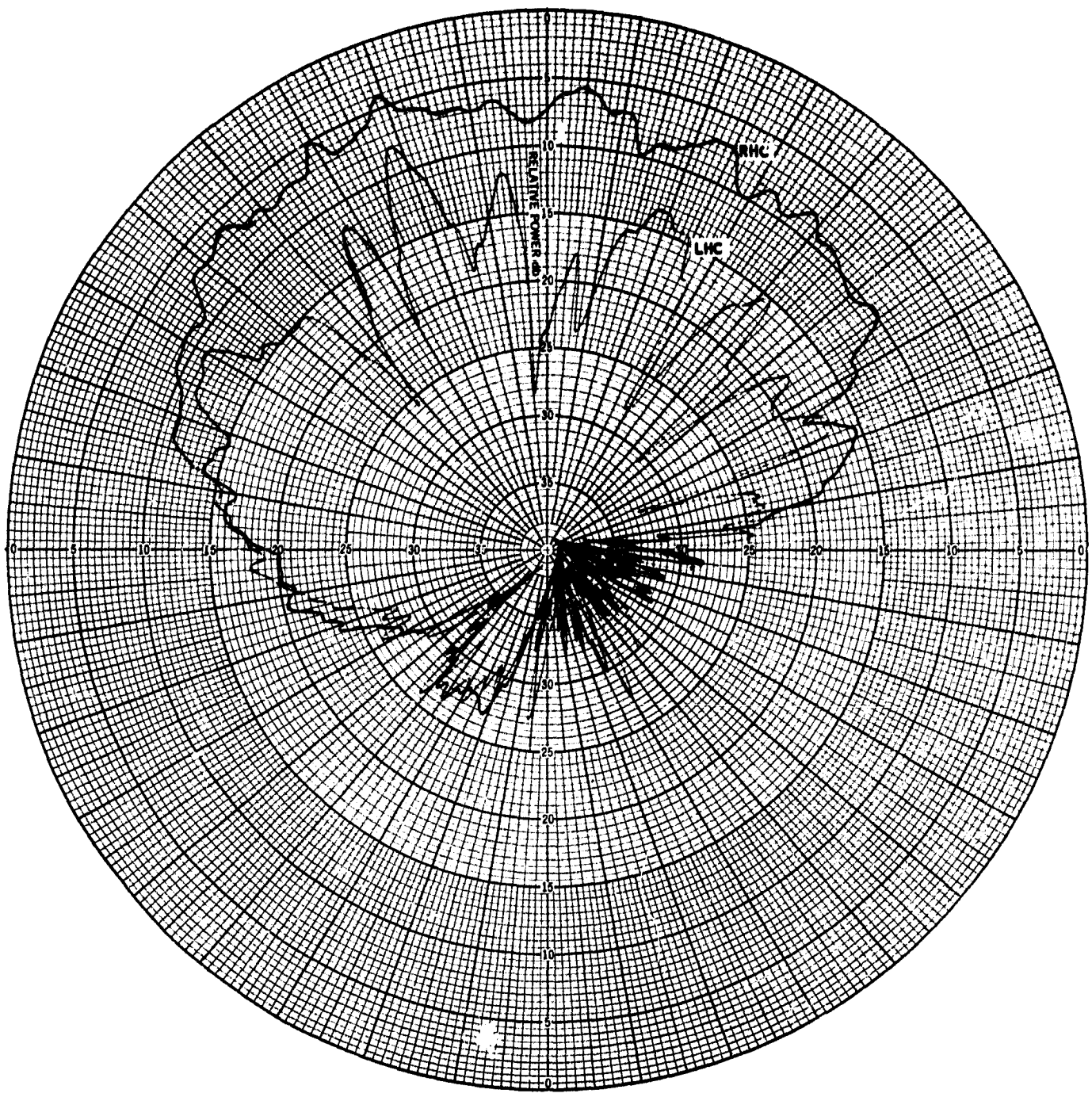

Fig. 23-15

THE JOHNS HOPKINS UNIVERSITY
APPLIED PHYSICS LABORATORY
SILVER SPRING MARYLAND

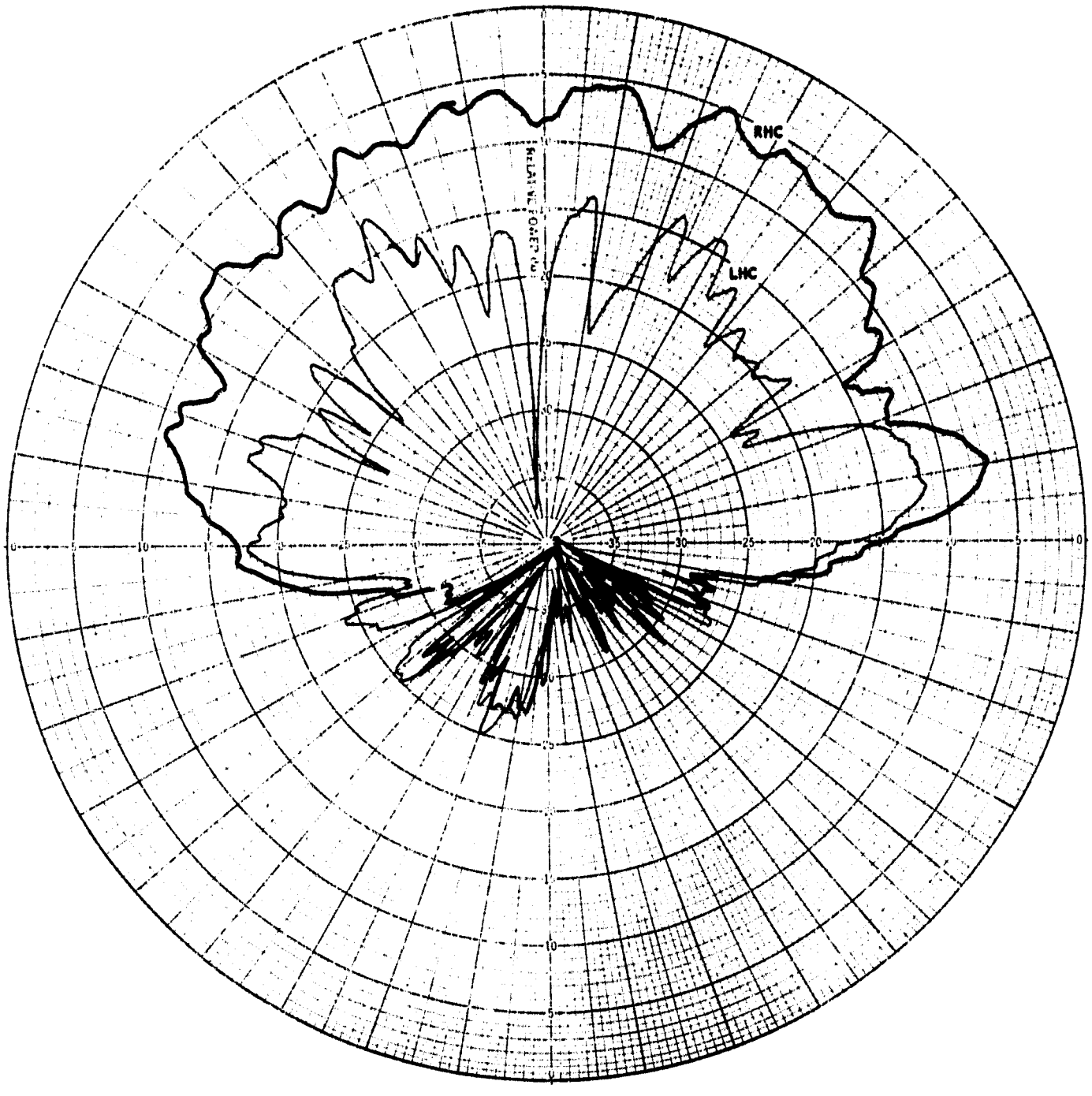

Fig. 23-16

THE JOHNS HOPKINS UNIVERSITY
APPLIED PHYSICS LABORATORY
SILVER SPRING MARYLAND

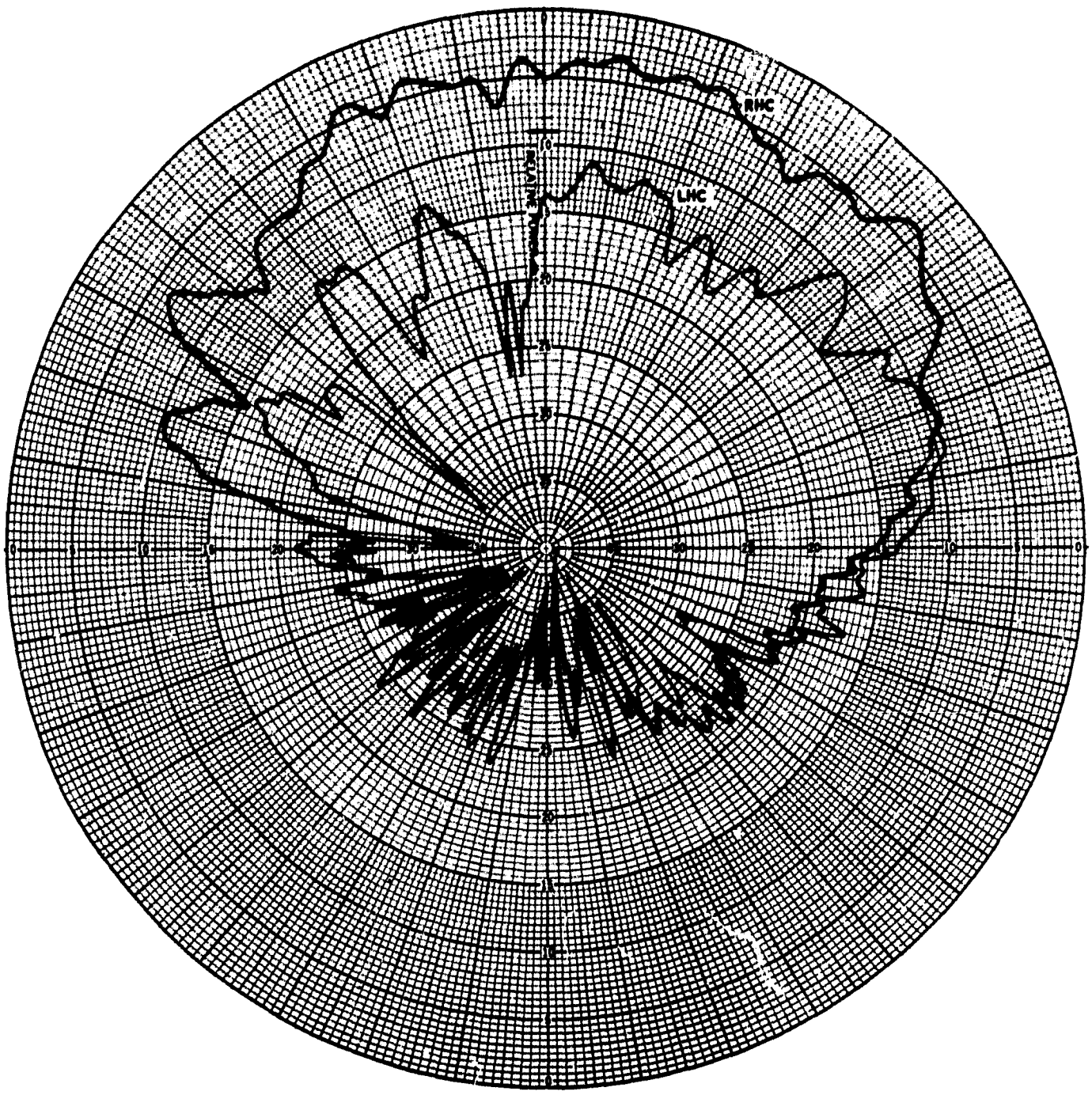

Fig. 23-17

THE JOHNS HOPKINS UNIVERSITY
APPLIED PHYSICS LABORATORY
SILVER SPRING MARYLAND

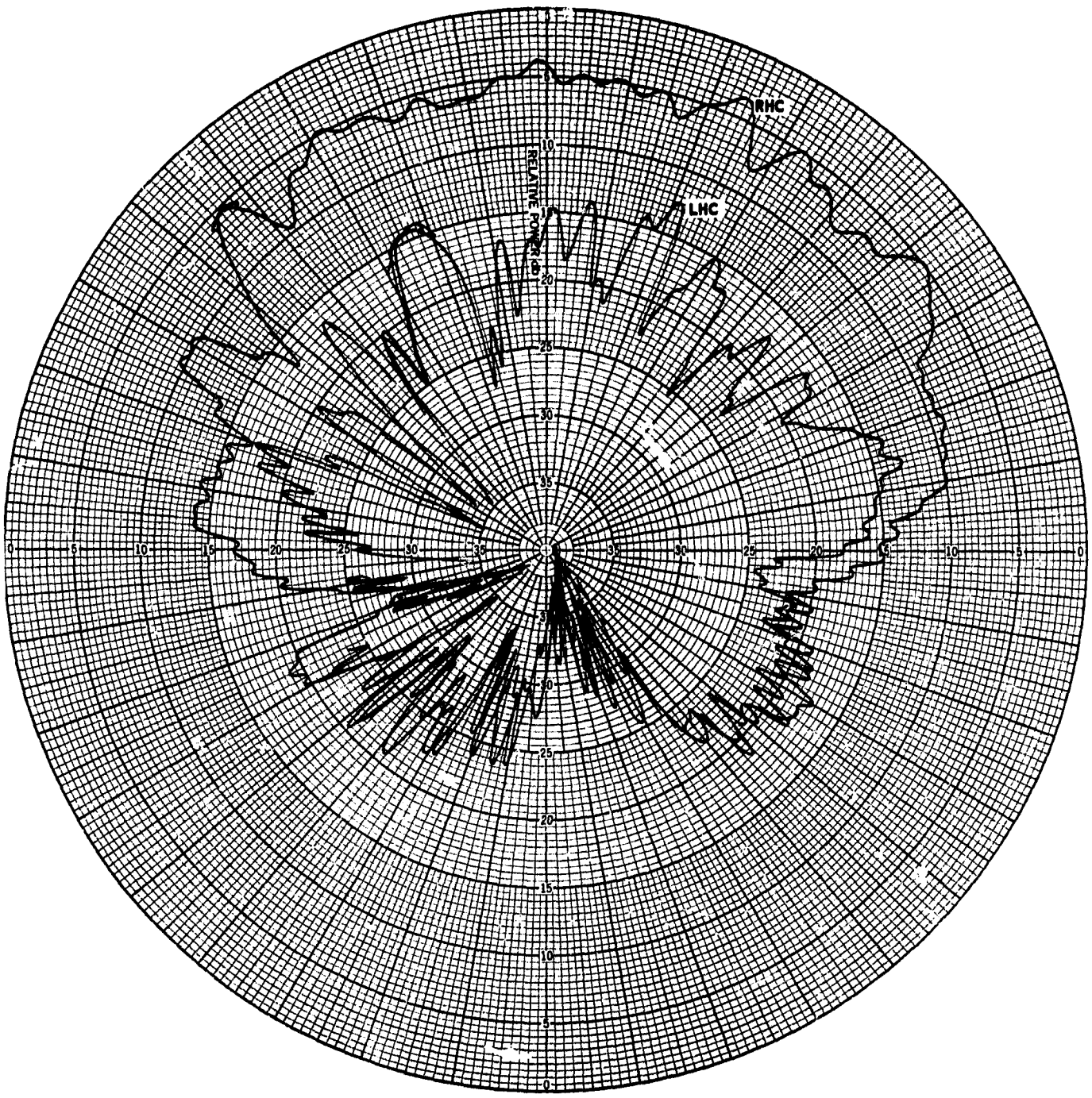

Fig. 23-18

THE JOHNS HOPKINS UNIVERSITY
APPLIED PHYSICS LABORATORY
SILVER SPRING MARYLAND

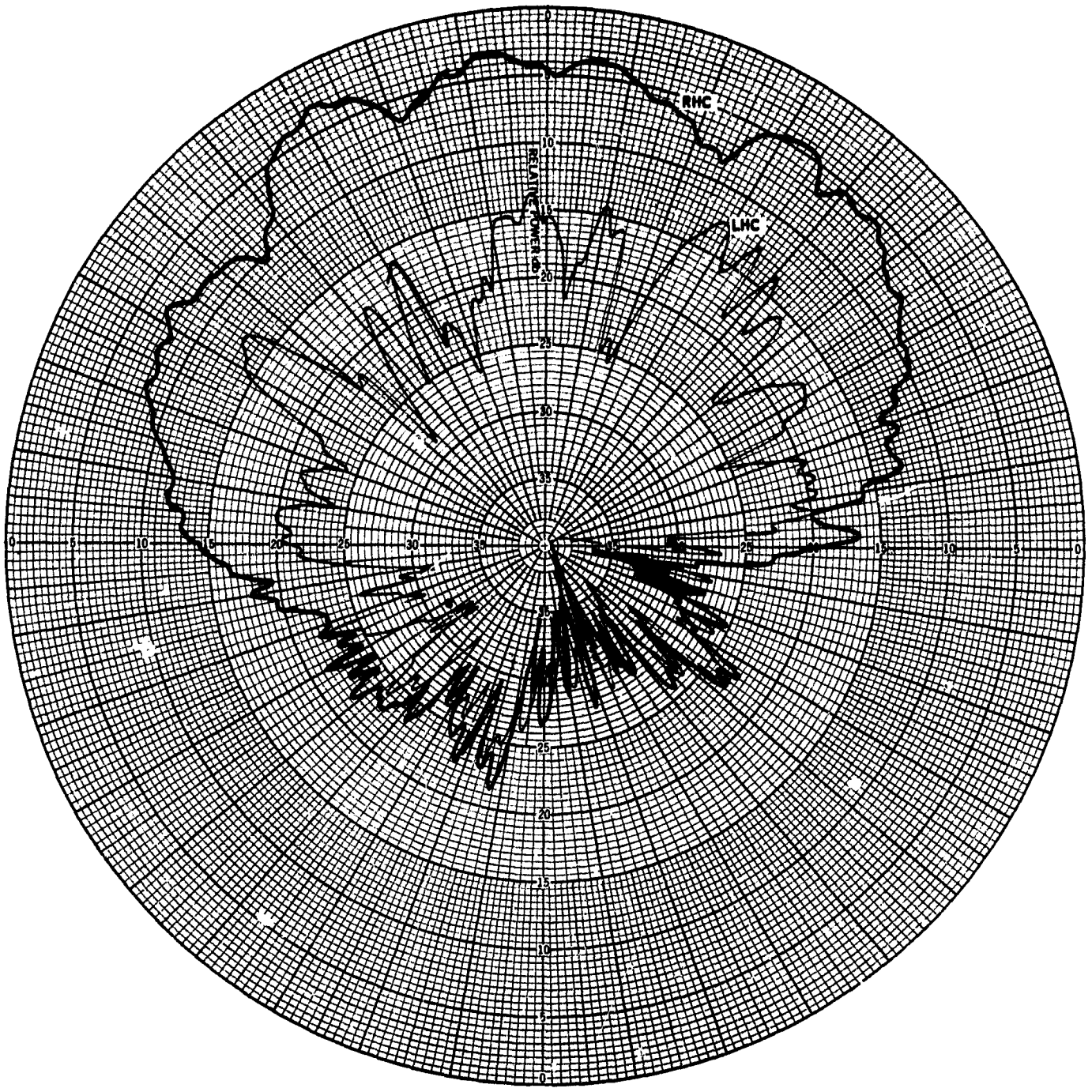

Fig. 23-19

THE JOHNS HOPKINS UNIVERSITY
APPLIED PHYSICS LABORATORY
SILVER SPRING MARYLAND

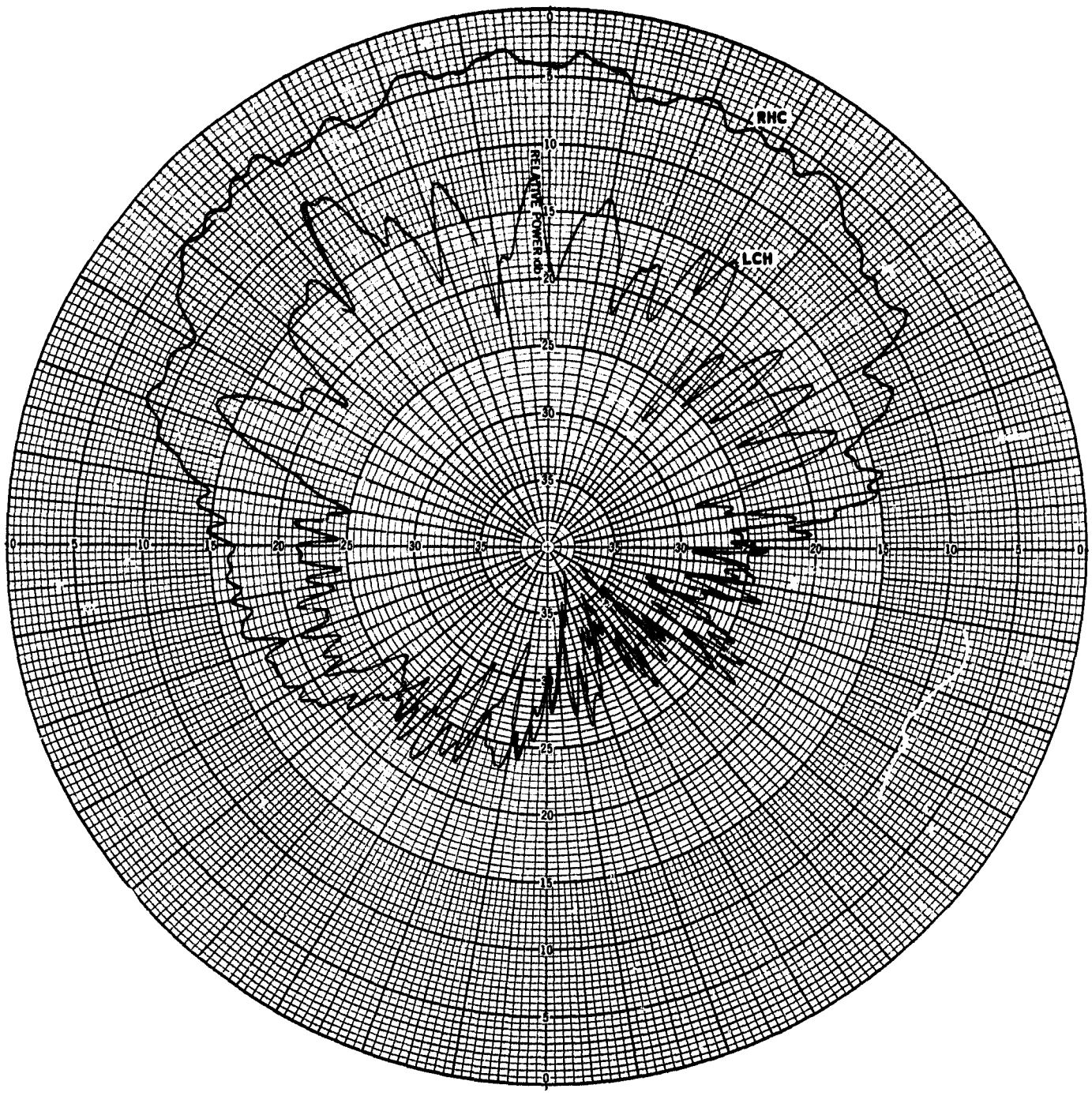

Fig. 23-20

THE JOHNS HOPKINS UNIVERSITY
APPLIED PHYSICS LABORATORY
SILVER SPRING MARYLAND

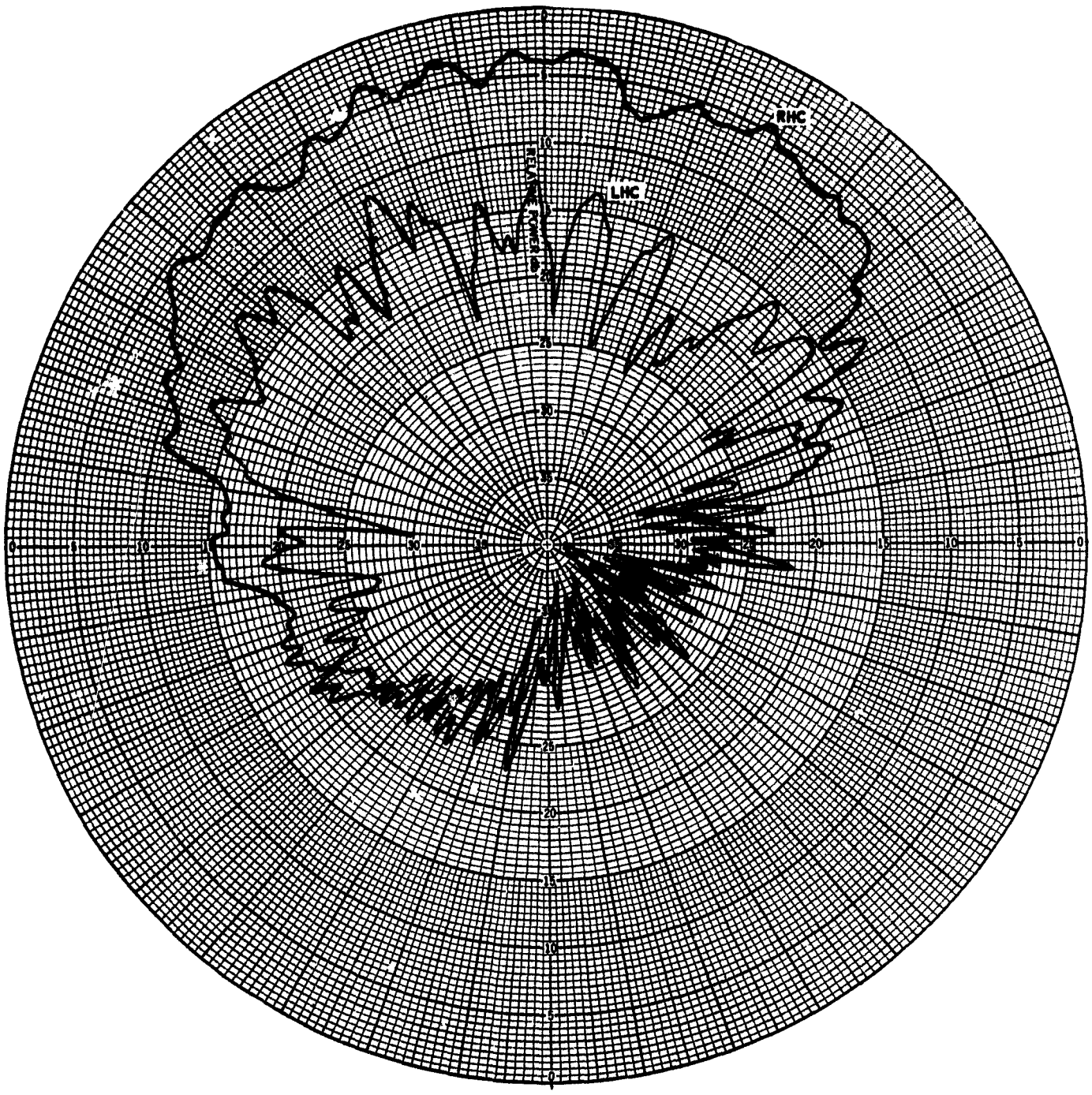

Fig. 23-21

THE JOHNS HOPKINS UNIVERSITY
APPLIED PHYSICS LABORATORY
SILVER SPRING MARYLAND

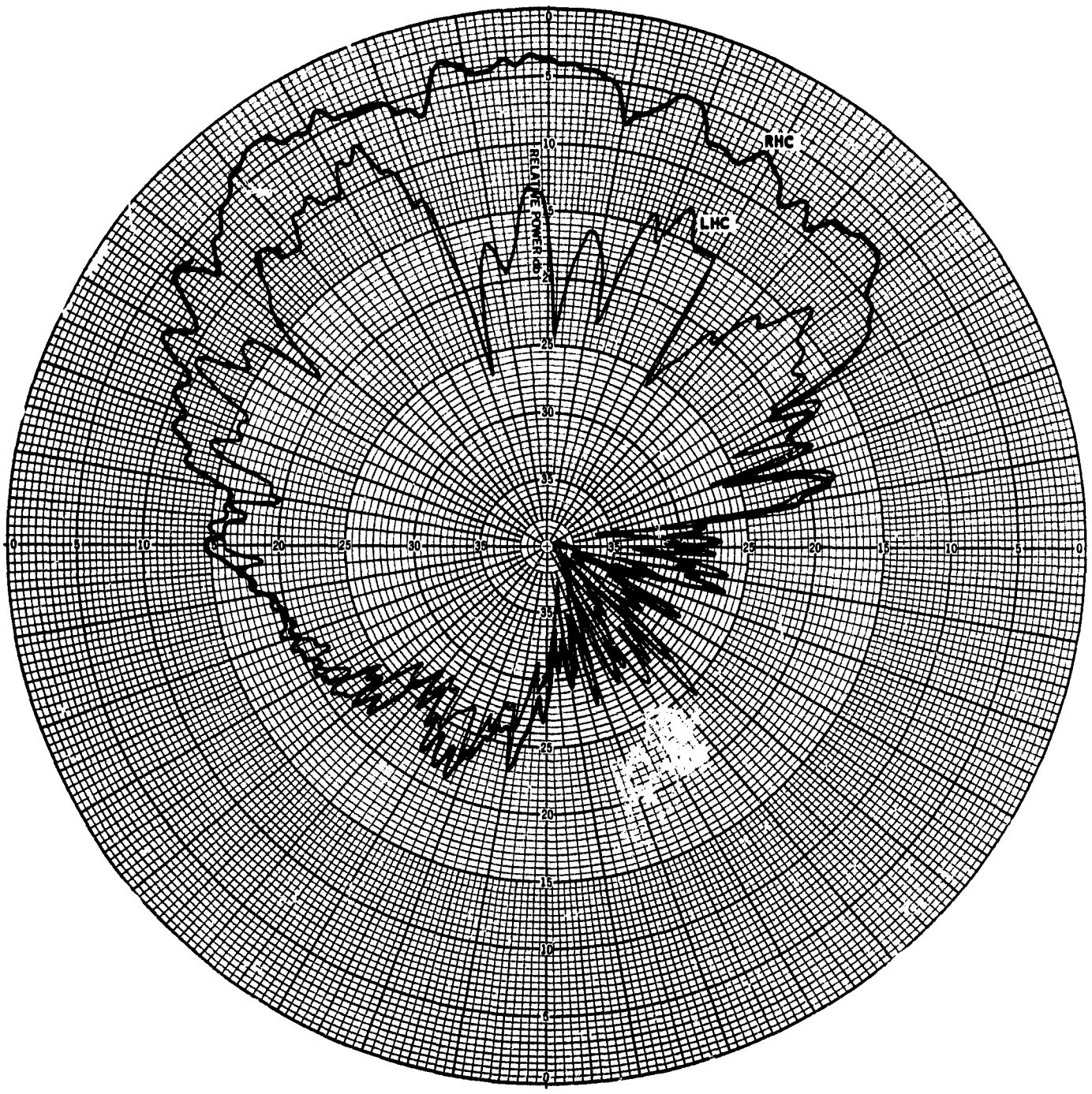

Fig. 23-22

THE JOHNS HOPKINS UNIVERSITY
APPLIED PHYSICS LABORATORY
SILVER SPRING MARYLAND

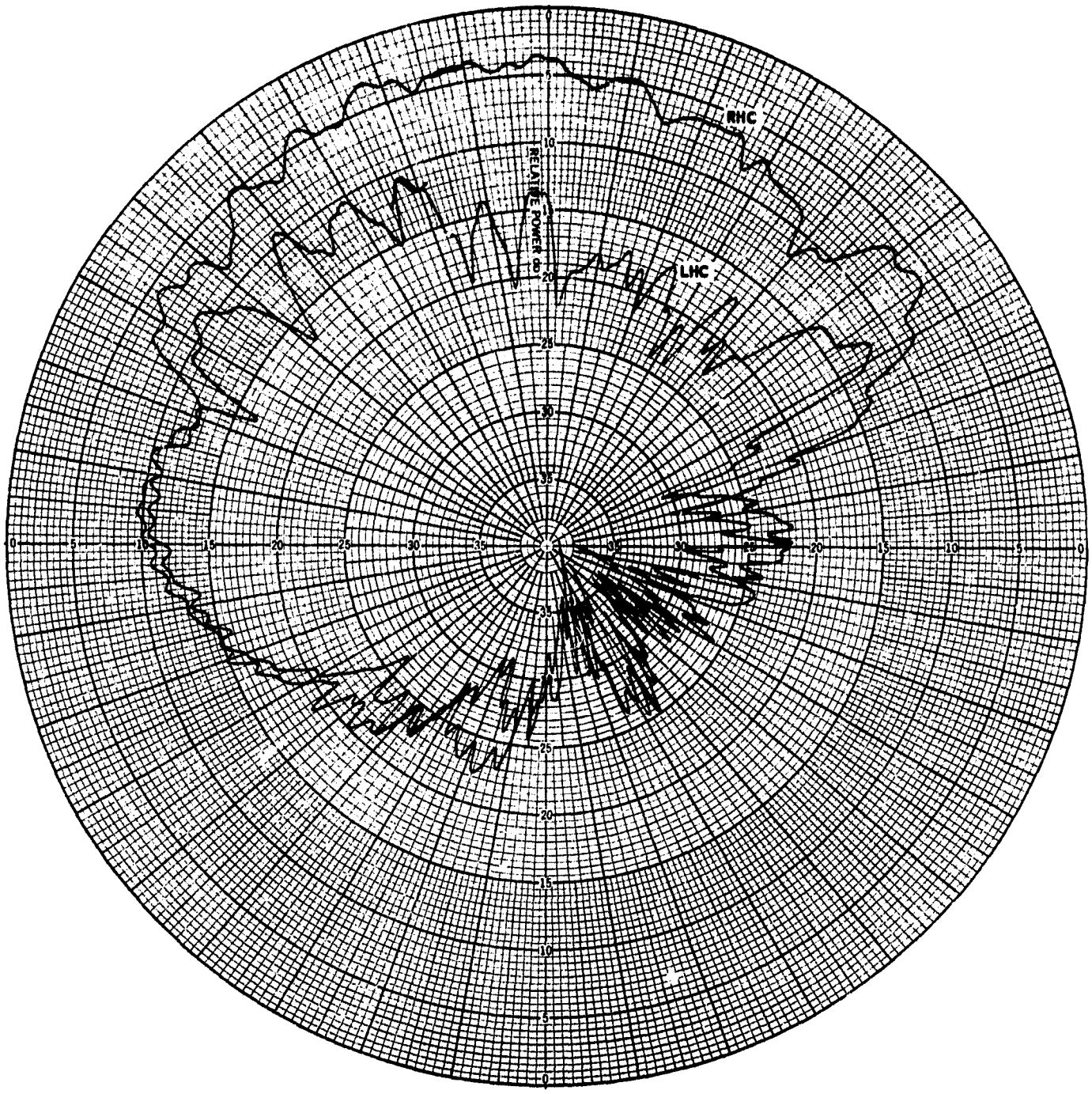

Fig. 23-23

THE JOHNS HOPKINS UNIVERSITY
APPLIED PHYSICS LABORATORY
SILVER SPRING MARYLAND

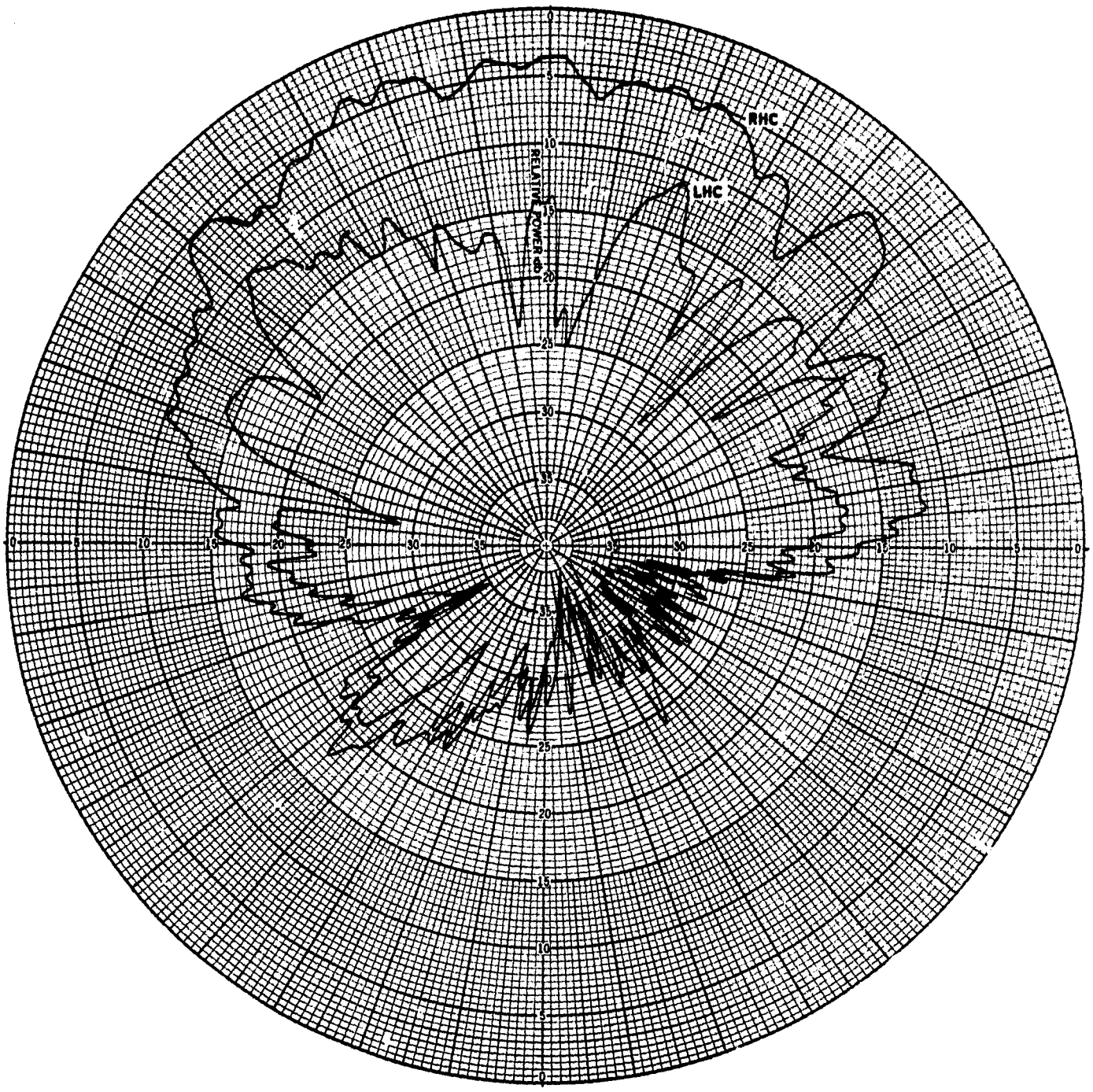

Fig. 23-24

THE JOHNS HOPKINS UNIVERSITY
APPLIED PHYSICS LABORATORY
SILVER SPRING MARYLAND

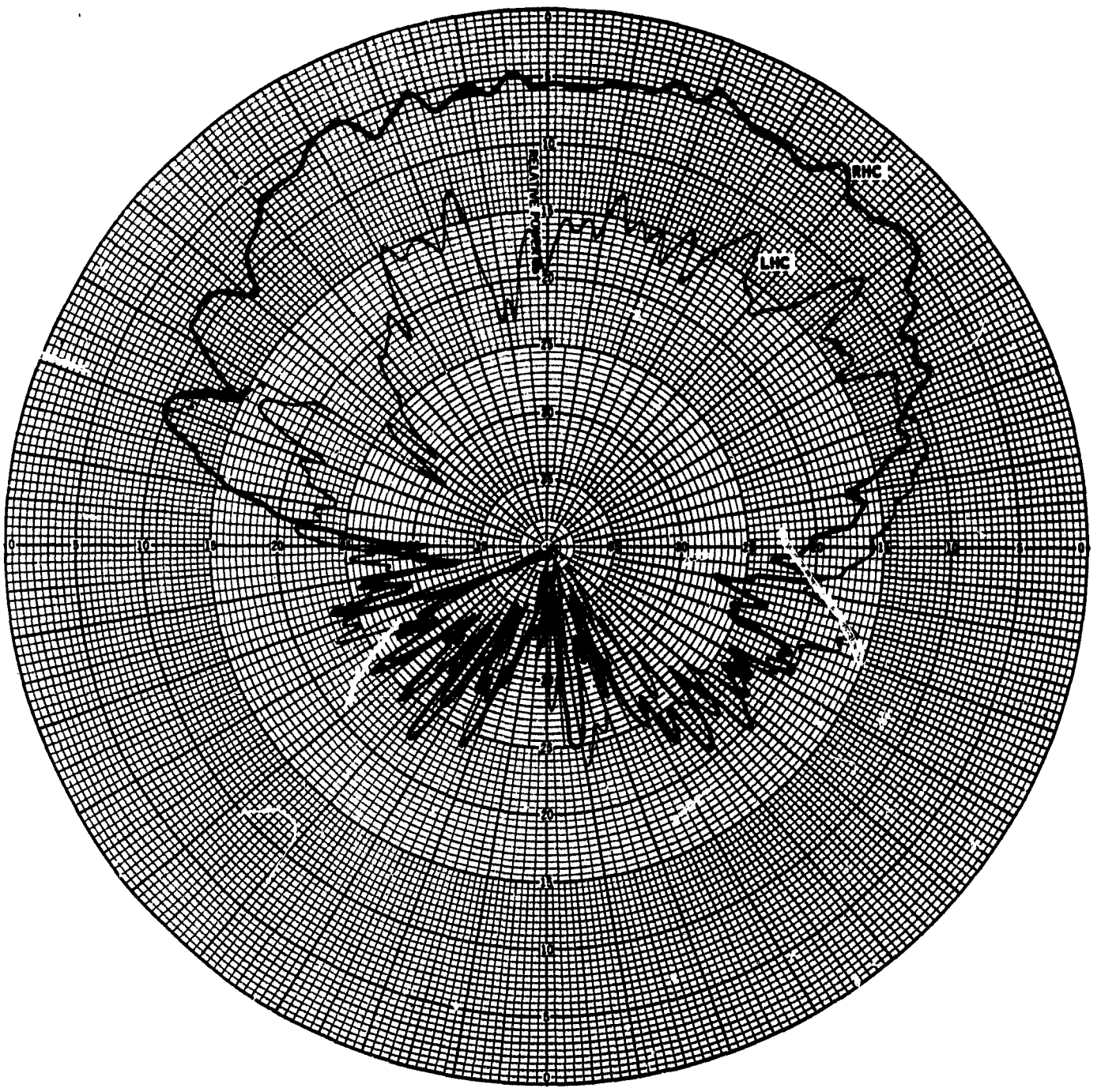

Fig. 23-25

THE JOHNS HOPKINS UNIVERSITY
APPLIED PHYSICS LABORATORY
SILVER SPRING MARYLAND

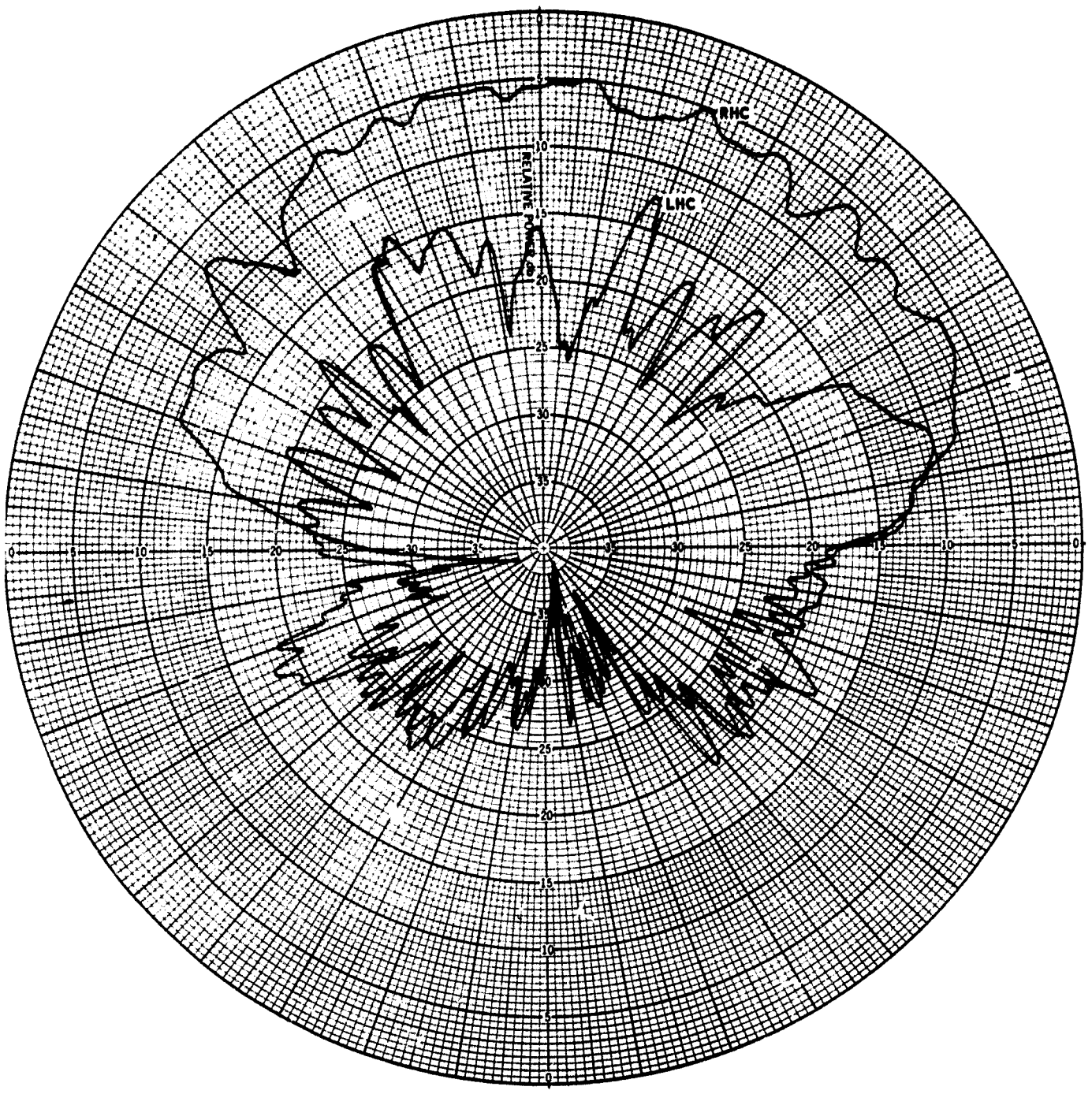

Fig. 23-26

THE JOHNS HOPKINS UNIVERSITY
APPLIED PHYSICS LABORATORY
SILVER SPRING MARYLAND

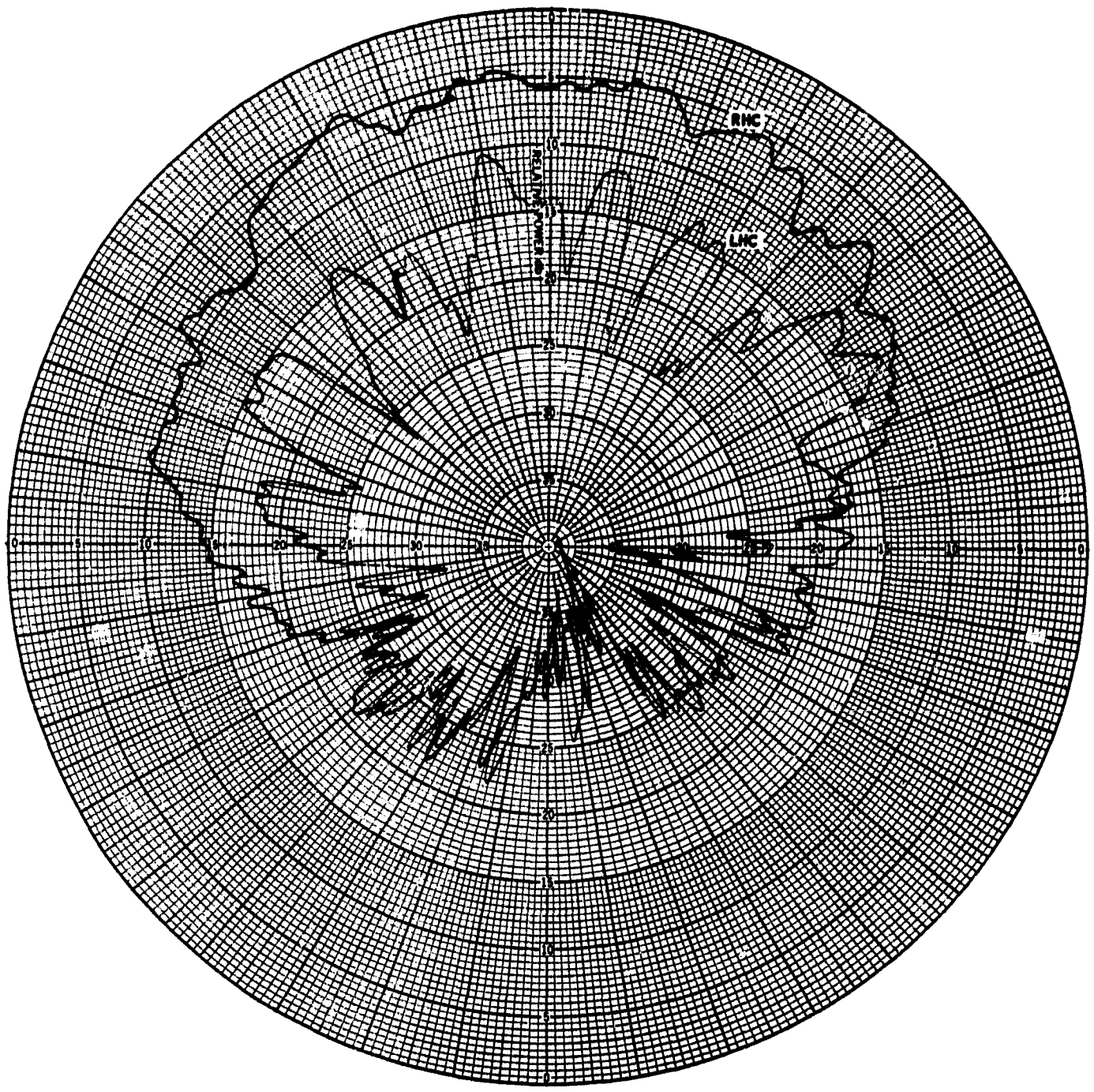

Fig. 23-27

THE JOHNS HOPKINS UNIVERSITY
APPLIED PHYSICS LABORATORY
SILVER SPRING MARYLAND

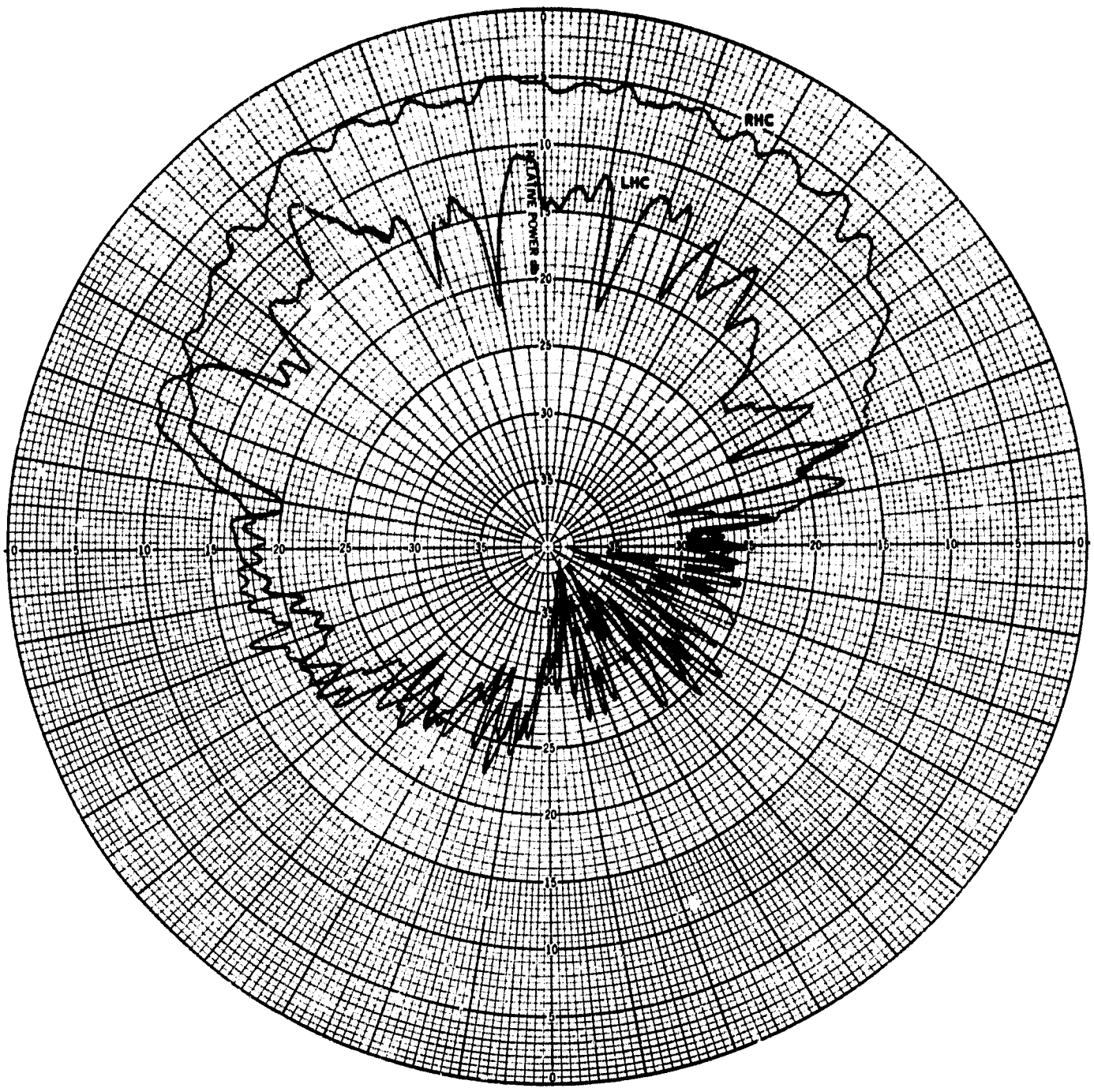

Fig. 23-28

THE JOHNS HOPKINS UNIVERSITY
APPLIED PHYSICS LABORATORY
SILVER SPRING MARYLAND

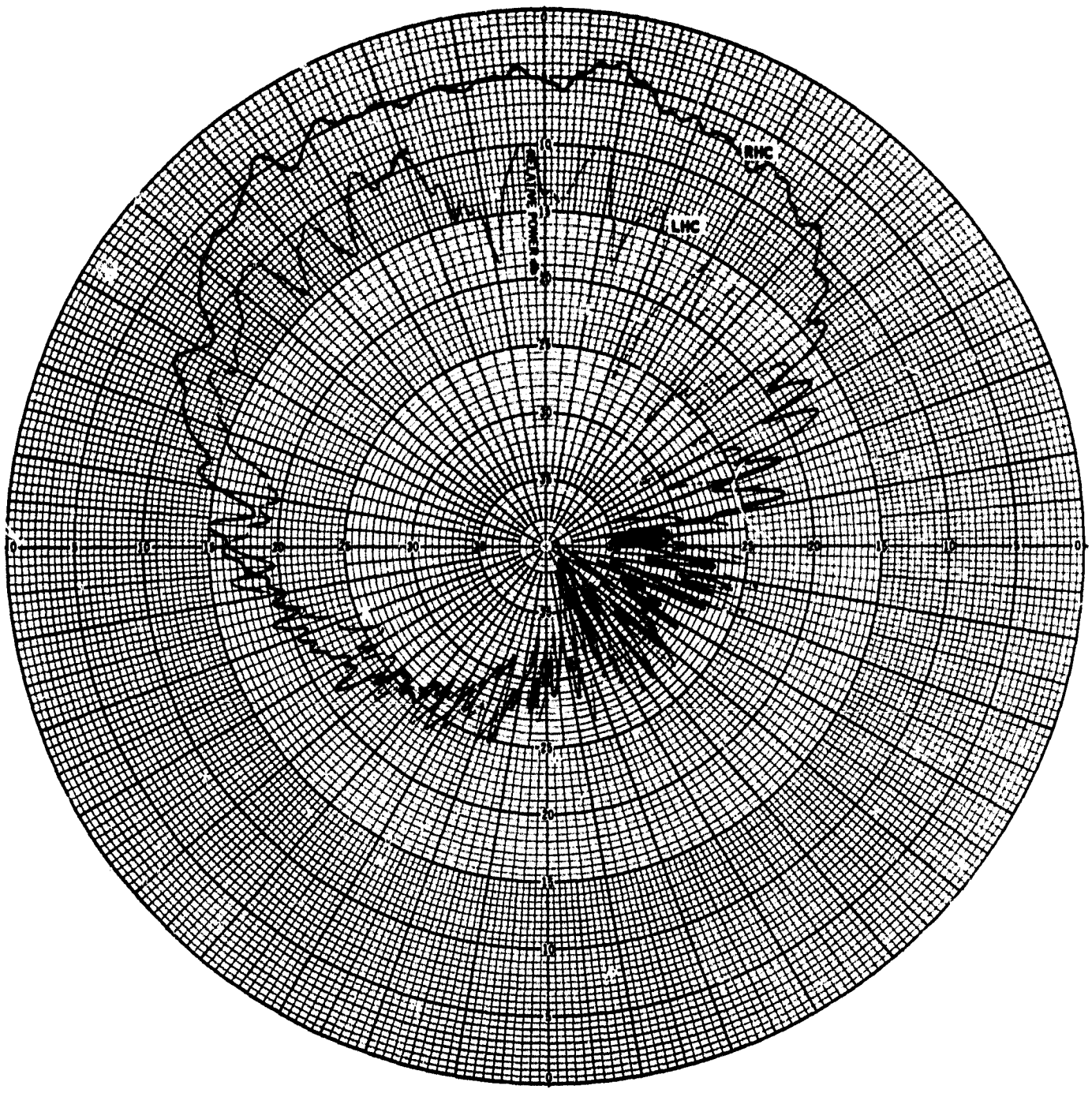

Fig. 23-29

THE JOHNS HOPKINS UNIVERSITY
APPLIED PHYSICS LABORATORY
SILVER SPRING MARYLAND

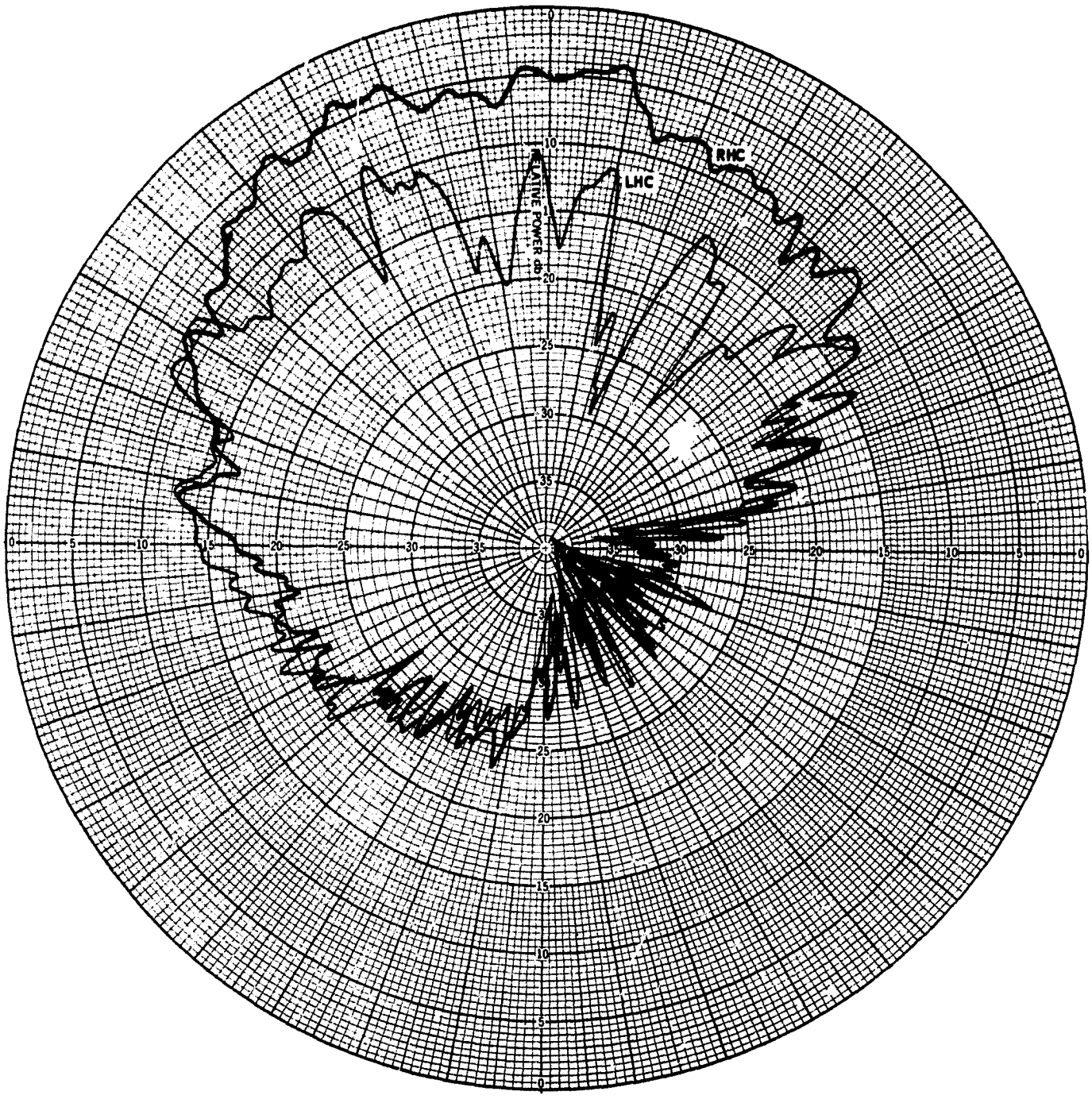

Fig. 23-30

THE JOHNS HOPKINS UNIVERSITY
APPLIED PHYSICS LABORATORY
SILVER SPRING MARYLAND

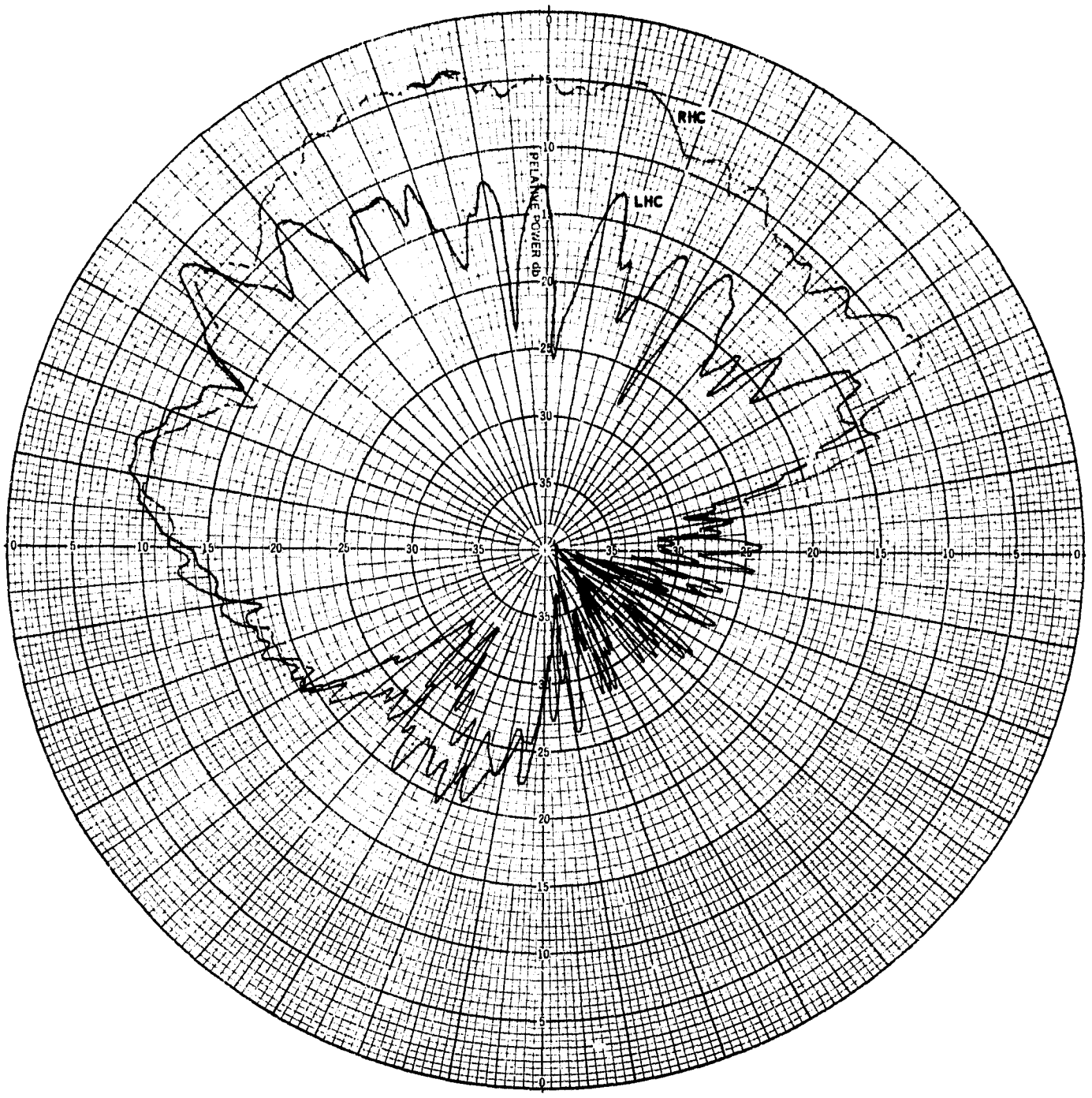

Fig. 23-31

THE JOHNS HOPKINS UNIVERSITY
APPLIED PHYSICS LABORATORY
SILVER SPRING MARYLAND

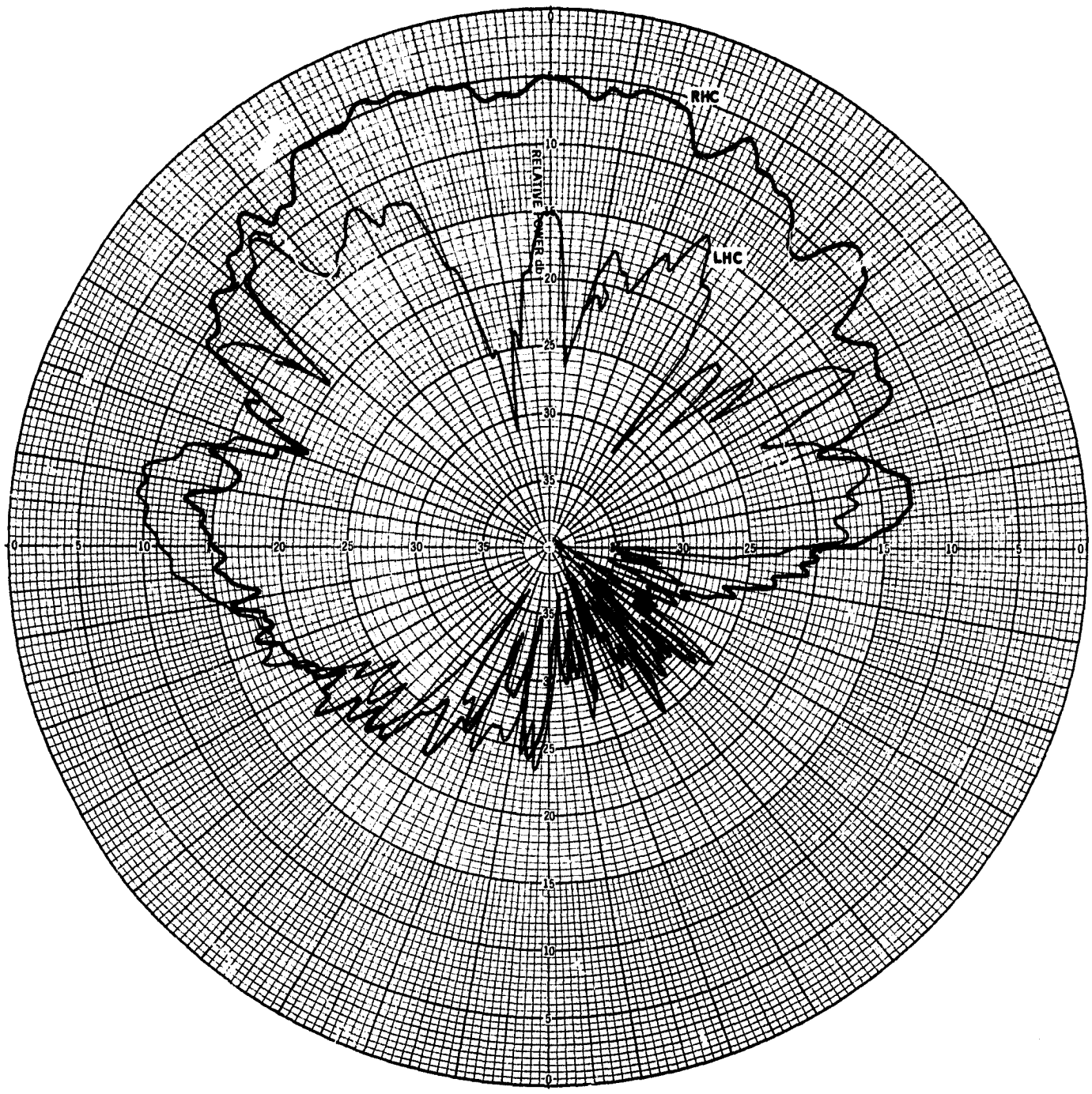

Fig. 23-32

THE JOHNS HOPKINS UNIVERSITY
APPLIED PHYSICS LABORATORY
SILVER SPRING, MARYLAND

GEOS-B C-Band Antenna Test Procedure

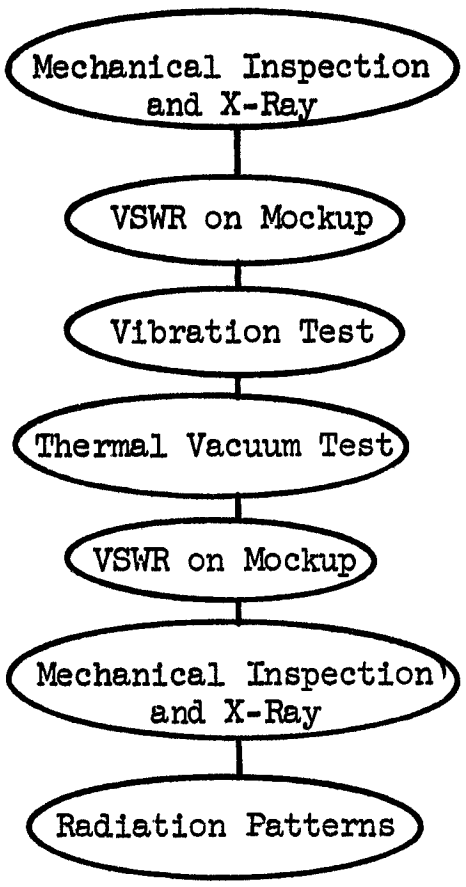

TEST FLOW DIAGRAM

Tests Performed and Typical Data

Mechanical Inspection and X-Ray - Causes for rejection in the past have been sprung center pins in the RF connector and cracks in the quartz window. Chips out of the surface of the quartz have no effect on the performance of the antenna and are acceptable. The X-ray (Figure 22) is used for visual checks and is a means of detecting damage after environmental testing.

VSWR on Mockup

The VSWR is measured at both frequencies on the RF mockup.

THE JOHNS HOPKINS UNIVERSITY
APPLIED PHYSICS LABORATORY
SILVER SPRING, MARYLAND

Vibration Test

The detected output of a slotted line is monitored with an oscilloscope during vibration. An intermittent or change in amplitude is cause for rejection of the antenna.

Thermal Vacuum Test

A sudden change in the VSWR measured with a slotted line during the test is cause for rejection. Typical VSWR vs. temperature data:

-95°F	1.2:1
+55°F	1.35:1
+155°F	1.4:1

Post Environmental Tests

VSWR, mechanical inspection and X-ray tests are repeated and the data compared with pre-environmental tests. Radiation patterns are measured as already discussed.

REFERENCES

1. "Performance Specification for GEOS-B Spacecraft," APL internal memo S4S-0-199 dated May 31, 1967.

2. "Frequency Independent Antennas," V. H. Rumsey (1957); I.R.E. National Convention Record, PI. 1, 114-118.

3. "Current Bands, Microwave Scanning Antennas," A. A. Oliner and R. G. Malech; R. C. Hansen, ED. New York Academic Press 1966, pp. 118-122.

4. "The Equangular Spiral Antenna," J. D. Dyson (1959); I.R.E. Transaction on Antennas and Properties, April, 181-187.

5. "A Broad-Band Spherical Satellite Antenna," H. B. Riblet (1960); I.R.E. Proceedings, Space Electronics Issue, April 1960, pp. 631-635.

6. "The Equangular Spiral Antenna on a Plane or Arbitrary Surface of Revolution," B. Storm (1961); APL CM-995 March, pp. 96-97.

7. "The Characteristics and Design of the Conical Log-Spiral Antenna," J. D. Dyson (1965); I.R.E. Transaction on Antenna and Properties, July pp. 488-499.

8. "Leaky Waves in Electromagnetic Phenomena, Electromagnetic Theory and Antennas," A. A. Oliner; E. C. Jordan, ED. New York Pergamon, 1963, pp. 837-856.

9. "Theoretical Brillouin (k-β) Diagram for Monopole and Dipole Arrays and Their Application to Log Periodic Antennas," R. Mittra and K. E. Jones; 1963 IEEE International Convention Record, Pt. 1 pp. 118-128.

10. "On the Solution of the Brillouin (k-β) Diagram of the Helix and Its Application to Helical Antennas," P. W. Klock and R. Mittra; 1963 G-Ap International Symposium Digest pp. 99-103.

11. "Theory of Frequency Scanning of Antennas," A. Schumorn and H. S. Tuan; I.R.E. Transaction on Antenna and Properties Vol. Ap-10 March 1962, pp. 144-150.

12. "A Traveling-Wave Directional Filter," F. S. Coale; I.R.E. Transaction MTT-4 pp. 256-260 (October 1956).

13. "Waveguide Transmission," G. C. Southworth; VanNostrand pp. 120-125.

14. "Antennas," J. D. Kraus; McGraw-Hill Book Company, Inc., 1950 pp. 430-431.